THE

LONDON, EDINBURGH, AND DUBLIN

PHILOSOPHICAL MAGAZINE

AND

JOURNAL OF SCIENCE.

[SEVENTH SERIES.]

OCTOBER 1937.

LII. *The "Converging Factor" in Asymptotic Series and the Calculation of Bessel, Laguerre and other Functions.* By JOHN R. AIREY, *D.Sc., Sc.D.**

IN the construction of tables of functions occurring in physical and mathematical problems, *e. g.*, Bessel functions, the series in ascending powers of the variable, such as

$$J_0(z)=1-\frac{z^2}{2^2}+\frac{z^4}{2^2.4^2}-\frac{z^6}{2^2.4^2.6^2}+\dots,$$

may be conveniently employed for small values of z. Although convergent for all values of z, it is not suitable when z is large, since the calculations become very difficult and laborious owing to the large number of terms and high powers necessary to be included. In finding the value [(1)] of e^{-10} to 24 places of decimals the calculation must be carried as far as the term z^{62}, the sum of the positive and negative powers being respectively

11013 . 232 920 103 323 139 721 376 087

and

11013 . 232 874 703 393 377 236 524 556.

* Communicated by the Author.

An earlier example occurs in the calculation of Airy's Integral [2],

$$\int_0^\infty \cos\frac{\pi}{2}(\omega^3 - m\omega)\, d\omega$$

for $m = -5{\cdot}6$, the largest value of the argument for which this particular integral was computed. It is remarked that it is impossible to make the calculations for larger values of m, even with ten-figure logarithms, on account of the divergence of the first terms of the series.

$$\int_0^\infty \cos\frac{\pi}{2}(\omega^3 - m\omega)\, d\omega$$

$$= C_1\left\{1 - \frac{1}{3}\cdot\frac{m^3}{3!} + \frac{4}{3}\cdot\frac{1}{3}\cdot\frac{m^6}{6!} - \frac{7}{3}\cdot\frac{4}{3}\cdot\frac{1}{3}\cdot\frac{m^9}{9!} + \cdots\right\}$$

$$+ C_2\left\{m - \frac{2}{3}\cdot\frac{m^4}{4!} + \frac{5}{3}\cdot\frac{2}{3}\cdot\frac{m^7}{7!} - \frac{8}{3}\cdot\frac{5}{3}\cdot\frac{2}{3}\cdot\frac{m^{10}}{10!} + \cdots\right\}.$$

For $m = \pm 5{\cdot}6$ the largest term in the series is 169·044826, and it is necessary to proceed as far as the 45th power of m. The result 0·000114 for $m = -5{\cdot}6$ is obtained by combining the sum of the positive terms, 614·149962 with the sum of the negative terms 614·149848. A very striking example of the application of the ascending series for large values of the argument is that given by Glaisher [3] in his paper on "Tables of the numerical values of the sine-integral, cosine-integral and the exponential integral." In calculating these functions to twelve places of decimals when the argument is 20, the first term rejected was the one containing z^{76}, and to show how extremely unmanageable the formulæ had become it is stated that these values required the formation of about twenty-two thousand figures exclusive of verifications. For larger values of the argument it is much more convenient to use the asymptotic series, *e. g.*,

$$Ei(z) = \frac{e^z}{z}\left(1 + \frac{1!}{z} + \frac{2!}{z^2} + \frac{3!}{z^3} + \cdots\right),$$

$$si(z) = -\frac{\cos z}{z}\left(1 - \frac{2!}{z^2} + \frac{4!}{z^4} - \frac{6!}{z^6} + \cdots\right)$$

$$- \frac{\sin z}{z}\left(\frac{1!}{z} - \frac{3!}{z^3} + \frac{5!}{z^5} - \frac{7!}{z^7} + \cdots\right),$$

and $$ci(z) = \frac{\sin z}{z}\left(1 - \frac{2!}{z^2} + \frac{4!}{z^4} - \frac{6!}{z^6} + \dots\right)$$

$$- \frac{\cos z}{z}\left(\frac{1!}{z} - \frac{3!}{z^3} + \frac{5!}{z^5} - \frac{7!}{z^7} + \dots\right).$$

These series, as far as the least term, were used by Glaisher for values of z greater than 17, the results being correct to about seven or eight decimal places. " To remove every shade of doubt that might attach to the use of these divergent series, the functions for $z=20$ were found from both formulæ—ascending and descending powers of the variable—and the agreement was perfect to the eighth place which was as far as the semi-convergent series could give correct results for the value of z."

Much greater accuracy can be obtained from the use of these asymptotic series than is here claimed. By a simple transformation of the divergent part of the asymptotic series, other series are obtained which are easily evaluated even when the argument is complex; and in the case of the Bessel functions, when the order of the function is imaginary or complex.

Although these asymptotic series begin by converging, they eventually become divergent. If the remaining terms after the smallest be omitted the sum of the terms already found will give the value of the function with an error less than the last included term : and the view generally held was that the degree of approximation could not be carried beyond this point. Lord Rayleigh [4], referring to the asymptotic expansions of Bessel functions, remarks that " series of this kind are strictly speaking not convergent at all, for when carried sufficiently far the sum of the series may be made to exceed any assignable quantity. But though ultimately divergent, they begin by converging, and when a certain point is reached the terms become very small. It can be proved that if we stop here the sum of the terms already obtained represents the required value of the function subject to an error which, in general, cannot exceed the last included term. Calculations founded on these series are therefore only approximate, and the degree of approximation cannot be carried beyond a certain point. In numerical calculations, therefore, we are to include only the convergent part."

In the case of asymptotic series of the first kind [5], *i.e.*, series in which the signs of the terms are alternately positive and negative, a much closer degree of accuracy than that represented by the least term can be secured by breaking up the divergent part of the asymptotic series into more tractable series, as many as eight, ten or more decimal places can be added to increase the accuracy of the result. To take a simple example, that of the exponential integral $Ei(-10)$, the value of the asymptotic series

$$1-\frac{1!}{x}+\frac{2!}{x^2}-\frac{3!}{x^3}+\frac{4!}{x^4}-\ldots$$

can be found to about four places of decimals when the calculations stop at the least term. However, by expressing the divergent part of the series as the product of a particular term—usually the least term—and a factor, for convenience called the "converging factor," it is possible to reduce the error to a unit in the seventeenth place of decimals and $Ei(-10)$ found to about 21 or 22 places, the accuracy of the result being increased by 13 places. To secure this degree of accuracy from the series in ascending powers it would be necessary to carry the calculations to sixty terms and for $Ei(-20)$ to nearly double that number of terms. If the argument z is complex, $\nu e^{i\theta}$ and β written for $e^{-i\theta}$, the various series derived from the divergent part of the asymptotic series can be readily computed by the method of differences and detached coefficients. For example, the series

$$6\beta^4-50\beta^5+225\beta^6-735\beta^7+\ldots,$$

which occurs in the term $\frac{1}{\nu^3}$ of the "converging factor" of the exponential integral [6],

6	50	225	735	1960	...
6	44	175	510	1225	
6	38	131	335	715	
6	32	93	204	380	
6	26	61	111	176	
6	20	35	50	65	
6	14	15	15	15	
6	8	1	0	0	

The sum of the series is

$$\frac{6\beta^4-8\beta^5+\beta^6}{(1+\beta)^7};$$

this gives the simple result $-\frac{1}{128}$ when the argument is real. $(\theta=0, \beta=1)$.

Exponential, Sine and Cosine Integrals.

For negative values of the argument the asymptotic series of the exponential integral is

$$1-\frac{1!}{z}+\frac{2!}{z^2}-\frac{3}{z^3}+\ldots,$$

the rth term, T_r, being $\frac{(r-1)!}{z^{r-1}}$. Put $z=ve^{i\theta}$, $\nu=r+h$, r an integer and h a fraction between -1 and $+1$, $\beta=e^{-i\theta}$, then the rth term and all the following terms are equivalent to

$$T_r\left[1-\frac{r}{z}+\frac{r(r+1)}{z^2}-\frac{r(r+1)(r+2)}{z^3}+\ldots\right]$$

$$=T_r\left[1-\frac{(\nu-h)\beta}{\nu}+\frac{(\nu-h)(\nu+1-h).\beta^2}{\nu^2}\right.$$

$$\left.-\frac{(\nu-h)(\nu+1-h)(\nu+2-h).\beta^3}{\nu^3}+\ldots\right]$$

$$=T_r\left[1-\left(1-\frac{h}{\nu}\right)\beta+\left(1-\frac{h}{\nu}\right)\left(1+\frac{1-h}{\nu}\right)\beta^2\right.$$

$$\left.-\left(1-\frac{h}{\nu}\right)\left(1+\frac{1-h}{\nu}\right)\left(1+\frac{2-h}{\nu}\right)\beta^3+\ldots\right].$$

The part of the series in the bracket independent of ν is, of course,

$$1-\beta+\beta^2-\beta^3+\ldots=\frac{1}{1+\beta}.$$

The other series are easily evaluated, *e. g.*, the series containing $\frac{1}{\nu^2}$ is

$$-2\beta^3+11\beta^4-35\beta^5+85\beta^6-\ldots,$$

the sum of which is

$$\frac{-2\beta^3+\beta^4}{(1+\beta)^5}.$$

The "converging factor," the factor by which T_r must be multiplied to evaluate this term and the following terms, becomes

$$\begin{aligned}
&\frac{1}{1+\beta}+\frac{1}{\nu}\left[\frac{\beta^2}{(1+\beta)^3}+\frac{\beta}{(1+\beta)^2}\cdot h\right]\\
&\qquad+\frac{1}{\nu^2}\left[\frac{-2\beta^3+\beta^4}{(1+\beta)^5}-\frac{\beta^2-2\beta^3}{(1+\beta)^4}h+\frac{\beta^2}{(1+\beta)^3}h^2\right]\\
&+\frac{1}{\nu^3}\left[\frac{6\beta^4-8\beta^5+\beta^6}{(1+\beta)^7}+\frac{2\beta^3-10\beta^4+3\beta^5}{(1+\beta)^6}h\right.\\
&\qquad\left.+\frac{-3\beta^3+3\beta^4}{(1+\beta)^5}h^2+\frac{\beta^3}{(1+\beta)^4}h^3\right]\\
&+\frac{1}{\nu^4}\left[\frac{-24\beta^5+58\beta^6-22\beta^7+\beta^8}{(1+\beta)^9}\right.\\
&\qquad-\frac{6\beta^4-52\beta^5+43\beta^6-4\beta^7}{(1+\beta)^8}h\\
&\qquad\left.+\frac{11\beta^4-28\beta^5-6\beta^6}{(1+\beta)^7}h^2-\frac{6\beta^4-4\beta^5}{(1+\beta)^6}\cdot h^3+\frac{\beta^4}{(1+\beta)^5}h^4\right].\\
&\qquad\qquad\ldots\qquad(1)
\end{aligned}$$

This form of the "converging factor" is not suitable for numerical computation. However, if we write $\theta=2\phi$, $\beta=e^{-i2\phi}$, $\sigma=\sec\phi$, and put $\alpha=e^{-i\phi}$, then $\frac{1}{1+\beta}=\frac{\sigma}{2\alpha}$ and (1) becomes

$$\begin{aligned}
&\frac{\sigma}{2\alpha}+\frac{\sigma^2}{4\nu}\left[\frac{\sigma}{2}\alpha+h\right]+\frac{\sigma^3}{8\nu^2}\left[\frac{\sigma^2}{4}(-2\alpha+\alpha^3)-\frac{\sigma}{2}(1-2\alpha^2)h+\alpha h^2\right]\\
&+\frac{\sigma^4}{16\nu^3}\left[\frac{\sigma^3}{8}(6\alpha-8\alpha^3+\alpha^5)+\frac{\sigma^2}{4}(2-10\alpha^2+3\alpha^4)h\right.\\
&\qquad\left.+\frac{\sigma}{2}(-3\alpha+3\alpha^3)h^2+\alpha^2h^3\right]
\end{aligned}$$

$$+\frac{\sigma^5}{32\nu^4}\left[\frac{\sigma^4}{16}(-24\alpha+58\alpha^3-22\alpha^5+\alpha^7)\right.$$
$$+\frac{\sigma^3}{8}(6-52\alpha^2+43\alpha^4-4\alpha^6)h$$
$$+\frac{\sigma^2}{4}(11\alpha-28\alpha^3+6\alpha^5)h^2$$
$$\left.+\frac{\sigma}{2}(6\alpha^2-4\alpha^4)h^3+\alpha^3 . h^4\right]+\ldots. \quad (2)$$

If ν is an integer and s written for $\sigma/2$ the "converging factor" as far as the term containing $\frac{1}{\nu^{10}}$ becomes

$$s.\alpha+\frac{1}{\nu}s^3.\alpha+\frac{1}{\nu^2}[s^5(-2\alpha+\alpha^3]+\frac{1}{\nu^3}[s^7(6\alpha-8\alpha^3+\alpha^5)]$$
$$+\frac{1}{\nu^4}[s^9(-24\alpha+58\alpha^3-22\alpha^5+\alpha^7)]$$
$$+\frac{1}{\nu^5}[s^{11}(120\alpha-444\alpha^3+328\alpha^5-52\alpha^7+\alpha^9)]$$
$$+\frac{1}{\nu^6}[s^{13}(-720\alpha+3708\alpha^3-4400\alpha^5$$
$$+1452\alpha^7-114\alpha^9+\alpha^{11})]$$
$$+\frac{1}{\nu^7}[s^{15}(5040\alpha-33984\alpha^3+58140\alpha^5-32120\alpha^7$$
$$+5610\alpha^9-240\alpha^{11}+\alpha^{13})]$$
$$+\frac{1}{\nu^8}[s^{17}(-40320\alpha+341136\alpha^3-785304\alpha^5+644020\alpha^7$$
$$-195800\alpha^9+19950\alpha^{11}-494\alpha^{13}+\alpha^{15})]$$
$$+\frac{1}{\nu^9}[s^{19}(362880\alpha-3733920\alpha^3+11026296\alpha^5$$
$$-12440064\alpha^7+5765500\alpha^9-1062500\alpha^{11}$$
$$+67260\alpha^{13}-1004\alpha^{15}+\alpha^{17})]$$
$$+\frac{1}{\nu^{10}}[s^{21}(-3628800\alpha+44339040\alpha^3-162186912\alpha^5$$
$$+238904904\alpha^7-155357384\alpha^9+44765000\alpha^{11}$$
$$-5326160\alpha^{13}+218848\alpha^{15}-2026^{17}+\alpha^{19})]+..$$
$$\ldots \quad 3)$$

The numerical coefficients in the expressions of two consecutive powers of ν are simply related: thus, the coefficients in the term containing $\frac{1}{\nu^6}$ are

$$720=6.120\,;\quad 3708=5.120+7.444\,;\quad 4400=4.444+8.328\,;$$

$$1452=3.328+9.52\,;\quad 114=2.52+10.1.$$

If ν is real and equal to $n+h$, the C.F. is

$$\frac{1}{2}+\frac{1}{4n}\left(\frac{1}{2}+h\right)-\frac{1}{8n^2}\left(\frac{1}{4}+\frac{h}{2}+h^2\right)-\frac{1}{16n^3}\left(\frac{1}{8}+\frac{h}{4}-h^3\right)$$
$$+\frac{1}{32n^4}\left(\frac{13}{16}+\frac{13h}{16}+\frac{7h^2}{4}+h^3-h^4\right)$$
$$-\frac{1}{64n^5}\left(\frac{47}{32}+\frac{47h}{16}+\frac{15h^2}{4}+\frac{15h^3}{4}+\frac{5h^4}{2}-h^5\right)$$
$$-\frac{1}{128n^6}\left(\frac{73}{64}+\frac{73h}{32}+\frac{13h^2}{16}-\frac{5h^3}{2}-5h^4-\frac{9h^5}{2}+h^6\right)+\ldots$$
$$\ldots \qquad (4)$$

This formula was used in extending the tables of the exponential integral as far as $\nu=20$ by intervals of 0·2, which were needed in constructing a table of the radiation integral [7]

$$\int_x^\infty \frac{dx}{x(e^x-1)}.$$

When ν is real, h zero, $\alpha=1$, $\sigma=1$, the calculations have been carried as far as the term $\frac{1}{\nu^{22}}$. If the "converging factor" is

$$\frac{1}{2}\left[1+\sum_{n=1}\frac{a_n}{(4\nu)^n}\right], \quad \ldots\ldots \quad (5)$$

the values of a_n are given in the table (p. 529).

The numbers in the table are derived from the numerical coefficients in (3) in a simple manner. For example,

$$a_6=-73=-720+3708-4400+1452-114+1,$$

and so on.

n.	a_n.				
1	+				1
2	−				1
3	−				1
4	+				13
5	−				47
6	−				73
7	+				2447
8	−				16811
9	−				15551
10	+			17	26511
11	−			189	94849
12	+			109	79677
13	+			29834	09137
14	−		4	84211	03257
15	+		13	50023	66063
16	+		1012	53200	47141
17	−		23203	31477	79359
18	+	1	30595	20092	04319
19	+	58	74028	26601	73759
20	−	1862	05713	25553	80307
21	+	16905	21942	11969	07793
22	+	5 27257	18724	48118	05207

(*a*) $Ei(-5)$. The exponential integral for argument $z=-5$ is given by

$$-\frac{e^{-5}}{5}\left[1-\frac{1}{5}+\frac{2!}{5^2}-\frac{3!}{5^3}+\frac{4!}{5^4}\times\text{C.F.}\right].$$

From (5) the C.F. $=0{\cdot}52372\ 087:$, $\frac{4!}{5^4}=0{\cdot}0384$,

their product $=0{\cdot}02011\ 08816$,

the bracket $=0{\cdot}85211\ 08816$,

and, finally,

$$Ei(-5)=-\frac{1}{5}\times 0{\cdot}00574\ 14779\ 57:$$

$$=-0{\cdot}00114\ 82955\ 91:$$

the correct value being $-0{\cdot}00114\ 82955\ 913$. There is thus an improvement in the accuracy of the calculation to the extent of seven or eight decimals even for this comparatively small value of the argument.

(*b*) $Ei\,(-10)$. The term, T_r in this case, is

$$-0{\cdot}00036\ 28800$$

and the C.F. is

$$0{\cdot}51218\ 19943\ 760:$$

thus one can add about thirteen places of decimals to the result of the calculation stopping at the least term

$$Ei\,(-10) = -0{\cdot}0^5\ 4156\ 9689\ 2968\ 5324,$$

the value given by Bauschinger [8], computed from the ascending series to twenty places,

$$-0{\cdot}0^5\ 4156\ 9689\ 2968\ 532.$$

(*c*) $Ei\,(-4{\cdot}5i)$.

Here $$\theta = \frac{\pi}{2},\quad \alpha = \cos\frac{\pi}{4} - i\sin\frac{\pi}{4} = \frac{1-i}{\sqrt{2}}.$$

$$\alpha^2 = -i,\quad \alpha^3 = \frac{-1-i}{\sqrt{2}},\ \text{etc.}\quad \sigma = \sqrt{2},\quad h = 0{\cdot}5.$$

The series representing this integral is

$$\frac{\sin\nu + i\cos\nu}{\nu}\left[1 + \frac{i}{\nu} - \frac{2!}{\nu^2} - \frac{3!\,i}{\nu^3}\cdot \times \text{C.F.}\right].$$

Making the above substitutions in (2), it is found that the C.F. is

$$\left(\frac{1}{2} + \frac{1}{2\nu} - \frac{7}{16\nu^2} + \frac{19}{32\nu^3} - \frac{311}{128\nu^4} + \ldots\right)$$

$$+ \left(\frac{1}{2} - \frac{1}{4\nu} - \frac{3}{16\nu^2} + \frac{3}{4\nu^3} + \frac{5}{128\nu^4} - \ldots\right)i.$$

Putting $\nu = 4{\cdot}5$, this becomes $0{\cdot}59 : +0{\cdot}44i$, the colon : representing approximately a half-unit in the last place of decimals; the product of this factor and the term $-\frac{3!\,i}{\nu^3}$ is equal to $0{\cdot}02897 - 0{\cdot}03917i$; finally, the bracket has the value

$$0{\cdot}93020 : +0{\cdot}18305i,$$

which, multiplied by

$$\frac{\sin\nu + i\cos\nu}{\nu} = \frac{2}{9}(-0{\cdot}977530 - 0{\cdot}210796i)$$

gives

$$Ei(-4{\cdot}5i) = -0{\cdot}19349 : -0{\cdot}08334i.$$

Since

$$Ei(-ix)=ci(x)-i\ si\ (x),$$

this result can be compared with *ci* (4·5) and *si* (4·5) from Glaisher's Tables [3].

In the first volume of mathematical tables issued by the Committee of the British Association the cosine integral for argument less than 5 is not given, but the difference between the integral and the natural logarithm of the argument, an arrangement which is both inconvenient and unnecessary.

(*d*) $Ei(-10i)$. The asymptotic expansion is given by

$$\frac{\sin\nu+i\cos\nu}{\nu}\left[1+\frac{i}{\nu}-\frac{2!}{\nu^2}-\frac{3!\,i}{\nu^3}+\frac{4!}{\nu^4}+\frac{5!\,i}{\nu^5}-\frac{6!}{\nu^6}\right.$$
$$\left.-\frac{7!\,i}{\nu^7}+\frac{8!}{\nu^8}+\frac{9!\,i}{\nu^9}\times\text{C.F.}\right].$$

In this case where ν is an integer, (3) can be used to calculate the C.F. as far as the term containing $\frac{1}{\nu^{10}}$: as in the previous example

$$\theta=\frac{\pi}{2},\quad \phi=\frac{\pi}{4},\quad \alpha=\cos\frac{\pi}{4}-i\sin\frac{\pi}{4};$$

with these substitutions the real and imaginary parts of the C.F. are

Real part :

$$\frac{1}{2}+\frac{1}{2^2\nu}-\frac{3}{2^3\nu^2}+\frac{13}{2^4\nu^3}-\frac{59}{2^5\nu^4}+\frac{185}{2^6\nu^5}+\frac{1309}{2^7\nu^6}-\frac{45387}{2^8\nu^7}$$
$$+\frac{832613}{2^9\nu^8}-\frac{12609823}{2^{10}\nu^9}+\frac{158544573}{2^{11}\nu^{10}}\cdots,$$

Imag. part :

$$\frac{1}{2}-\frac{1}{2^2\nu}+\frac{1}{2^3\nu^2}+\frac{3}{2^4\nu^3}-\frac{55}{2^5\nu^4}+\frac{599}{2^6\nu^5}-\frac{5823}{2^7\nu^6}+\frac{49595}{2^8\nu^7}$$
$$-\frac{266743}{2^9\nu^8}-\frac{2679473}{2^{10}\nu^9}+\frac{141494849}{2^{11}\nu^{10}}-\cdots,$$

which give the C.F. to five places of decimals, viz.,

$$0{\cdot}52191+0{\cdot}47633i.$$

The product of this factor and $\frac{9!\,i}{\nu^9}$, which is $0{\cdot}0003\ 6288i$, is

$$-0{\cdot}0001\ 7285+0{\cdot}0001\ 8939i,$$

and the complete bracket is

$$0{\cdot}9819\ 1035+0{\cdot}0948\ 8539i$$

$\sin 10=-0{\cdot}5440\ 2111$, $\cos 10=-0{\cdot}8390\ 7153$,

and

$$Ei(-10i)=-0{\cdot}04545\ 64329-0{\cdot}08755\ 12675 : i,$$

which may be compared with [9]

$ci(10)=-0{\cdot}04545\ 64330$ and $si(10)=-0{\cdot}08755\ 12674$.

(*e*) $Ei\left(-5e^{i\frac{\pi}{6}}\right)$. Since

$$Ei(-z)=-\frac{e^{-z}}{z}\left(1-\frac{1}{z}+\frac{2!}{z^2}-\frac{3!}{z^3}+\frac{4!}{z^4}\times\text{C.F.}\right)$$

and

$$z=5\left(\cos\frac{\pi}{6}+i\sin\frac{\pi}{6}\right)=\frac{5(\sqrt{3}+i)}{2},\quad \nu=5,\quad \theta=\frac{\pi}{6},$$

the bracket

$$=\left(1-\frac{\sqrt{3}}{2\nu}+\frac{1}{\nu^2}\right)+i\left(\frac{1}{2\nu}-\frac{\sqrt{3}}{\nu^2}+\frac{6}{\nu^3}\right)$$
$$-\frac{12}{\nu^4}(1+i\sqrt{3})\times\text{C.F.}$$

Now

$$e^{-z}=e^{\nu\cos\theta}\left[\cos(\nu\sin\theta)-i\sin(\nu\sin\theta)\right],$$

$$\log_{10}e^{\nu\cos\theta}=\bar{2}{\cdot}1194497 :,\quad \frac{1}{z}=\frac{1}{5}\cdot\frac{\sqrt{3}-i}{2},$$

$\cos(\nu\sin\theta)=-0{\cdot}8011436$, $\sin(\nu\sin\theta)=-0{\cdot}5984721$:

and

$$\frac{e^{-z}}{z}=-0{\cdot}00261\ 4867-0{\cdot}00030\ 9975i.$$

The C.F. calculated from (3) as far as the term $\frac{1}{\nu^4}$, by substituting

$$\phi=15^\circ,\ \sigma=\sec 15^\circ,\ \alpha=e^{-i\phi},$$

gives

$$0{\cdot}52505 : +0{\cdot}12671 : i,$$

and the bracket is

$$0{\cdot}8609\ 278+0{\cdot}0588\ 242i,$$

giving the result

$$Ei\,(-5e^{\frac{i\pi}{6}})=0{\cdot}0022\ 3298+0{\cdot}0004\ 2068i,$$

compared with the value from the ascending series

$$0{\cdot}0022\ 3299+0{\cdot}0004\ 2066i.$$

Without the use of the " converging factor " the result is

$$0{\cdot}0022\ 022+0{\cdot}0003\ 816,$$

with errors of three or four units in the fifth place of decimals.

Logarithmic Γ Function.

The series in ascending powers, viz.,

$$\log_e \Gamma(1+z)=\frac{1}{2}\log_e\left(\frac{\pi z}{\sin \pi z}\right)-\frac{1}{2}\log_e\left(\frac{1+z}{1-z}\right)+C_1 z\,.$$
$$-C_3x^3-C_5x^5\ \ldots,$$

where

$$C_1=1-\gamma=0{\cdot}42278\ 43351,$$

$$C_3=\frac{1}{3}\sum_2^\infty n^{-3}=0{\cdot}06735\ 23010:$$

$$C_5=\frac{1}{5}\sum_2^\infty n^{-5}=0{\cdot}00738\ 55510 : {}^{(10)} \text{ and so on,}$$

is suitable for computing this function when $|z| \leqslant 1$. Thus, when $z=i$, the first term is real and the remaining terms imaginary,

$$\log_e \Gamma(1+i)=-0{\cdot}65092\ 31993-0{\cdot}30164\ 03205i.$$

The asymptotic expansion (Stirling's Series), which may be used for larger values of the argument z, is

$$\log \Gamma(z)=(z-\tfrac{1}{2})\log_e z-z+\tfrac{1}{2}\log_e 2\pi + \frac{B_1}{2z}-\frac{B_2}{12z^3}+\frac{B_3}{30z^5}-\dots$$

The term containing the rth Bernoullian number is

$$\frac{B_r}{(2r-1)\,2r\,.\,z^{2r-1}} \quad \text{and} \quad B_r=\frac{(2r)!}{2^{2r-1}\,.\,\pi^{2r}}\sum_{n=1}^{\infty}\frac{1}{n^{2r}}.$$

If $z=\nu e^{i\theta}$, then this term of the Bernoullian series and all the following terms can be represented by

$$\frac{(2r-2)!}{2^{2r-1}\pi^{2r}z^{2r-1}}\left[\Sigma\frac{1}{n^{2r}}-\frac{(2r-1)2r}{2^2\pi^2\nu^2}e^{-2i\theta}\Sigma\frac{1}{n^{2r+2}} + \frac{(2r-1)\,2r\,(2r+1)(2r+2)}{2^4\pi^4\nu^4}e^{-4i\theta}\Sigma\frac{1}{n^{2r+4}}-\dots\right] \quad \dots \quad (1)$$

Put $t=2\pi\nu=(2r-1)-\eta$, where r is an integer fixed by the chosen value of ν and η lies between -1 and $+1$, $\beta=e^{-i\theta}$, and A is the coefficient outside the bracket. Thus (1) becomes

$$A\left[\Sigma\frac{1}{n^{2r}}-\frac{(t+\eta)(t+1+\eta)}{t^2}\beta^2\Sigma\frac{1}{n^{2r+2}} + \frac{(t+\eta)(t+1+\eta)(t+2+\eta)(t+3+\eta)}{t^4}\beta^4\Sigma\frac{1}{n^{2r+4}}-\dots\right],$$

and proceeding as in the case of the exponential integral we find the "converging factor" as far as the t^{-2} term.

$$\frac{1}{1+\beta^2}+\left[\frac{-\beta^2+3\beta^4}{(1+\beta^2)^3}+\frac{-2\beta^2}{(1+\beta^2)^2}\eta\right]\frac{1}{t} + \left[\frac{11\beta^4-30\beta^6+7\beta^8}{(1+\beta^2)^5}+\frac{-\beta^2+14\beta^4-9\beta^6}{(1+\beta^2)^4}\eta + \frac{-\beta^2+3\beta^4}{(1+\beta^2)^3}\eta^2\right]\frac{1}{t^2}\dots$$

$$+\frac{1}{2^{2r}}\left\{\frac{1}{1+\gamma^2}+\left[\frac{-\gamma^2+3\gamma^4}{(1+\gamma^2)^3}+\frac{-2\gamma^2}{(1+\gamma^2)^2}\eta\right]\frac{1}{t}+\cdots\right\}$$

$$+\frac{1}{3^{2r}}\left\{\frac{1}{1+\delta^2}+\left[\frac{-\delta^2+3\delta^4}{(1+\delta^2)^3}+\frac{-2\delta^2}{(1+\delta^2)^2}\eta\right]\frac{1}{t}+\cdots\right\}+\cdots,$$

where $\gamma=\frac{\beta}{2}$, $\delta=\frac{\beta}{3}$, etc.

If $\nu=3$, $2r$ is approximately equal to 20 and $\frac{1}{2^{2r}}$ is about 10^{-6}, *i. e.*, the term of which the coefficient is $\frac{1}{2^{2r}}$ only affects the converging factor by less than a unit in the sixth place of decimals and may therefore be omitted.

Limiting the calculation to the first term, writing

$$s=\frac{\sec\theta}{2}, \text{ and } \frac{1}{1+\beta^2}=\frac{s}{\beta},$$

the converging factor becomes

$$\frac{s}{\beta}+\left[s^3\left(-\frac{1}{\beta}+3\beta\right)-2s^2.\eta\right]\frac{1}{t}$$

$$+\left[s^5\left(\frac{11}{\beta}-30\beta+7\beta^3\right)+s^4\left(-\frac{1}{\beta^2}+14-9\beta^2\right)\eta\right.$$

$$\left.+s^3\left(-\frac{1}{\beta}+3\beta\right)\eta^2\right]\frac{1}{t^2}$$

$$+\left[s^7\left(\frac{6}{\beta^3}-\frac{183}{\beta}+511\beta-245\beta^3+15\beta^5\right)\right.$$

$$+s^6\left(\frac{22}{\beta^2}-208+222\beta^2-28\beta^4\right)\eta$$

$$\left.+s^5\left(\frac{18}{\beta}-60\beta+18\beta^3\right)\eta^2+s^4(4-4\beta^2)\eta^3\right]\frac{1}{t^3}$$

$$+\left[s^9\left(-\frac{274}{\beta^3}+\frac{4303}{\beta}-12216\beta+8634\beta^3-1422\beta^5\right.\right.$$

$$\left.+31\beta^7\right)$$

$$+s^8\left(\frac{6}{\beta^4}-\frac{627}{\beta^2}+4568-6314\beta^2+1850\beta^4-75\beta^6\right)\eta$$

$$+s^7\left(\frac{11}{\beta^3}-\frac{433}{\beta}+1491\beta-875\beta^3+70\beta^5\right)\eta^2$$

$$+s^6\left(\frac{6}{\beta^2}-114+170\beta^2-30\beta^4\right)\eta^3$$

$$+s^5\left(\frac{1}{\beta}-10\beta+5\beta^3\right)\eta^4\Big]\frac{1}{t^4}+\ldots\ldots\ldots\ldots \quad (2)$$

If the argument is taken along the "semi-imaginary" axis, *i. e.*, $\theta=\frac{\pi}{4}$,

$$s=\frac{1}{\sqrt{2}} \text{ and } \beta=\cos\frac{\pi}{4}-i\sin\frac{\pi}{4}=\frac{1-i}{\sqrt{2}}.$$

To take an extreme case, viz., to find $\log_e\Gamma(1+i)$ from the asymptotic series, $z=1+i$, $\nu=\sqrt{2}$,

$$\log_e z=\frac{1}{2}\log_e 2+i\frac{\pi}{4}, \quad t=2\pi\sqrt{2};$$

whence $r=5$ and $\eta=0\cdot114$. Substituting these values in (2), the converging factor is found to be approximately $0\cdot52+0\cdot50i$, and the product of this and the term

$$\frac{B_5}{90z^9}, \ [=0\cdot0^4263(1-i)]$$

is $$0\cdot0^4427-0\cdot0^400 : i.$$

The sum of the series up to the B_4 term is

$$-0\cdot650948-0\cdot301637 : i.$$

Adding the above product, we get the value of $\log_e\Gamma(1+i)$, about two units in error in the sixth place of decimals, viz.,

$$\log_e\Gamma(1+i)=-0\cdot650921-0\cdot301638i.$$

Naturally, with this very small value of z, only one or two decimal places can be added to the result.

Gauss [11] calculated $\log_e\Gamma(1+i)$ to seven places of decimals from $\log_e\Gamma(11+i)$, using, apparently, Stirling's Series as far as the term $\frac{B_3}{30z^5}$, B_3 being the least

Bernoullian number. The difference equation gave the value of

$$\log_{10}\Pi(i)=\bar{1}\cdot 7173075-17^\circ\,16'\,57''\cdot 693i,$$

or $$\log_e\Gamma(1+i)=-0\cdot 6509235:-0\cdot 3016399i.$$

When $z=10+i$ the asymptotic series may be used as far as $\frac{B_{32}}{63.64z^{63}}$, which is approximately equal to $0\cdot 0^{28}4$, *i. e.*, with an accuracy of some 27 decimal places.

Confluent Hypergeometric Function.

This function $M(\alpha.\gamma.x)$ is closely related to the exponential integral, and is defined by the series

$$M(\alpha.\gamma.x)=1+\frac{\alpha}{\gamma}x+\frac{\alpha(\alpha+1)}{\gamma(\gamma+1)}\cdot\frac{x^2}{2!}+\frac{\alpha(\alpha+1)(\alpha+2)}{\gamma(\gamma+1)(\gamma+2)}\cdot\frac{x^3}{3!}+\cdots,$$

satisfying the differential equation

$$x.\frac{d^2y}{dx^2}+(\gamma-x).\frac{dy}{dx}-\alpha.y=0.$$

Attention has been drawn to the importance of this function [12] in the solution of differential equations of the second order, *e. g.*,

$$\frac{d^2y}{dx^2}+(px+q)\frac{dy}{dx}+(lx^2+mx+n)y=0,$$

$$\frac{d^2y}{dx^2}+\left(p+\frac{q}{x}\right)\frac{dy}{dx}+\left(l+\frac{m}{x}+\frac{n}{x^2}\right)y=0,$$

and Laplace's equation

$$(a_2+b_2x)\frac{d^2y}{dx^2}+(a_1+b_1x)\frac{dy}{dx}+(a_0+b_0x)y=0.$$

The function plays an important rôle in the solution of many physical problems, such diverse problems as the deflexion of electrons, collision of proton and neutron, hyperfine structure, and the positron theory, and it has been stated that for the further development of the quantum theory the main gaps are those which seem likely to be filled by more accurate numerical computations.

The asymptotic expansion of $\mathrm{M}(\alpha.\gamma.x)$ is

$$\frac{\Gamma(\gamma)}{\Gamma(\gamma-\alpha)}.(-x)^{-\alpha}\left\{1-\frac{\alpha(\alpha-\gamma+1)}{x}+\frac{\alpha(\alpha+1)(\alpha-\gamma+1)(\alpha-\gamma+2)}{2!\,x^2}-\dots\right\}$$

$$+\frac{\Gamma(\gamma)}{\Gamma(\alpha)}e^{x}x^{\alpha-\gamma}\left\{1+\frac{(1-\alpha)(\gamma-\alpha)}{x}+\frac{(1-\alpha)(2-\alpha)(\gamma-\alpha)(\gamma-\alpha+1)}{2!\,x^2}+\dots\right\}.$$

Among the functions which can be expressed in terms of the confluent hypergeometric function there are :

Incomplete gamma function

$$\gamma(n,x)=\int_0^x e^{-t}t^{n-1}dt=\frac{1}{n}.e^{-x}.x^{n}\mathrm{M}(1,n+1,x).$$

Integrals of the type

$$\int_0^x e^{-a^m x^m}dx=x\mathrm{M}\left(\frac{1}{m},\frac{m+1}{m},-a^m x^m\right).$$

Laguerre function

$$\mathrm{L}_p^q(x)=\frac{\Gamma(q+p+1)}{\Gamma(p+1)\,\Gamma(q+1)}.\mathrm{M}(-p,q+1,x).$$

Bessel functions, imaginary argument

$$\Gamma\left(\frac{\gamma+1}{2}\right).\mathrm{I}_{\frac{\gamma-1}{2}}\left(\frac{x}{2}\right)=2^{1-\gamma}.e^{-\frac{x}{2}}.x^{\frac{\gamma-1}{2}}.\mathrm{M}(\tfrac{1}{2}\gamma,\gamma,x).$$

Bessel functions, real argument

$$\mathrm{J}_\nu(x)+i\mathrm{Y}(x)=\left(\frac{x}{2}\right)^{\nu}\frac{e^{-ix}}{\Gamma(\nu+1)}.\mathrm{M}(\nu+\tfrac{1}{2},2\nu+1,2ix),$$

and the ω function of Cunningham [13], an important generalization of the Hermite functions. The differential equation of $\omega_{n,m}(\xi)$ is

$$\xi\frac{d^2y}{d\xi^2}+(\xi+1+m)\frac{dy}{d\xi}+\left(n+1+\frac{m}{2}\right)y=0,$$

the solution of which is

$$\mathrm{M}\left(n+1+\frac{m}{2},m+1,-\xi\right)\text{ or }e^{-x}\mathrm{M}\left(\frac{m}{2}-n,m+1,\xi\right).$$

Incomplete Gamma Function.

The asymptotic expansion of this function

$$\int_z^\infty t^{r-1} e^{-t}\, dt$$

is

$$z^{r-1}e^{-z}\left\{1-\frac{1-r}{z}+\frac{(1-r)(2-r)}{z^2}\cdots\right.$$
$$\left.(-)^{n-1}\frac{(1-r)(2-r)\ldots(n-1-r)}{z^{n-1}}\times\text{C.F.}\right\}.$$

The variable z, r, and n (an integer) being known, if we put $n-r=m$ and $z=m+h$, both m and h can be found; h is a small quantity between -1 and $+1$. Thus if $z=4$, and $r=\frac{3}{4}$, then, if $n=5$, $m=\frac{17}{4}$ and $h=-\frac{1}{4}$. The converging factor in this particular case is found by the foregoing method to be of the same form as that of the exponential integral for real values of the variable, viz.,

$$\frac{1}{2}+\frac{1}{4m}\left(\frac{1}{2}+h\right)-\frac{1}{8m^2}\left(\frac{1}{4}+\frac{h}{2}+h^2\right)-\frac{1}{16m^3}\left(\frac{1}{8}+\frac{h}{4}-h^3\right)$$
$$+\frac{1}{32m^4}\left(\frac{13}{16}+\frac{13h}{8}+\frac{7h^2}{4}+h^3-h^4\right)-\ldots$$

The converging factor in the three cases where $h=-\frac{1}{4}, -\frac{1}{2}, -\frac{3}{4}$ are

$$h=-\frac{1}{4};\ \frac{1}{2}+\frac{1}{4.4m}-\frac{3}{16.8m^2}-\frac{5}{64.16m^3}+\frac{127}{256.32m^4}$$
$$-\frac{943}{1024.64m^5}-\frac{2643}{4096.128m^6}+\frac{190907}{16384.256m^7}\cdots,$$

$$h=-\frac{1}{2};\ \frac{1}{2}-\frac{1}{4.8m^2}-\frac{1}{8.16m^3}+\frac{1}{4.32m^4}-\frac{21}{32.64m^5}$$
$$-\frac{23}{64.128m^6}+\frac{229}{32.256m^7}\cdots;$$

$$h=-\frac{3}{4};\ \frac{1}{2}-\frac{1}{4.4m}-\frac{7}{16.8m^2}-\frac{23}{64.16m^3}-\frac{41}{256.32m^4}$$
$$-\frac{841}{1024.64m^5}-\frac{2479}{4096.128m^6}+\frac{64225}{16384.256m^7}\cdots$$

Use was made of these formulæ in computing the integrals

$$\int_x^\infty x^{-\alpha}e^{-x}\,dx, \quad \alpha=\frac{1}{4},\ \frac{1}{2},\ \frac{3}{4}$$

required in the construction of tables of the radiation integrals $\int_x^\infty \frac{dx}{x^a(e^x-1)}$.

For $\int_4^\infty x^{-\frac{1}{4}}e^{-x}\,dx$ the converging factor is 0·51338, thus increasing the accuracy of the result by five places of decimals; the value of the integral so found is 0·0123 1169, with a possible error of a unit in the eighth place of decimals. From Pearson's table [14] of the incomplete gamma function this value is approximately 0·0123 1167 :

In the example just given ν is real, but the converging factor can also be applied in the case where ν is imaginary, *e. g.*, in calculating $\mathrm{M}(i,\ 1+i,\ -x)$, of which the expansion is

$$\frac{\Gamma(1+i)}{x^i}-\frac{i}{xe^x}\left[1-\frac{1-i}{x}+\frac{(1-i)(2-i)}{x^2}-\frac{(1-i)(2-i)(3-1)}{x^3}+\ldots\right].$$

If $x=4$, $r=i$, and $n=4$, $m=4-i$, $h=i$, and $\frac{1}{m}=\frac{4+i}{17}$.

Making these substitutions, the converging factor is

$$\frac{1}{2}+\frac{2+9i}{136}+\frac{61-6i}{9248}+\frac{3454+2555i}{314432}-\frac{7393+5830i}{42672752}-\ldots$$
$$=0\cdot5321+0\cdot0735i.$$

Therefore

$$1-\frac{1-i}{4}+\frac{(1-i)(2-i)}{16}-\frac{(1-i)(2-i)(3-i)}{64}\times\text{C.F.}$$
$$=(0\cdot8125-0\cdot0115)+(0\cdot0625+0\cdot0831:)\,i$$
$$=0\cdot8010+0\cdot1456:i.$$

Also $\Gamma(1+i)=0\cdot49801:-0\cdot15495i,$

and $4^{-i}=0\cdot183457-0\cdot983028i$ [15].

Whence

$$\mathrm{M}(i,\ 1+i,\ -4)=-0\cdot06029-0\cdot52166i.$$

From the series in ascending powers of x,

$$\mathrm{M}(i,\ 1+i,\ -4) = -0{\cdot}060296 - 0{\cdot}521665i.$$

Integrals $\int_0^x e^{-a^m x^m} dx$.

Integrals of the above type include the Error Function, which has been extensively tabulated [16], and the integral $\int_0^x e^{-x^4} dx$, which appears in electrical conductivity problems in gases [17]. In connexion with this integral the asymptotic series is given in the form ($\lambda = x^4$),

$$\frac{\Gamma\left(\frac{5}{4}\right)}{x} - \frac{1}{4\lambda} \cdot e^{-\lambda}\left[1 - \frac{3}{(2x^2)^2} + \frac{3{\cdot}7}{(2x^2)^4} - \cdots\cdots \pm \frac{3 \cdot 7 \cdot 11 \ldots (4n-1)}{(2x^2)^{2n}}(1-\theta)\right],$$

with the remark that the ratio of two consecutive terms is $\frac{4n-1}{2x^2}$, which for sufficiently large values of n increases without limit. When x is large ($n < x^4$) the resulting error is less than the last calculated term. Since the general integral is equal to

$$x\mathrm{M}\left(\frac{1}{m},\ \frac{m+1}{m},\ -a^m x^m\right),$$

$$\gamma - \alpha = 1 \text{ and } \alpha - \gamma + 1 = 0 \text{ in } \mathrm{M}(\alpha . \gamma . x),$$

with the result that only the first term, unity, remains in the first asymptotic series. When

$$x = 1{\cdot}5,\ \ x^4 = \rho + h = 5{\cdot}0625,\ \ r = \tfrac{1}{4},$$

the integral may be computed with an accuracy of 8 or 9 places of decimals. If

$$n = 5,\ \rho = 4{\cdot}75 \text{ and } h = 0{\cdot}3125,$$

or

$$n = 6,\ \rho = 5{\cdot}75 \text{ and } h = -0{\cdot}6875,$$

and the converging factor can be computed from the series in the preceding section

$$\frac{1}{2} + \frac{1}{4\rho}\left(\frac{1}{2} + h\right) - \frac{1}{8\rho^2}\left(\frac{1}{4} + \frac{h}{2} + h^2\right) - \ldots$$

to five or six decimals, giving for the value of the integral

$$0{\cdot}9995\ 4149:$$

Laguerre Function $L_p^q(z)$.

Among the numerous physical problems, into the solution of which the Laguerre function enters, may be mentioned the theory of scattering of protons by protons, photoelectric absorption for X-rays, cosmic ray absorption, vibrational isotope effect, and Coulomb wave functions in repulsive fields [18].

In the last case the Laguerre function expressed in terms of the confluent hypergeometric function is proportional to

$$M(L+1-i\eta,\ 2L+2,\ 2i\rho);$$

the regular solution of the differential equation

$$\frac{d^2M}{d\rho^2}+\left\{1-\frac{2\eta}{\rho}-\frac{L(L+1)}{\rho^2}\right\}M=0$$

is $$e^{-i\rho}.\rho^{L+1}.M(L+1-i\eta,\ 2L+2,\ 2i\rho).$$

For the regions of small energy, η large, by change of variables $M=\zeta f$ and $\zeta=i(8\rho\eta)^{\frac{1}{2}}$, the differential equation becomes

$$\left[\frac{d^2}{d\zeta^2}+\frac{1}{\zeta}\frac{d}{d\zeta}+1-\frac{(2L+1)^2}{\zeta^2}+\frac{\zeta^2}{16\eta^2}\right]f=0.$$

If the term $\frac{\zeta^2}{16\eta^2}$ is neglected the differential equation is that of the ordinary Bessel function.

For the Laguerre function $L_n(u)$ Sommerfeld [19] has given the following expression:

$$L_n(u)=e^{i\pi n}\left[\frac{u^n}{\Gamma(1+n)}-\frac{n}{u}\cdot\frac{e^u(-u)^{-n}}{\Gamma(1-n)}\right],$$

which is equivalent to taking only the first terms, unity, in the two asymptotic series of $M(-n,\ 1,\ x)$. The numerical results obtained from this formula are considerably in error and of little practical value. Sexl [20]

had previously included three or four terms in the asymptotic series, viz.:

$$L_n(u) = \frac{e^{i\pi n} u^n}{\Gamma(n+1)}\left[1 - \frac{n^2}{u} + \frac{n^2(n-1)^2}{2!\,u^2} - \dots\right]$$
$$- \frac{n}{u} e^{i\pi n} \frac{e^u (-u)^{-n}}{\Gamma(1-n)}\left[1 + \frac{(n+1)^2}{u} + \frac{(n+1)^2(n+2)^2}{u^2} + \dots\right].$$

This function may also be expressed in terms of an integral involving the Bessel function [21], $I_0(x\sqrt{u})$, and also in terms of the Hankel Cylinder Functions [22] of order $\frac{1}{3}$ and $\frac{2}{3}$.

As an example of the application of the converging factor method calculate the value of $M(1-i,\ 2,\ 3i)$.

Now

$$M(1-i,\ 2,\ i\rho)$$
$$= \frac{\Gamma(2)}{\Gamma(1+i)} (-i\rho)^{-1+i} \left\{1 - \frac{(1-i)i}{i\rho} + \frac{(1-i)(2-i)(-i)(1-i)}{2!\,(i\rho)^2} - \dots\right\}$$
$$+ \frac{\Gamma(2)}{\Gamma(1-i)} e^{i\rho} (i\rho)^{-1-i} \left\{1 + \frac{i(1+i)}{i\rho} + \frac{i(1+i)(1+i)(2+i)}{2!\,(i\rho)^2} + \dots\right\},$$

and $$(-i\rho)^{-1+i} = \frac{i}{\rho} e^{\frac{\pi}{2}} (\cos \log_e \rho + i \sin \log_e \rho)$$

$$e^{\frac{\pi}{2}} = 4{\cdot}8104\ \ 7738$$

$$\frac{1}{\Gamma(1+i)} = 1{\cdot}8307444 + 0{\cdot}5696\ \ 076 : i,$$

and $$3^i = \cos \log_e 3 + i \sin \log_e 3$$
$$= 0{\cdot}4548\ \ 3242 + 0{\cdot}8905\ \ 7704i.$$

For the first asymptotic series of $M(1-i,\ 2,\ ir)$, if T_r is the term

$$\frac{(1-i)(2-i)\dots(r-i)(-i)(1-i)\dots(r-1-i)}{r!\,(ir)^r},$$

the C.F. in this case is, as far as the $\frac{1}{r^3}$ term,

$$\left(\frac{1}{2}+\frac{1}{4r}+\frac{1}{8r^2}+\frac{1}{16r^3}-\ldots\right)+\left(\frac{1}{2}+\frac{3}{4r}+\frac{1}{8r^2}-\frac{5}{16r^3}+\ldots\right)i,$$

and for the second asymptotic series the conjugate of this expression.

When $\rho=r=3$, $T_r=0{\cdot}18518 : +0{\cdot}06173i$,

and the C.F. $=0{\cdot}592+0{\cdot}758i$ approximately.

Their product is $0{\cdot}1769+0{\cdot}0628i$, and the two asymptotic series are, respectively, $1{\cdot}618 : -0{\cdot}267 : i$, $1{\cdot}618 : +0{\cdot}267 : i$. Finally, $M(1-i,\ 2,\ 3i)=0{\cdot}186+2{\cdot}621i$, compared with the value from the ascending series $0{\cdot}1859+2{\cdot}6217i$.

The value of the function calculated from the asymptotic series as far as the least term is $0{\cdot}260+3{\cdot}662 : i$, and using the first term only of the two series, $0{\cdot}043+0{\cdot}611i$, which bears no relation to the true value of the function.

It may be of interest to set down the values for L=0 as in the above example, L=1, L=2.

$$M(1-i,\ 2,\ 3i)=0{\cdot}1859\ \ 1843 : +2{\cdot}6217\ \ 1393i,$$

$$M(2-i,\ 4,\ 3i)=0{\cdot}1168\ \ 0548 : +1{\cdot}6471\ \ 2320i,$$

$$M(3-i,\ 6,\ 3i)=0{\cdot}0986\ \ 1954+1{\cdot}3906\ \ 7558i\ [23].$$

Bessel Functions, $K_\nu(z)$, $J_\nu(z)$.

(*a*) The asymptotic expansion of $K_\nu(z)$ may be written in the form

$$\sqrt{\frac{\pi}{2z}}\cdot e^{-z}\left\{1+\frac{4\nu^2-1}{8z}+\ldots\right.$$
$$\left.\frac{(4\nu^2-1)(4\nu^2-9)\ldots[4\nu^2-(4n-1)^2]}{(2n)!\,(8z)^{2n}}\times\text{C.F.}\right\},$$

and the converging factor then becomes

$$1+\frac{[4\nu^2-(4n+1)^2]}{(2n+1)8z}+\frac{[4\nu^2-(4n+1)^2][4\nu^2-(4n+3)^2]}{(2n+1)(2n+2)(8z)^2}+\ldots$$

If z is real and equal to $n+h$, writing $\gamma=\frac{1-4\nu^2}{4}$, and

carrying out the summations as in the previous examples, the factor simplifies to

$$\frac{1}{2}+\frac{1}{4n}\left(\frac{1}{4}+h\right)-\frac{1}{16n^2}\left(\frac{1}{8}+\frac{h}{2}+2h^2+\gamma\right)$$
$$-\frac{1}{64n^3}\left(\frac{1}{16}+\frac{h}{4}-4h^3-\frac{\gamma}{2}\right)\ldots$$

Similar but more complicated factors occur when z is complex. If $z=(n+h)e^{2i\theta}$, the first three terms of the real and imaginary parts of the converging factor, f $\sigma=\sec\theta$, $\tau=\tan\theta$, and γ as before is $\frac{1-4\nu^2}{4}$,

$$\frac{1}{2}+\frac{\sigma^2}{16n}(1+4h)-\frac{\sigma^2}{128n^2}\{2\sigma^2(1+4h)$$
$$+(8\gamma-1+3\tau^2-4h+4h\tau^2+16h^2)\}\ldots$$
$$+i\tau\left[\frac{1}{2}-\frac{\sigma^2}{16n}+\frac{\sigma^2}{128n^2}\{2\sigma^2-(3-\tau+8h+16h^2)\}\ldots\right].$$

For $z=5e^{i\frac{\pi}{4}}$, the argument taken along the semi-imaginary axis, $\theta=\frac{\pi}{8}$ and

$$\text{Ker}\,(5)+i\,\text{Kei}\,(5)=-0{\cdot}0115117+0{\cdot}0111876i.$$

(*b*) The two Bessel functions of fractional order $J_{\pm\frac{1}{4}}(x)$ are given by

$$J_{\frac{1}{4}}(x)=\sqrt{\frac{2}{\pi x}}\left[P_{\frac{1}{4}}(x).\sin\left(x+\frac{\pi}{8}\right)+Q_{\frac{1}{4}}(x).\cos\left(x+\frac{\pi}{8}\right)\right],$$

$$J_{-\frac{1}{4}}(x)=\sqrt{\frac{2}{\pi x}}\left[P_{-\frac{1}{4}}(x).\cos\left(x-\frac{\pi}{8}\right)-Q_{-\frac{1}{4}}(x)\sin\left(x-\frac{\pi}{8}\right)\right]$$

When x is an integer, n and $\gamma=\frac{1-4\nu^2}{4}$,

$$CF_P=\frac{1}{2}+\frac{1}{8n}-\frac{1}{4n^2}\left(\frac{3}{8}+\frac{\gamma}{2}\right)+\frac{1}{8n^3}\left(\frac{13}{16}+\frac{\gamma}{2}\right)$$
$$-\frac{1}{16n^4}\left(\frac{59}{32}-\frac{7\gamma}{8}-\frac{\gamma^2}{4}\right)+\frac{1}{32n^5}\left(\frac{185}{64}-\frac{57\gamma}{8}-\frac{3\gamma^2}{2}\right)\ldots.$$

and

$$\mathrm{CF_Q} = \frac{1}{2} + \frac{3}{8n} - \frac{1}{4n^2}\left(\frac{3}{8} + \frac{\gamma}{2}\right) - \frac{1}{8n^3}\left(\frac{1}{16} + \frac{\gamma}{2}\right)$$

$$+ \frac{1}{16n^4}\left(\frac{61}{32} + \frac{23\gamma}{8} + \frac{\gamma^2}{4}\right) - \frac{1}{32n^5}\left(\frac{709}{64} + \frac{41\gamma}{8} + \gamma^2\right)\ldots,$$

when

$$n=5, \quad \mathrm{CF_P}=0{\cdot}52107, \quad \mathrm{CF}=0{\cdot}57028,$$

$$\mathrm{P}_{\pm\frac{1}{4}}(5)=0{\cdot}99805\ 88187:, \quad \mathrm{Q}_{\pm\frac{1}{4}}(5)=-0{\cdot}01836\ 83506:$$

$$\text{Bracket } (\mathrm{J}_{\frac{1}{4}})=-0{\cdot}78742\ 29801.$$

$$\text{Bracket } (\mathrm{J}_{-\frac{1}{4}})=-0{\cdot}12295\ 81443,$$

and

$$\mathrm{J}_{\frac{1}{4}}(5)=-0{\cdot}28097\ 20667,$$

$$\mathrm{J}_{-\frac{1}{4}}(5)=-0{\cdot}04387\ 45181.$$

(*c*) The calculation of the ber, bei functions proceeds on similar lines.

$$\mathrm{I}_0(x\sqrt{i}) = \mathrm{ber}\ x + i\ \mathrm{bei}\ x$$

$$= \frac{e^{x/\sqrt{2}}}{\sqrt{2\pi x}}\left\{\cos\left(\frac{x}{\sqrt{2}} - \frac{\pi}{8}\right) + i\sin\left(\frac{x}{\sqrt{2}} - \frac{\pi}{8}\right)\right\}$$

$$\times\left\{\mathrm{P}_0\left(xe^{-\frac{i\pi}{4}}\right) + i\mathrm{Q}_0\left(xe^{-\frac{i\pi}{4}}\right)\right\}$$

$$+ \frac{ie^{-x/\sqrt{2}}}{\sqrt{2\pi x}}\left\{\cos\left(\frac{x}{\sqrt{2}} + \frac{\pi}{8}\right) - i\sin\left(\frac{x}{\sqrt{2}} + \frac{\pi}{8}\right)\right\}$$

$$\times\left\{\mathrm{P}_0\left(xe^{-\frac{i\pi}{4}}\right) - i\mathrm{Q}_0\left(xe^{-\frac{i\pi}{4}}\right)\right\}.$$

The second term is no other than $\frac{i}{\pi}$ (Ker $x + i$ Kei x), which was, by most mathematicians, including Kummer and Kirchhoff, regarded as a negligible series. This term must be retained, not on account of any question of symmetry, but because it forms an essential part of the function. No amount of manipulation of the remainder of the first series will compensate for the neglect of the second series. Through the omission of the so-called

negligible series the first zero of ber x is erroneously given as 2·835, instead of the value, correct to three places, 2·849. Tables of sin, cos, sinh and cosh $\frac{x}{\sqrt{2}}$ to twelve places have been constructed over the range 0·0 to 20·0 by 0·1 intervals [24].

The series $P_\nu(z)$ may be written as

$$1-\frac{(4\nu^2-1)(4\nu^2-9)}{2!\,(8z)^2}+\frac{(4\nu^2-1)(4\nu^2-9)(4\nu^2-25)(4\nu^2-49)}{4!\,(8z)^4}$$

$$+(-)^n\frac{(4\nu^2-1)(4\nu^2-9)\ldots[4\nu^2-(4n-3)^2][4\nu^2-(4n-1)^2]}{(2n)!\,(8z)^{2n}}$$

$$\times \text{C.F.}_P.$$

Put $z=(n+h)e^{i\theta}$, $\frac{1-4\nu^2}{4}=\gamma$, $\sigma=\sec\theta$, and $\alpha=e^{i\theta}$, the converging factor C.F.$_P$ becomes

$$\frac{\sigma}{2}\alpha-\frac{\sigma}{2n}\left[\frac{\sigma^2}{8}(\alpha-3\alpha^{-1})-h\sigma\right]$$

$$-\frac{\sigma^2}{4n^2}\left[\frac{\gamma}{2}-\frac{\sigma^3}{32}(11\alpha-30\alpha^{-1}+7\alpha^{-3})\right.$$

$$\left.-\frac{h\sigma^2}{4}(\alpha^2-8+3\alpha^{-2})+\frac{h^2\sigma}{2}(3\alpha-\alpha^{-1})\right]$$

$$+\frac{\sigma^3}{8n^3}\left[\frac{\sigma\gamma}{8}(\alpha^2+8-5\alpha^{-2})+h\gamma(\alpha-\alpha^{-1})\right.$$

$$+\frac{\sigma^4}{128}(6\alpha^3-183\alpha+511\alpha^{-1}-245\alpha^{-3}+15\alpha^{-5})$$

$$-\frac{h\sigma^3}{16}(22\alpha^2-123+88\alpha^{-2}-7\alpha^{-4})$$

$$\left.-\frac{3h^2\sigma^3}{8}(\alpha^3-15\alpha+15\alpha^{-1}-\alpha^{-3})+2h^2\sigma(\alpha^2-1)\right]+\ldots.$$

Similarly, if $Q_\nu(z)$ is written in the form

$$\frac{4\nu^2-1}{8z}-\frac{(4\nu^2-1)(4\nu^2-9)(4\nu^2-25)}{3!\,(8z)^3}+\ldots$$

$$+(-)^{n-1}\frac{(\nu^2-1)(4\nu^2-9)\ldots[4\nu^2-(4n-5)^2][4\nu^2-(4n-3)^2]}{(2n-1)\,!\,(8z)^{2n-1}}$$

$$\times \text{C.F.}_Q,$$

with the same notation, the converging factor C.F.$_Q$ is

$$\frac{\sigma}{2}\alpha+\frac{\sigma}{2n}\left[\frac{\sigma^2}{8}(\alpha+5\alpha^{-1})+h\sigma\right]$$

$$-\frac{\sigma^2}{4n^2}\left[\frac{\gamma}{2}+\frac{\sigma^3}{32}(\alpha+30\alpha^{-1}-19\alpha^{-3})\right.$$

$$\left.+\frac{h\sigma^2}{4}(\alpha^2+8-5\alpha^{-2})+\frac{h^2\sigma}{2}(3\alpha-\alpha^{-1})\right]$$

$$+\frac{\sigma^3}{8n^3}\left[\frac{\sigma\gamma}{8}(\alpha^2+4-9\alpha^{-2})+h\gamma(\alpha-\alpha^{-1})\right.$$

$$-\frac{\sigma^4}{128}(2\alpha^3+29\alpha-413\alpha^{-1}+455\alpha^{-3}-65\alpha^{-5})$$

$$-\frac{h\sigma^3}{16}(2\alpha^4+87\alpha^2-136+19\alpha^{-2})$$

$$\left.+\frac{h^2\sigma^2}{8}(3\alpha^3+35\alpha-59\alpha^{-1}+5\alpha^{-3})+2h^3\sigma(\alpha^2-1)\right]+\ldots$$

For the ber, bei functions,

$$\theta=-\frac{\pi}{4},\ \sigma=\sqrt{2},\ \alpha=e^{i\theta},\ \gamma=\frac{1}{4},$$

the converging factors become

$$\text{C.F.}_P=\left(\frac{1}{2}+\frac{1}{4n}-\frac{7}{8n^2}+\frac{71}{16n^3}-\ldots\right)$$

$$+\left(-\frac{1}{2}+\frac{1}{2n}-\frac{17}{16n^2}+\frac{13}{4n^3}-\ldots\right)i,$$

$$\text{C.F.}_Q=\left(\frac{1}{2}+\frac{3}{4n}-\frac{13}{8n^2}+\frac{49}{8n^3}-\ldots\right)$$

$$+\left(-\frac{1}{2}+\frac{1}{2n}-\frac{5}{16n^2}-\frac{3}{4n^3}+\ldots\right)i.$$

With the help of these converging factors the first term of $I_0(5\sqrt{i})$ can be calculated to about six places of decimals, viz.,

$$-6{\cdot}226519+0{\cdot}119697i,$$

to which must be added the product of $\frac{i}{\pi}$ and the " negligible " series,

$$-0{\cdot}0035611-0{\cdot}0036643i,$$

giving the result

$$\mathrm{I}_0(5\sqrt{i})=\mathrm{ber}\ 5+i\ \mathrm{bei}\ 5=-6{\cdot}230080+0{\cdot}116033i,$$

the error being one or two units in the last place.

(*d*) Bessel functions, imaginary order, occur, of course, much less frequently in physical problems than those of real order. Böcher [25] found the potential within a solid bounded by two coaxial cylinders and four planes, two through the axis of the cylinders and two perpendicular to this axis, involving, under special conditions, Bessel functions whose order or index is imaginary, whilst functions whose order is complex and argument real are required in the investigation of the De Sitter universe.

The Bessel function of imaginary order $\mathrm{J}_i(x)$ for $x=4$ has been computed from the series in ascending powers of x and from the asymptotic series.

$$\mathrm{J}_i(x)=\left(\frac{2}{\pi x}\right)^{\frac{1}{2}}\left[\mathrm{P}_i(x)\cos\left(x-\frac{2i+1}{4}\pi\right)\right.$$
$$\left.-\mathrm{Q}_i(x)\sin\left(x-\frac{2i+1}{4}\right)\pi\right],$$

where

$$\mathrm{P}_i(x)=1-\frac{5.13}{2!\,(8x)^2}+\frac{5.13.29.53}{4!\,(8x)^4}-$$

and

$$\mathrm{Q}_i(x)=-\frac{5}{8x}+\frac{5.13.29}{3!\,(8x)^3}-\frac{5.13.29.53.85}{5!\,(8x)^5}+\ldots.$$

When x is an integer, as in this example, the converging factor for $\mathrm{Q}_i(n)$ is

$$\frac{1}{2}+\frac{3}{8n}-\frac{1}{4n^2}\left(\frac{3}{8}+\frac{\gamma}{2}\right)-\frac{1}{8n^3}\left(\frac{1}{16}+\frac{\gamma}{2}\right)$$
$$+\frac{1}{16n^4}\left(\frac{61}{32}+\frac{23\gamma}{8}+\frac{\gamma^2}{4}\right)-\frac{1}{32n^5}\left(\frac{709}{64}+\frac{41\gamma}{8}+\gamma^2\right)\ldots,$$

and for $P_i(n)$

$$\frac{1}{2}+\frac{1}{8n}-\frac{1}{4n^2}\left(\frac{3}{8}+\frac{\gamma}{2}\right)+\frac{1}{8n^3}\left(\frac{13}{16}+\frac{\gamma}{2}\right)$$
$$-\frac{1}{16n^4}\left(\frac{59}{32}-\frac{7\gamma}{8}-\frac{\gamma^2}{4}\right)+\frac{1}{32n^5}\left(\frac{185}{64}-\frac{57\gamma}{8}-\frac{3\gamma^2}{2}\right)\cdots,$$

and $\gamma=\frac{1-4\nu^2}{4}=\frac{5}{4}$, when $\nu=i$ and for $n=4$,

$$C.F_Q=0{\cdot}5776 \quad \text{and} \quad C.F_P=0{\cdot}5182.$$

The last term of the Q series is

$$+0{\cdot}0010\ 6043,$$

and of the P series

$$+0{\cdot}0009\ 4859:$$

$$P_i(4)=+0{\cdot}9713501 \text{ and } Q_i(4)=-0{\cdot}1481589.$$

Finally

$$J_i(4)=-0{\cdot}9805664+0{\cdot}070697i,$$

the value $-0{\cdot}9805664+0{\cdot}070695i$ being obtained from the ascending series. If the calculation is carried as far as the least term the result is

$$J_i(4)=-0{\cdot}9801+0{\cdot}0712i.$$

The Bessel function of imaginary order and complex argument $J_i\left(4e^{\frac{i\pi}{4}}\right)$ has also been computed by both methods.

From the ascending series

$$J_i\left(4e^{\frac{i\pi}{4}}\right)=-0{\cdot}51967-0{\cdot}52763i.$$

For the asymptotic series the converging factors are

P series : $\left(\frac{1}{2}+\frac{1}{4n}-\frac{9}{8n^2}+\frac{79}{16n^3}\cdots\right)$
$$+\left(\frac{1}{2}-\frac{1}{2n}+\frac{17}{16n^2}-\frac{23}{8n^3}\cdots\right)i,$$

Q series : $\left(\frac{1}{2}+\frac{3}{4n}-\frac{15}{8n^2}+\frac{107}{32n^3}\cdots\right)$
$$+\left(\frac{1}{2}-\frac{1}{2n}+\frac{5}{16n^2}+\frac{11}{8n^3}\cdots\right)i.$$

The last term of the P series is real and equal to

$$0{\cdot}0009486 \text{ with converging factor } 0{\cdot}57+0{\cdot}40i,$$

the last term of the Q series is complex and equal to $0{\cdot}0007498\ (1+i)$ with converging factor $0{\cdot}62+0{\cdot}41i$.

The final result gives

$$J_i\left(4e^{\frac{i\pi}{4}}\right) = -0{\cdot}51970-0{\cdot}52764 : i,$$

and without the converging factor

$$-0{\cdot}51909-0{\cdot}52690i.$$

The " converging factor " method has been extensively employed in the construction of tables of Bessel, Neumann and other functions for the Mathematical Tables Committee of the British Association.

Neumann functions [26] or Bessel functions of the second kind, of zero and unit orders : $G_0(x)$ and $G_1(x)$.

Bessel functions, $Y_0(x)$ and $Y_1(x)$ according to Neumann's definition [27].

Lommel-Weber functions [28] $\Omega_0(x)$, $\Omega_1(x)$, $\Omega_{\frac{1}{2}}(x)$, and $\Omega_{-\frac{1}{2}}(x)$ where asymptotic series such as

$$B_0(x) = \frac{1}{x} - \frac{1}{x^3} + \frac{3^2}{x^5} - \frac{3^2 5^2}{x^7} + \ldots,$$

$$B_{\frac{1}{2}}(x) = \frac{1}{x}\left\{1 - \frac{1\cdot 3}{(2x)^2} + \frac{1.3.5.7}{(2x)^4} - \frac{1.3.5.7.9.11}{(2x)^6} + \ldots\right\},$$

have to be calculated.

Confluent hypergeometric function [29], $M(\alpha.\gamma.x)$ for various values of the parameters, α and γ.

Exponential, sine and cosine integrals [30].

Probability integral and its integrals [31].

References.

(1) J. W. L. Glaisher, " Tables of the Exponential Function," Trans. Camb. Phil. Soc. xiii. pt. 3, pp. 243–272 (1883).

(2) G. B. Airy, Trans. Camb. Phil. Soc. viii. pp. 596–599 (1849).

(3) J. W. L. Glaisher, Phil. Trans. Roy. Soc. clx. pp. 367–387 (1870).

(4) Rayleigh, ' Collected Works,' i. p. 190 (1874); Stokes, Math. and Physical Papers, ii. p. 337 (1883); Bromwich, ' Theory of Infinite Series,' first edition, pp. 262, 326; Borel, ' Séries divergentes,' p. 3; Schafheitlin, ' Theorie der Besselschen Funktionen,' pp. 51, 52.

(5) Stieltjes, 'Annales de l'École Norm Sup.' (3), t. 3, p. 201 (1886); a memoir which deserves to be much more widely known.

(6) Compare Bromwich (Reference 4), p. 303.

(7) A. Pannekoek, Monthly Notices, Roy. Astron. Soc. xcvi. pp. 789–792 (1936).

(8) Bauschinger, *Archiv. d. Math. u. Phys.* pp. 28–34 (1843).

(9) J. R. Airey, "Tables of the Exponential, Sine and Cosine Integrals," Report, Math. Tables Comm., British Assoc. (1927).

(10) Stieltjes, 'Acta Mathematica,' x. pp. 299–302 (1887), for sums of reciprocal powers.

(11) Gauss, ' Werke,' Band iii. p. 230. The calculation discovered in a note-book of date about 1847.

(12) H. A. Webb and J. R. Airey, " The Practical Importance of the Confluent Hypergeometric Function," Phil. Mag. xxxvi. pp. 129–141 (1918); J. R. Airey, Report of the Math. Tables Comm., British Assoc. (1926), (1927). Both reports include tables of the function for various values of the parameters, α and γ.

(13) E. Cunningham, Proc. Royal Soc. lxxxi. (1908).

(14) ' Tables of the Incomplete F Function,' edited by K. Pearson, His Majesty's Stationery Office, London.

(15) J. R. Airey, " Tables of $\sin \log_e x$ and $\cos \log_e x$," Phil. Mag. series 7, vol. xx. p. 731 (1935).

(16) Burgess, Trans. Roy. Soc. Edin. xxxix. pp. 257–321 (1898).

(17) Schumann, ' Elektrische Durchbruchfeldstärke von Gasen,' pp. 234–5 (Springer, Berlin); F. Emde, *Zeit. für angewandte Math. u. Mech.* Band xiv. Heft 6 (1934).

(18) Yost, Wheeler, and Breit, Phys. Rev. xlix. second series, p. 174 (1936).

(19) A. Sommerfeld, *Annalen d. Phys.* xi. p. 257 (1931); O. Scherzer, *Annalen d. Phys.* xiii. p. 137 (1932).

(20) T. Sexl, *Zeit. für Physik*, lvi. pp. 62–72 (1929), and lxxxi. p. 163 (1933).

(21) Epstein and Muskat, Proc. Nat. Acad. xv. p. 405 (1929).

(22) J. A. Gaunt, *Zeit. für Phys.* lix. p. 511 (1930).

(23) E. R. Wicher, ' Terrestrial Magnetism,' xli. p. 389 (1936), for the extension to the case $L=2$.

(24) J. R. Airey, " The Circular and Hyperbolic Functions, Argument $x/\sqrt{2}$," Phil. Mag. series 7, vol. xx. p. 721 (1935).

(25) Boole, Phil. Trans. Roy. Soc. p. 239 (1844); Hankel, *Math. Annalen*, i. (1869); Lommel, *Math. Annalen*, iii. pp. 481–486 (1871); Böcher, Annals of Mathematics, vi. pp. 137–160 (1892); Debye, *Münchener Sitzungsberichte*, xl. (1910); Emde u. Rühle, *Jahresber. d. Deutschen Math. Verein*, xliii. (1934).

(26) J. R. Airey, Report Math. Tables Comm., Brit. Assoc. 1913.

(27) J. R. Airey, Reports, 1914 and 1915.

(28) J. R. Airey, Reports, 1924 and 1925.

(29) J. R. Airey, Reports, 1926 and 1927.

(30) J. R. Airey, Reports, 1927 and 1928.

(31) J. R. Airey, Report, 1928.

LIII. *Geiger-Müller Counters for Radiochemical Investigations.* *By* F. T. Hamblin, *B.Sc., A.I.C., and* C. H. Johnson, *Ph.D., Department of Physical and Inorganic Chemistry, Bristol University* *.

THE study of chemical processes with the aid of artificially produced radioactive isotopes of common elements has led to interesting results, and promises to become a method of widespread application. The Geiger-Müller counter [1] affords an apparently simple means of obtaining quantitative data, but an inexperienced person is confronted with the difficulty that the literature [2] is mainly helpful to those who are already well acquainted with the technique. How should a normal counter behave? We are not aware of the existence of any publication which sets out to describe in sufficient detail the construction of a counting mechanism, to lay stress upon essential particulars, and to point out the numerous pitfalls in operation. This paper is an attempt to present a *complete* description of a basic counting apparatus which should enable anyone to reproduce it without difficulty. The electrical circuit is probably the simplest in common use and does not require shielding. The apparatus has a maximum counting speed of about 1200 per minute, and can therefore be safely employed to register β-ray impulses at *recorded* rates up to, say, four hundred a minute. Corrections must be applied for simultaneous arrivals. The smaller the rate of counting the greater the necessity for absolute reliability, and our experience proves that this can be attained by close attention to detail. A defective or insufficiently controlled counting mechanism will give rise to erroneous values for the decay periods of radio-elements, and this is undoubtedly responsible for much of the confusion existing at the present time. Another matter in need of airing is that workers are not always careful to state whether their results are corrected for coincident impulses, nor, when correct ions are made, the method employed.

* Communicated by C. H. Johnson, Ph.D.

Geiger-Müller Counters.

The counter consists of a closed metal casing maintained at a high negative potential with respect to a fine wire passing along its axis. An electron emitted by a radioactive substance enters the casing, ionizes the enclosed gas (usually air at low pressure), and produces a momentary discharge. The small impulse is amplified and automatically recorded. The highest efficiency is obtained by placing radioactive material symmetrically around the counter. This condition is best fulfilled in a cylindrical counter such as that described by Juliusburger,

Fig. 1.

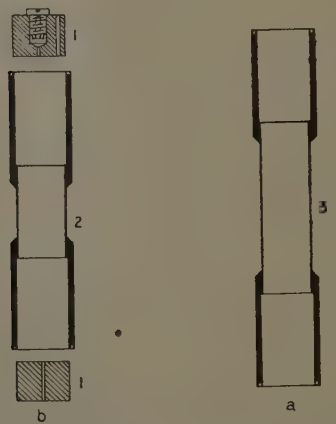

1, ebonite end-pieces; 2 and 3, counter casings.

Topley, and Weiss [3], made from seamless aluminium tubing. Our most successful counters were of similar design with important modifications (fig. 1).

The Casing.

"Duralumin" can be turned and polished more easily than aluminium, and was therefore used; before turning the 1-inch rod was rolled to close the pores. The overall length of the counter casing shown in fig. 1 (*a*) is 8·4 cm., and the length of the thin central portion (the window through which electrons enter) 3·0 cm.

The interior is recessed 2·2 cm. from each end, the internal diameter at the ends is 1·35 cm. and in the middle 1·30 cm. The wall thickness at the ends of the casing is 0·08 cm. The ebonite plugs are 1·1 cm. deep and the fine central holes 0·5 mm. diameter. The thread on the central brass screw must be coarse to avoid tearing the ebonite, *e. g.*, 1 BA; the screw is hollowed out and filled with solder. The counter casing shown in fig. 1 (*b*) is practically identical with fig. 1 (*a*), except that the window is only 0·9 cm. in length. The thickness of the window must not be less than 0·08 mm. or it buckles during subsequent evacuation. *So thin a window is seldom gas-tight.* Generally speaking a McLeod gauge is required to detect the leakage, which nevertheless is more likely than anything else to be the cause of rapid deterioration of the counter. A thicker window will stop a considerable proportion of the electrons. The remedy is to coat the thinnest window that may be used with shellac varnish, whereby the absorption of electrons is not materially increased. The composition of the shellac solution is 15 parts by weight of orange shellac and 1·5 of dibutyl phthalate (plasticizer) in about 150 parts of methylated spirits. It should be filtered before application. The casing is cleaned with warm alcohol and dried, a *thin* layer of almost boiling varnish laid on the window with a camel-hair brush and rotated over a hot-plate causing the shellac to set evenly upon the metal. It is then placed for one hour in an oven at about 90° C., at which temperature the shellac flows and hardens without crinkling. The process is repeated twice, with a final heat treatment of several hours' duration. A well-finished window is pale yellow and perfectly smooth. Before applying the varnish the casing is thoroughly cleaned with water, followed by immersion for some hours in hot absolute alcohol. *The polished interior must not be contaminated by grease or fluff.*

Ebonite End-pieces.

The resistance between the casing and the central wire must be much greater than that of the leak-resistance in the amplifying circuit, therefore the plugs through which the wire passes need to be made of *finest quality ebonite.* Several commercial grades of ebonite and other

synthetic materials proved unsatisfactory. The casing is recessed to support the plugs which fit the tube snugly (fig. 1). New plugs should be left to soak in absolute alcohol, and afterwards baked for two hours at 110° C. before use.

Preparation and Insertion of the Wire.

Tungsten wire, 0·045 mm. diameter, is suspended and gently passed between finger and thumb in order to detect irregularities. It may be necessary to reject

Fig. 2.

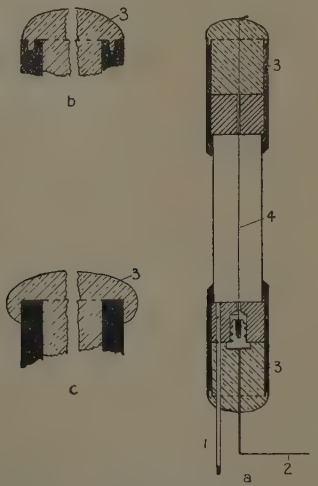

1, glass tube for evacuation of counter; 2, lead to circuit; 3, wax; 4, fine tungsten wire.

three or four feet in process of selecting a suitably smooth piece, say 4 in. long. The wire is held under tension and cautiously scrubbed with cotton-wool soaked in concentrated nitric acid, then with water until free from acid, and finally with alcohol. The brass screw in the ebonite end-piece (only one is so fitted) is removed, and a short length of copper-wire, 26 S.W.G., soldered to the head; a blob of solder is placed on the tip, and into th s is dipped one end of the tungsten wire. The

attachment will be firm provided the soldering iron is sufficiently hot, which is a point of importance, because the wire is eventually stretched taut and might become detached. A counter with a slack wire may respond to stimuli, but its "characteristics" (see later section) are impaired. Adhering dirt and flux are washed off the junction, the tungsten wire is again cleansed with alcohol and threaded through the fine hole in the centre of the ebonite plug; the brass piece is screwed home and the plug placed in the casing. At this stage a short length of tapered soft glass tubing is inserted in a narrow hole in the plug. The tubing is constricted above the tapered portion to facilitate sealing off and to prevent subsequent cracking around the seal. Through this tube the counter is later evacuated. It will be noted from fig. 2 (*a*) that neither the soldered tip of the brass screw nor the glass tube projects beyond the face of the ebonite inside the casing. Just-molten wax is poured on top of the plug and gently-warmed with a non-luminous flame. Care is taken in sealing the rim of the casing and around the protruding copper-wire and glass tube, *places where the wax is most likely to crack.* The wax having been allowed to set, the free end of the tungsten wire is passed through the other plug, which is then pushed into the casing; the counter is suspended by the wire, thus kept taut, and molten wax run in. The insulating properties of the wax can be ruined by overheating, *and for the same reason luminous or smoky flames should not be used.*

Wax.

The wax must be highly insulating and contain no volatile matter, should melt easily and yet not be so fluid as to penetrate into the interior of the counter. Cracks quickly develop if it is too soft or too brittle. Solubility in alcohol is desirable since this facilitates its removal when necessary. No commercial wax, that we could discover, satisfied all these requirements, but a mixture of rosin and beeswax, recommended by Juliusburger, Topley, and Weiss [3], is excellent. Two parts by weight of beeswax are heated at 120° C. for a short time *to expel water*, and five parts of powdered rosin are added gradually with stirring until homogeneous. The pale yellow product should be stored in a stoppered pyrex

tube. Narrow circular grooves are cut in both ends of the counter casing, fig. 2 (*b*), and filled with wax immediately after varnishing the window. By this means a wax-to-wax junction is provided near the very vulnerable edge, reducing the likelihood of cracks developing there and also avoiding the necessity of running wax over the edge, fig. 2 (*c*), a procedure [3] which lowers the efficiency of the counter by widening the air-space between the window and the vessel containing radioactive substance.

Evacuation.

This is effected by a pyrex glass apparatus consisting of a mercury diffusion-pump backed by a Hyvac oil-pump and McLeod gauge. A horizontal tube of soft glass, fitted with side tubes for attachment to counters projecting vertically downwards and a mercury manometer, is connected to the pumps and gauge by a ground-joint. For ease of manipulation it is convenient to employ soft glass tubing in the counters. A large cylindrical pyrex bulb containing P_2O_5 provides a reservoir of dry air which is filled through a train of P_2O_5 tubes. Well ground taps connect the various parts of the apparatus which performs several functions. *The gas-tightness of counters can be rigorously tested.* Evacuation for twelve hours or more at a pressure of 10^{-6} cm. is by far the most efficient method for removing traces of water. Ultimately the counters are filled with dry air at a pressure of $7{\cdot}5 \pm 0{\cdot}2$ cm. and sealed off. The complete removal of water from the interior of a counter is essential, because its presence gives rise to high "background" counts and to the phenomenon of "double-kicking," which will be described in later sections. Therefore leakage of air, however small, cannot be tolerated.

Mounting.

Various means were tried of clamping the counter in a vertical position, using gentle pressure on the casing for making contact with the H.T. batteries, but sooner or later, however light the pressure, the counter invariably sprang a leak.

The plan finally adopted with success was to support the counter in a cubical block of low-melting paraffin

wax and make the electrical connexion by means of a blob of mercury buried in the wax in contact with the casing (fig. 3). Before determining the " characteristics " of a newly completed counter *it must be put aside for at least twenty-four hours in order to settle down.* The operating voltage of the counter generally falls some 30 volts during the first twenty-four hours after sealing off, and then remains steady. Counters should be kept at an even temperature and protected from dust.

Electrical Circuit.

A valuable review of Geiger counter circuits has recently been compiled by Wynn Williams [4]. Ours

Fig. 3.

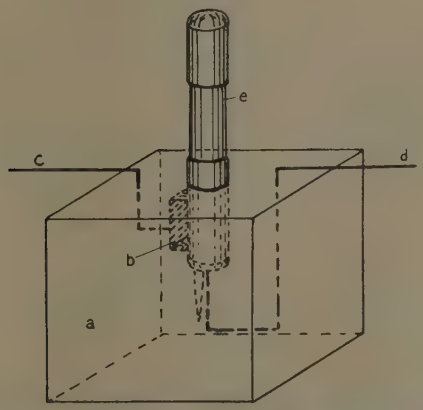

a, paraffin wax block ; *b*, mercury ; *c*, lead to high voltage negative ; *d*, lead to circuit ; *e*, Geiger-Müller counter.

is perhaps the simplest possible (fig. 4), and is modelled upon that used by Fay and Paneth [5].

H.T. Batteries.

Consisted of twelve 120 volt dry batteries in series, with plug-in holes at 12 volt increments, efficiently insulated by glass and rubber sheets from each other *and from the amplifying circuit and counter* which stood upon the same bench. For fine adjustment of the voltage an additional dry battery was included, which

enabled changes of 1·5 volts to be made by means of a wander-plug attachment. The potential applied to counters was in the neighbourhood of 1200 v. At air pressures between 7 and 8 cm. of mercury we found the working voltage to rise by about 70 volts per cm. increase of pressure. The leads from the H.T. supply were heavy-rubber coated flex supported above the bench on insulating glass stands.

Valves.

The amplifying valve was a Mullard P.M.3 or P.M. 3A, and the thyratron an Osram G.T.1 Gas-filled Relay.

Fig. 4.

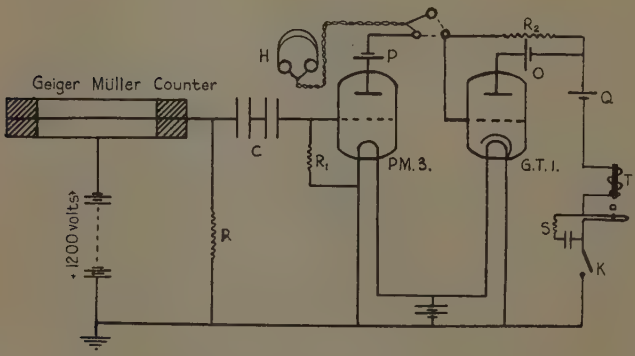

The circuit.

It was convenient to mount them in a box with a glass window, so that flashes from the relay valve could be observed. The mode of operation of the P.M.3 is abnormal, in that reception of an impulse by the grid results in its becoming more negative, with consequent *fall* in current through the anode circuit. The voltage swing produced on the grid of the thyratron is controlled by the resistance R_2 (fig. 4), which must also be adjusted in accordance with the characteristic curve of the P.M.3 to ensure efficient amplification; $R_2 \simeq 2 \times 10^5\ \omega$ is suitable. The grid leak-resistance R_1 should be $8 \pm 2 \times 10^6\ \omega$; a grid-bias battery is unnecessary in the case of a P.M.3 valve.

Condensers.

The smaller the capacity of the coupling condensers, C, the sharper are the impulses fed on to the grid of the P.M.3 valve, but they will also be feebler, and with a single stage of amplification satisfactory operation is obtained with 0·0002 and 0·0003 μF in series. Best quality condensers are essential.

Leak-resistance.

The correct adjustment of the high resistance, R, *is extremely important*, since for every air-filled counter there is a fairly narrow range of resistance, approximately

Fig. 5.

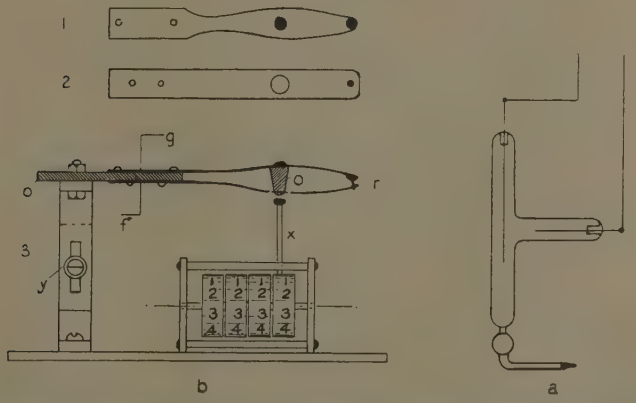

a. High resistance. *b*. 1 and 2, plan of top and bottom strips of contact breaker respectively; 3, side elevation of telephone call-counter arrangement. *o*, ebonite; *g* and *f*, connecting leads; *r*, platinum points; *x*, movable arm; *y*, brass supporting bracket.

10^9 to 10^{10} ω, within which the counting characteristics of the circuit are satisfactory. This will be discussed in a subsequent section. The mode of construction of the leak-resistance is illustrated in fig. 5 (*a*), for which we are indebted to the Department of Physics. Two tungsten electrodes are sealed into a pyrex glass vessel filled with an anhydrous solution of absolute ethyl alcohol in pure xylene. The proportions of alcohol and xylene can only be found by experiment. Externally the electrodes are spot-welded to nickel wires. Several

of these are filled with varying proportions of the constituents by alternately heating to expel air and cooling with the open end under the liquid. The tubes are allowed to stand for some hours and their resistances measured before sealing. They do not polarize in use, but the resistances increase with age, as shown by the following observations.

TABLE I.

Tube.	May 1936. $\omega \times 10^{-9}$.	December 1936. $\omega \times 10^{-9}$.
1	0·96	1·2
2	6·2	7·9
3	8·9	10·9

Telephone-call Counter.

An amplified impulse from the Geiger counter reduces the negative potential on the grid of the thyratron and initiates a discharge through the solenoid of a telephone-call counter, T, thereby raising a pivoted iron plate which causes the registration of one unit. The discharge in the thyratron, once started, continues unless the anode circuit is broken, when the grid regains control within 10^{-3} seconds. It is therefore necessary to break the anode circuit as soon as an impulse has been registered, and this is effected by attaching a light brass arm, x (fig. 5 (*b*)), with a smooth head vertically to the plate, so that when the latter moves up the head knocks against a contact-breaker.

The top of our contact-breaker consists of a steel leaf spring with a small ebonite stud near the tip, as shown in fig. 5 (*b*); the lower fixed contact is of stout copper strip. The points of contact are tipped with *platinum*, and must be cleaned occasionally with fine emery paper. By reducing the masses of moving parts, adjusting the tension in the leaf spring and the spring in the call counter, the position of the contact breaker, and by keeping the bearings oiled it is possible greatly to increase the maximum counting speeds of commercial call-counters. We are able to obtain a *steady* maximum speed of 2000 per minute in spite of a disadvantageously high solenoid resistance. The hammer needs to be set very carefully

with respect to the ebonite stud on the contact-breaker. Excessive arcing across the breaker is liable to produce spurious high counts, since the anode circuit is then not completely broken, which may cause the registration of two or more units per single impulse, i. e., "*double kicking.*" Therefore a spark-quenching device, S, 0·01 μF and 500 ω in series across the gap, is included, which permits a more delicate adjustment of the hammer and consequent gain in speed. The counting speed increases with the voltage applied to the solenoid, but the latter is limited, as the plate voltage on the P.M.3 valve should not exceed 150 v. Very occasionally the moving parts of the telephone-counter stick momentarily whilst in use, causing continuous discharge in the thyratron, so a tapping-key, K, is placed near the observer whereby the anode circuit can be instantly broken. Another matter which demands special attention is *the negative bias on the grid of the thyratron.* Weak impulses will not be registered if the bias is too large; too small a bias results in "double kicking" on account of the finite duration of individual impulses. A good plan is to alter the voltage applied from battery P until the thyratron is just unstable in operation and then increase P by about 8 volts; P $\triangleq$ 55 v., Q $\triangleq$ 100 v., O $\triangleq$ 120 v. gives satisfactory performance with the P.M.3 valve.

Recognition of "double-kicking" requires practice, since two or more impulses will often arrive close together in normal circumstances. A method of testing the behaviour is to include a pair of head-phones, H, in the anode lead of the amplifying valve and count the number of almost simultaneous arrivals occurring over a period of, say, fifteen minutes, and compare this with the number recorded by the telephone-counter during an equal interval of time. The method can also be used to ascertain whether all the impulses from the Geiger counter are registered by the call-counter. Moreover, the audible clicks from a healthy counter are sharper than from one in poor condition. For these reasons *it is advisable to have available a pair of head-phones* which can be switched in when required.

The Characteristics of Geiger-Müller Counters.

We define the *zero voltage* as being the highest H.T.

voltage that can be applied to the Geiger counter withou response when surrounded by a feebly radioactive substance such as potassium chloride. As the voltage is progressively raised the number of impulses registered per minute by the telephone-call counter increases. Types of voltage-count curves which may be obtained are exemplified in fig. 6 (i.).

Curves c and d possess almost flat portions, $\frac{dn}{dv} \rightarrow 0$, of which the voltage span may vary in individual cases between 10 and 50 volts. A "flat" of not less than

Fig. 6 (i.).

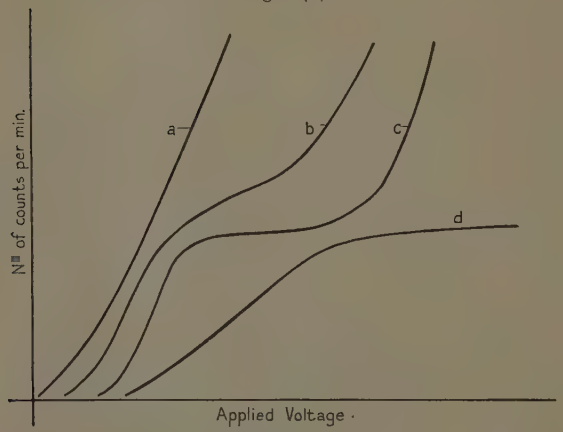

20 volts is adquate provided the counter is gas-tight and due attention is paid to other conditions of operation. The working voltage is set at the mid-point (if anything to the low voltage side) of the flat in order that small fluctuations shall not sensibly alter the counting efficiency. We have frequently found that of a pair of casings, identical as far as visual examination can decide, one will invariably give rise to a characteristic curve of type (a) or (b), and is therefore useless, whereas the other will possess a satisfactory flat nine times out of ten that it is made up. Fig. 6 (ii.) demonstrates the effect upon the flat of varying the magnitude of the leak-resistance; $R_1 = 4 \times 10^8\ \omega$, $R_2 = 6 \times 10^9\ \omega$, $R_3 = 9 \times 10^9\ \omega$. The flat

is *flattened and extended* by increasing the resistance, but the maximum counting speed of the circuit is thereby reduced, and consequently it is not always possible to arrange a satisfactory compromise between these opposing influences. In practice the largest resistance compatible with a high maximum speed is employed.

The following experiment throws some light upon the characteristic curve. Estimates are made of the number of impulses (about 60 a minute on the flat) from the Geiger counter with a small radium source at a convenient distance away, at a series of increasing H.T. voltages, first by means of *head-phones* in the anode lead of the

Fig. 6 (ii.).

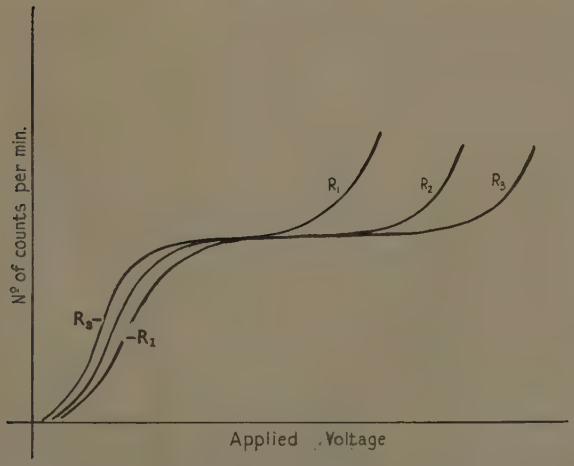

P.M.3 valve, and then automatically on the telephone-call counter. The results are represented in fig. 7, *x* head-phones, *y* call-counter.

At voltages lower than v_1, some of the impulses are too feeble to trigger the thyratron. From v_1 to v_2 all the impulses are effective, but above v_2 the strongest impulses are so prolonged that the thyratron is still unstable after the telephone-counter has registered and "double-kicking" occurs. As the voltage is raised further the effect becomes intensified. It has also been shown that the flat *determined by head-phones* is extended

and made flatter by increasing the leak-resistance, as was observed when the impulses were automatically recorded.

Maximum Counting Speed.

This very important quantity must be understood to refer to *the circuit as a whole*, and not to the telephone-call counter. With the apparatus described maximum counting speeds of 1200 ± 50 per minute are consistently obtained. The call-counter working in conjunction with the thyratron alone (the latter having been made unstable by breaking the circuit at battery P) is capable of rather

Fig. 7.

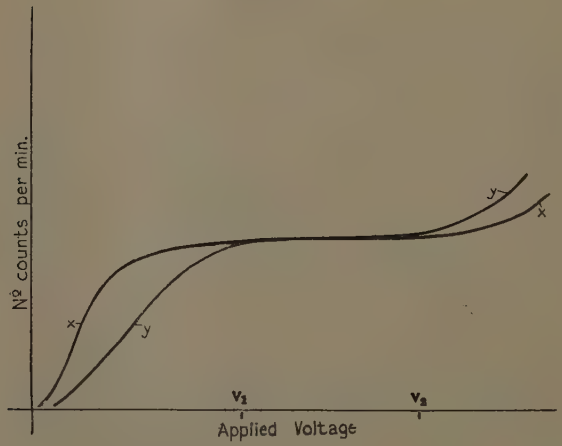

more than 2000. The maximum speed of the circuit is conveniently determined by placing 0·1 millicurie of a radium salt near, but not too near, the Geiger counter for periods of, say, ten seconds. As the rad um is gradually brought closer the call-counter slows up, and finally ceases altogether; a noise like the tearing of cloth is heard in the head-phones. Considerably higher maximum speeds than 1200 per minute can be obtained by slight reduction of the negative bias on the grid of the thyratron, but these are somewhat unsteady and accompanied by the tearing noise in the head-phones.

They are probably not genuine, and since steadiness is essential we invariably work at the lower speed.

The Background Count.

Allowance must be made for the ionization, mainly caused by cosmic radiation, which is always superimposed upon that due to a radioactive substance. The unevenness of the background count is illustrated in Table II., which shows the number of times a given count was registered in successive *half*-minutes over a period of some seventy minutes.

TABLE II.

ount.	2.	3.	4.	5.	6.	7.	8.	9.	10.	11.	12.	13.	14.	15.	16.	17.	18.	19.	20.
umber of times ecorded.	0	1	1	3	8	17	22	13	9	18	18	7	4	12	9	1	1	1	2

Readings vary from 3 to 20 per *half* minute (mean 20·8 per minute), but when dissected into five-minute intervals the fluctuations are from 17 to 22 impulses per minute. These figures emphasize the importance of the time of observation in statistical analyses of results. A freshly made large counter, fig. 1 (*a*), gives rise to a background count of 14 ± 2 per minute, increasing sometimes with use over the course of weeks to, say, 16 ± 2. The background count of one with smaller window area, fig. 1 (*b*), is about 5 per minute, and the electron sensitivity *per unit area of window* is equal to that of the larger counter. Consequently when small quantities of radioactive material are under investigation it is preferable to use this type rather than partly surround the window of a large counter.

Methods of Presenting Radioactive Substances to the Counter.

Powders are conveniently placed around the counter in containers similar to those invented by Juliusburger, Topley, and Weiss [3], *i. e.*, in the annular space between a tube of thin cellophane (nearest the counter) and an outer tube of glass. We find it advantageous to make *both* tubes of celluloid (thickness 0·1 mm.), rolling them

on cylindrical wooden mandrels of appropriate dimensions, fixing with seccotine, and supporting on a brass ring as in fig. 8 (*a*). The same amount of overlap, and hence constant absorption of β-particles, is ensured by using celluloid sheets of the same size. For convenience when filling it is well to make the inner cylinder protrude above the other. The radioactive substance must be dry or the celluloid will buckle. Tests with powdered KCl proved that maximum response is obtained when the width of the annular space, hence of the brass ring, is 2·0 mm.

Four such containers were constructed and filled with KCl, so that when slipped over the counter the salt completely enveloped the window. Five-minute runs were

Fig. 8.

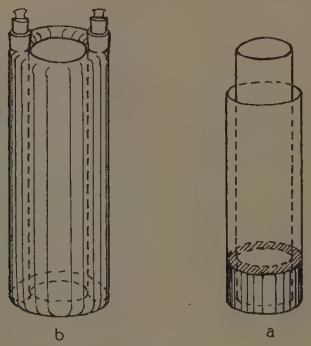

made with each in turn, and the average number of impulses recorded *per minute* were respectively 192, 190, 197, and 194, showing a satisfactory degree of reproducibility. Rotating the cylinders produced no sensible alteration in the average number of counts.

When experimenting with radio-bromine [6], we used a *pyrex* glass cell, fig. 8 (*b*), the inner wall of which was extremely thin. Filled with a cold saturated solution of KCl the number of impulses registered per minute, over and above the background, was 37. Soda glass would considerably augment the background count, because it contain potassium.

Other Types of Geiger-Müller Counters.

Experiments were made with counter-casings of various shapes and sizes. Special attention was given to those constructed from seamless brass tubing of *rectangular* section (*cf.* Fay and Paneth [5]), the windows of which were made by cutting away one side and soldering on a piece of thin copper-foil. These were less efficient than the cylindrical type and offered no compensating advantages. For purposes of comparison the characteristics of the large and small cylindrical counters and of a very large rectangular counter are summarized in Table III.

TABLE III.

Counter.	Area of window (cm.)^2.	Background (per minute).	Uncorrected excess counts produced by KCl (per minute).
Fig. 1 (*a*)	12·0	15	175
Fig. 1 (*b*)	3·7	5	68
Rectangular.....	20·4	72	26

Running-in and Testing the Counter.

In order to achieve stability a counter must be run-in before commencing an experiment. A container of KCl is slipped over it and connexion made to the H.T. batteries. Half-an-hour is usually sufficient, but the time required varies somewhat for different counters.

Routine Testing.

As a matter of *routine* attention should be given to the contacts on the batteries and elsewhere. Vigilance must be exercised against the occurrence of "double-kicking," which, unless caused by the Geiger counter, may be cured by adjusting the contact breaker or the negative bias on the grid of the thyratron. The points of the contact breaker should be cleaned. Dirty points introduce an additional high resistance in the anode circuit, thereby reducing the efficiency of the thyratron, as explained in the section on valves. It is well to listen to the impulses in the head-phones. Then follows

the determination of zero voltage, the count (using a mixture of NaCl and KCl) at both extremities of the flat, the background count, and finally the maximum counting speed of the circuit.

At the end of an experiment the characteristics must be re-determined, for counters deteriorate with extraordinary suddenness. The useful life of a counter is a matter of weeks, or even months. Their careers are often terminated by accidental damage to the wax seal, with consequent entry of water vapour. When this happens it is sometimes convenient to cut the tip off the glass tube, remove it by cautious warming, and insert another. After carefully sealing the wax the counter is evacuated and filled with dry air as previously described; but the flat is shortened by such treatment, and sooner or later the counter must be completely dismantled and rebuilt. After much use a counter gradually deteriorates, the symptoms being considerably reduced maximum speed, blurred "clicks" in the head-phones, and a poor flat.

It may be mentioned that after counting at high speed a counter is somewhat unstable; it is therefore our invariable practice to allow a minute or two for adjustment to new conditions *whenever the container is changed.*

Correction for Coincident Impulses.

With an apparatus of finite resolving power two or more impulses arriving within the shortest time required for registration will be counted as one. A correction is therefore necessary.

In a note immediately following this paper Mr. H. Todd derives a correction formula based upon the assumption that the resolving power of the instrument is constant, *i. e.*, independent of the rate of counting. In order to use the formula a further assumption must be made, namely, that the maximum counting speed, the reciprocal of which is taken to be the minimum time required for registration of an impulse, is correctly determined by bringing radium near the counter. Since the too close approach of radium produces paralysis the validity of this assumption is open to question. However, an Appendix to Todd's paper shows that the formula has been tested experimentally with satisfactory results.

Todd makes the interesting deduction that it is inadmissible, indeed *meaningless*, to correct an observed rate of counting larger than the maximum rate divided by e, *i. e.*, approximately one-third of the maximum counting speed.

A check upon the applicability of the formula and the performance of our counting mechanism is the determination of decay periods of radio elements. In the case of radio-*iodine*, using on different occasions both large and small Geiger counters, fig. 1 (*a*) and (*b*), the following values were obtained :—25·5, 26·0, 26·0, 25·0, 25·0. Mean : 25·5 min. Fermi and his collaborators [7], who used an electrometer, gave 25 min. The half-life of radio-*chlorine* measured in three separate experiments was 36·0, 36·5, 35·0. Mean : 36·0 min. The time given by Olson, Libby, Long, and Halford [8] for radio-chlorine was 37 minutes. The statistical distribution of the *corrected* counts was apparently satisfactory in each experiment ; there was no evidence of a different rate of decay when the counts were large (*e.g.*, observed count 330 ; corrected count 500) than when they were small (*e. g.*, observed count 70 ; corrected count 75).

Acknowledgments.

It is a pleasure to express our thanks to Prof. F. A. Paneth, Dr. J. W. J. Fay, and Dr. P. B. Moon for guidance at the outset of our investigations. Also to Drs B. Topley and J. Weiss. The Thrissell Engineering Company of Bristol took much trouble in turning the counter casings. Grants in aid of the research were received from the Royal Society and from the Bristol Colston Society.

References.

(1) *Phys. Zeit.* xxix. p. 839 (1928) ; *ibid.* xxx. p. 489 (1929).
(2) Barasch, Proc. Phys. Soc. xlvii. p. 824 (1935) ; Moon, J. Sci. Instr. xiv. p. 189 (1937).
(3) Hughes, Juliusburger, Masterman, Topley, and Weiss, J. C. S. p. 1525 (1935).
(4) Reports on the Progress of Physics, iii. p. 239 (1936).
(5) J. C. S. p. 384 (1936).
(6) Hamblin and Johnson, ' Nature,' cxxxviii. p. 504 (1936).
(7) Amaldi, D'Agostino, Fermi, Pontecorvo, Rasetti, and Segrè, Proc. Roy. Soc. A, cxlix. p. 522 (1935).
(8) J. A. C. S. pp. 1313 & 2467 (1936).

LIV. *Note on the Correction to be applied to the Results obtained by using a Geiger Counter.* *By* H. Todd, *B.A.*, *Department of Mathematics, Bristol University* *.

IT is clear that any method of counting irregular impulses which uses an interrupter with a definite maximum rate (*i. e.* minimum resolving time), must be subject to error as a result of the events to be counted often being so close in time that two or more of them are counted as one. It is the object of this note to obtain the correction necessary to estimate the true count from the count given by the instrument, and to find the limit of usefulness of a counter of given maximum rate.

It can be proved that the probability that m random points on a line of unit length shall lie in a range of length $1/n$ is

$$\left(\frac{m}{n^{m-1}} - \frac{m-1}{n^m}\right).$$

Suppose that the counter has a maximum rate of n per minute; that it is counting impulses with a true average rate of μ per minute, and that the count given by the instrument is m per minute. Consider the events of one minute as points at random on a straight line of length unity: there will be $\frac{1}{2}\mu(\mu-1)$ pairs of points, so that we may expect to find in the long run that

$$\frac{\mu(\mu-1)}{2}\left(\frac{2}{n} - \frac{1}{n^2}\right)$$

pairs are each within a length $\frac{1}{n}$, *i.e.*, the counter would fail to separate them. Further, there will be

$$\frac{\mu(\mu-1)(\mu-2)}{6}\left(\frac{3}{n^2} - \frac{2}{n^3}\right)$$

sets of three points which lie, each three, in a length $\frac{1}{n}$, and so on for bigger groups.

* Communicated by C. H. Johnson, Ph.D.

Suppose there are n_1 twos, n_2 threes, n_3 fours, n_4 fives, and no sixes. Then each five counts as five fours, each four as four threes, each three as three twos: so the n_4 fives count as $5n_4$ fours, therefore there are only n_3-5n_4 *independent* fours. These count as $4(n_3-5n_4)$ threes, and the n_4 fives count as $10n_4$ threes, therefore the number of *independent* threes is

$$n_2-4(n_3-5n_4)-10n_4=n_2-4n_3+10n_4.$$

These count as $3(n_2-4n_3+10n_4)$ twos, and the independent fours as $6(n_3-5n_4)$ twos, and the fives as $10n_4$ twos; therefore the number of independent twos is

$$n_1-3(n_2-4n_3+10n_4)-6(n_3-5n_4)-10n_4 \\ =n_1-3n_2+6n_3-10n_4.$$

Collecting these results together we have

$n_1-3n_2+6n_3-10n_4$ independent twos,
$n_2-4n_3+10n_4$ independent threes,
n_3-5n_4 independent fours,
and n_4 fives.

The counter will reckon each of these groups as a simple event, so the observed count will be

$$m=\mu-(n_1-3n_2+6n_3-10n_4)-2(n_2-4n_3+10n_4) \\ -3(n_3-5n_4)-4n_4,$$

$$=\mu-n_1+n_2-n_3+n_4.$$

Clearly the argument is quite general and does not depend on stopping at groups of five, so we have, finally,

$$m=\mu-n_1+n_2-n_3+n_4-n_5+\ldots$$

$$=\mu-\frac{\mu(\mu-1)}{2!}\left(\frac{2}{n}-\frac{1}{n^2}\right)+\frac{\mu(\mu-1)(\mu-2)}{3!}\left(\frac{3}{n^2}-\frac{2}{n^3}\right)\ldots$$

the series stopping at the last term greater than unity. We can find m without serious error by summing this series to $(\mu+1)$ terms, which gives

$$m=1+(\mu-1)\left(1-\frac{1}{n}\right)^{\mu},$$

and this can be replaced by the simpler formula

$$m=\mu e^{-\frac{\mu}{n}},$$

as it can be proved without difficulty that

$$1+(\mu-1)\left(1-\frac{1}{n}\right)^{\mu}>\mu e^{-\frac{\mu}{n}}>(\mu-1)\left(1-\frac{1}{n}\right)^{\mu}.$$

In practice we always observe m and wish to estimate μ, so that the formula must be reversed: this reversion gives

$$\mu=m+\frac{m^2}{n}+\frac{3m^3}{2n^2}+\frac{8m^4}{3n^3}+\cdots$$

$$=m\sum_{r=1}^{\infty}\frac{r^{r-1}}{r!}\left(\frac{m}{n}\right)^{r-1}.$$

This series will converge, by the ratio test, if

$$\operatorname*{Lt}_{r\to\infty}\frac{m}{n}\left(\frac{r+1}{r}\right)^{r}<1,$$

i. e.,

$$m<\frac{n}{e}.$$

Clearly the maximum m allowable must be less than n/e, and in practice it is found that any m near this value cannot be counted efficiently for reasons which must now be studied in detail.

The first thing we notice about the formula is that the m has a definite maximum value:

$$\frac{dm}{d\mu}=e^{-\frac{\mu}{n}}\left(1-\frac{\mu}{n}\right),$$

so that for $\mu=n$, m attains the maximum value n/e: then further as μ increases from n to infinity m diminishes from n/e to zero. This is so obviously false that there must be something in the derivation of the correction formula that makes it inapplicable for values of μ equal to or greater than n. If we return to the first part of the argument we see that, in writing the result

$$m=\mu-(n_1-3n_2+6n_3-10n_4)$$
$$-2(n_2-4n_3+10n_4)-3(n_3-5n_4)-4n_4,$$

we have tacitly assumed that the impulses coming in, μ in number, can be grouped in ones, twos, threes, etc.,

and that each one, or " burst " of two, or of three, is counted as one by the instrument : and, in fact, that all these " bursts " are separated from each other by an interval greater than the minimum resolving time of the counter. But as μ increases, the time will come when every impulse is separated from the next by an interval less than the resolving time of the counter and then the argument breaks down completely.

The following diagram is designed to illustrate what will occur :—

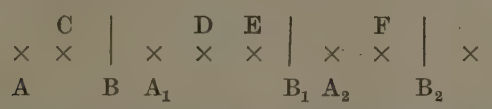

Suppose the crosses on the line all represent impulses and the distances on the line represent the intervals of time between their arrivals at the instrument : suppose, also, that AB represents the resolving interval of the counter. The impulse A is counted and the next one C is ignored : the third impulse A_1 is counted, so from A_1 measure the resolving interval $A_1B_1(=AB)$; clearly the impulses D and E will be ignored, and the next one to be counted will be A_2, and so on. It will now be clear that the more impulses there are, the more the number counted will approach to n, the full possible count for the instrument, and that the original argument no longer applies, because there is no minimum resolving interval which is void of impulses.

It is possible from this to judge how far the formula $m=\mu e^{-\frac{\mu}{n}}$ can be relied upon ; in fact, we can see at once that there must not be as much as nearly one impulse per resolving interval of the counter, or, μ must be less than n.

We can now examine more closely the practical limits o ` usefulness of the correction formula : first suppose that $\mu=n$ and that the formula holds so far ; then $m=\mu e^{-\frac{\mu}{n}}=n/e$, so we have an observed count of n/e and an added correction of $(n-n/e)$. This correction, being considerably bigger than the observation, can hardly be considered as satisfactory. Let us lay down the not unreasonable rule that the added correction shall not

exceed one-half the observed count, then we have for the limiting case,

$$m=\left(m+\frac{m}{2}\right)e^{-\left(m+\frac{m}{2}\right)\frac{1}{n}},$$

or

$$\frac{3m}{2n}=\log_e\frac{3}{2},$$

or $m=n\times 0{\cdot}27$ very nearly.

This, then, is about the largest observed count m which can safely be corrected.

The calculation of μ from the observed m is not straightforward, because the terms of the series giving μ do not, as a rule, decrease very rapidly: we can, however, proceed as in the following example.

Suppose $n=1000$ and $m=240$, then we have

$$\begin{aligned}\mu&=m+\frac{m^2}{n}+-\\&=240+58+21+9+-\\&=328.\end{aligned}$$

This value of μ must be too small, as all the terms of the series are positive. So put $\mu=330$ in the first formula, giving

$$\begin{aligned}m&=330\,e^{-\frac{330}{1000}}\\&=330-109+18-2\\&=237\,;\end{aligned}$$

now try $\mu=340$, giving

$$\begin{aligned}m&=340-116+20-2\\&=242.\end{aligned}$$

So by linear interpolation, the required μ for $m=240$ is

$$330+\frac{3}{5}(340-330)=336,$$

which can be verified, for

$$\begin{aligned}336e^{-\frac{336}{1000}}&=336-113+19-2\\&=240.\end{aligned}$$

Summary.

(i.) The maximum count (n) of the instrument is to be obtained by bringing up a source of impulses that is sufficiently rapid to give a clear count and not so frequent that the impulses (which, in fact, all have some "spread") run together.

(ii.) Any observed count m should not be greater than about one-quarter of n, the maximum count.

(iii.) The correction formula does not apply at all when m is nearly approaching n/e.

(iv.) The formula giving μ from m will almost always need correction by interpolation from the inverse formula $m=\mu e^{-\frac{\mu}{n}}$, as shown in the example given.

Dept. of Mathematics,
University of Bristol.

Appendix. By F. T. Hamblin, B.Sc., A.I.C.

Experimental Verification of the Correction Formula previously deduced.

The formula given above is obtained by considering a perfect system in which the resolving time is independent of the rate of counting. It is doubtful whether this assumption is strictly true in practice.

When a powerful radioactive source (*i.e.*, one containing a little radium salt) is brought near to a Geiger counter the observed counts/min. increase to a certain limit and then begin to decrease. In the previous section it has been shown that the correction formula gives the result that m increases with μ to a maximum value of $\frac{n}{e}$ when $\mu=n$. A further increase in μ causes a decrease in m. Schiff [1], who obtained an identical formula by a different method, thought that the two effects were related and that the correction formula gave a complete explanation of the phenomenon observed when a radium source approaches a Geiger counter. He therefore considered that the resolving time of the counter is $\frac{1}{n.e}$.

The decrease in m after reaching its maximum value is often very sudden in practice, and not gradual as required

by the correction formula. Impulses from the Geiger counter can be heard by including a pair of head-phones in the anode circuit of the first amplifying valve, and normally they are sharp clicks. If, however, radium is brought up to the counter so that the observed counts begin to fall, a noise like tearing cloth is heard occasionally together with the clicks. The former increases as the radium is brought nearer to the counter and, finally, no clicks are heard at all. The falling off in the observed count is thus a complicated effect. Todd has also given reasons on theoretical grounds why the correction formula is not valid with observed counts greater than $\frac{n}{e}$ and suggests that the resolving time of the counter is $\frac{1}{n}$.

A number of experiments were carried out to find the value for the resolving time which gave the best correction formula and to test the formula itself. Some representative results are given below.

Graphs with μ as ordinate and m as abscissa were drawn for the two resolving times and used to correct observed counts.

Experiment 1.

A small quantity of powdered uranium nitrate was sealed in two thin glass tubes X and Y respectively. The number of counts/min. A, obtained by placing one of the tubes X near the counter was observed. The other tube Y, was now brought near and the combined effect C, of X and Y found ; X was now removed and the number of counts/min. B, due to Y alone, noted. This procedure was repeated a number of times.

Stability was achieved by allowing the counter one and a half minutes to settle down after each movement of the radioactive sources. The number of counts/min. were determined in each case as the mean of four consecutive minute readings.

The background count/min. for five consecutive minutes was found at various intervals throughout the test and the mean value (19 counts/min.) taken. The maximum speed/min. was also determined by putting a radium source near the counter for ten seconds on three occasions

at the beginning and end of the test and taking the mean, which was 1200 counts/min.

The sum of the excess corrected counts/min. due to X and Y alone should equal the excess corrected counts/min. obtained with X and Y together. The fourth and fifth columns in Table I. give values of A, B, and C corrected according to formula $m=\mu e^{-\frac{\mu}{n}}$ (hereafter called formula I.), and the sixth and seventh columns give the corresponding values corrected by the formula $m=\mu e^{-n\mu}$ (hereafter called formula II.).

TABLE I.

A.	B.	C.	(A corrected +B corrected) −38.	(C corrected) −19.	(A corrected +B corrected) −38.	(C corrected) −19.
129	64	170	173	182	162	161
97	204	249	320	299	280	252
105	99	175	186	190	175	168
179	182	302	394	413	347	317
102	127	188	217	209	201	181
70	181	228	254	271	228	228
72	226	246	323	302	281	249
67	150	182	205	197	188	175
115	101	187	201	209	188	180
83	80	145	136	147	132	133
110	120	200	218	227	203	194
126	119	213	236	241	219	210
144	103	209	240	240	220	195
77	81	128	131	125	126	115
80	137	189	211	211	188	182
122	131	204	246	232	227	199
Totals			3691	3695	3365	3139

In individual cases the agreement is often poor owing to statistical fluctuations, but on adding together the results of sixteen experiments corrected according to formula I. the agreement is very good.

Experiment 2,

This consisted in placing an uranium nitrate source near the Geiger counter and measuring the counts/min. C, which it produced at various distances from the counter. The counts/min. were determined as the mean of four consecutive minute readings, the counter having been allowed to settle down for one and a half minutes after the source had been moved. The excess corrected counts/min. multiplied by the square of the distance d of the source from the central wire of the counter, should be independent of d. The maximum count/min. and the background count/min. were determined as in the first experiment and found to be 1200 and 15 respectively.

In Table II. C is the mean of four measurements of four minutes each, C′ and C″ are the values of C corrected according to formula I. and formula II. respectively.

TABLE II.

d.	C.	C′−15.	$(C'-15)\times d^2\times 10^{-3}$.	C″−15.	$(C''-15)\times d^2\times 10^{-3}$.
10	333	500	50	359	36
12	269	350	50	281	41
15	193	220	50	191	43
20	129	130	52	120	48
25	87	78	49	75	47
30	66	55	50	53	48
40	45	32	51	31	50

Experiment 3.

Separate samples of uranium nitrate and sodium chloride were finely ground. A portion of the sodium chloride was well mixed with the uranium nitrate and the activity Q, of the whole measured. A volume of the powdered sodium chloride equal to that of the mixture was now added and the whole well mixed. The activity of the resulting product was then measured and this mixture further diluted with an equal volume of the sodium chloride. The activity of the product was measured and the process repeated. The excess corrected counts/min. should be halved at each dilution. The maximum speed/min. and the background count/min.

were determined as in the previous experiments and found to be 1200 and 14 respectively. In Table III. Q is a mean value from ten consecutive minute readings, Q′ and Q″ are values of Q corrected according to formula I. and formula II. respectively.

TABLE III.

Q.	Q′−14.	Q″−14.
358	566	392
234	288	240
138	142	130

Experiment 4.

A further test is indicated at the end of the previous paper in which decay periods of various radio-elements were given. Fermi and collaborators[2] determined half period values with an electrometer and thus eliminated the necessity of correcting for coincident counts. With good experimental technique this method can be considered to give absolute values. Decay periods of radio-chlorine and radio-iodine were determined using the first correction formula, and the mean values obtained were 36·0 and 25·5 mins. respectively. Fermi gives the decay periods as 35·0 and 25·0 mins. respectively. There was no evidence of a different rate of decay at different portions of the decay curve. With the second formula the rate of decay was slower when the recorded counts/min. were large (about 400) than when they were small (about 50).

From these experiments it is clear that the best results are obtained when the resolving time is taken as $\frac{1}{n}$ and not $\frac{1}{n.e}$. Each of the experiments involves to some extent a differential method and this tends to mask the difference between the two formulæ.

Owing to the complicated nature of the system (circuit and counter) it is doubtful whether a rigid correction formula could be obtained which is applicable to every system. It is therefore necessary to carry out some

or all of the tests given above on any new system to make sure that an adequate correction formula is being employed.

References.

(1) Schiff, Phys. Rev. l. p. 88 (1936).
(2) Amaldi, D'Agostino, Fermi, Pontecorvo, Rasetti and Segré, Proc. Roy. Soc. A, cxlix. p. 522 (1935).

Dept. of Physical and
Inorganic Chemistry,
Bristol University.

LV. *An Apparatus for the Production of Radioactive Elements by means of Radium.* *By* F. T. Hamblin, *B.Sc., A.I.C.**

Summary.

An apparatus is described for the production of radioactive elements which gives adequate protection to the operator with ease of manipulation.

Introduction.

ARTIFICIALLY radioactive elements are often conveniently prepared by bombardment of stable elements with neutrons [1]. When the formation of a radio-element is due to the capture of a neutron by the nucleus "slow" neutrons are found to be very much more effective than "fast." Slow neutrons are obtained by slowing down with water or paraffin wax those produced from a "bomb" containing an intimate mixture of a radium salt (or radon) and beryllium dust. The neutrons collide with the hydrogen atoms, and gradually lose energy until they are in thermal equilibrium with the surrounding molecules.

The usual method of producing the radio-elements has been to sink the neutron source in a block of paraffin wax or a vessel of water, and place the substance to be irradiated with neutrons in tubes sunk in the medium about 7 cm. from the source [1]. Alternatively the

* Communicated by C. H. Johnson, Ph.D.

substance was placed in the annular space of a double-walled glass tube suspended in a bucket of water, and the bomb lowered into the central tube.

If continual use is being made of large sources it is necessary to protect the operator, owing to the injurious effects on the human body of the radiations from radium or radon.

The best practical screening material is lead, but when working with radio-elements of short life it is essential that the irradiated substance shall be available for use as quickly as possible after the "bomb" has been removed, and therefore the massive protection must not prevent the apparatus from being rapidly operated.

Distance is the only real protection from the radiations, and the apparatus was therefore housed in a waterproof shed about thirty yards from the laboratory. This also removed any effect of the γ-rays from the source on the Geiger counters in the laboratory. In estimating the protection required it must be borne in mind that the operator is only near to the apparatus for a few minutes each day, viz., whilst placing substances to be irradiated and removing them later. The apparatus described here was designed to combine adequate protection when using sources containing less than 500 millicuries of radium with ease of manipulation, and proved very satisfactory in practice.

Details of Construction.

The shed was lit by electricity controlled by an automatic switch fixed to the door for convenience when working at night. When necessary, in cold weather, the shed was heated by radiator lamps connected to an auxiliary circuit. The apparatus was supported on three stout shelves fixed to the sides of the shed, and is shown diagrammatically in fig. 1.

The lead block A, 6 inch diameter, has a $\frac{1}{2}$-inch diameter hole drilled through it to within $\frac{3}{4}$ inch of the top; from there the hole is reduced to $\frac{1}{10}$ inch diameter. The block is machined all over to the shape indicated in fig. 1. The radium bomb is enclosed in a duraluminium container with 0·009 inch walls, the top of the container is made with a wall thickness of $\frac{1}{10}$ inch, and a screw plug fitted

with a hole for suspending it on a stout greased silk cord. The cord passes over a smooth steel rod embedded

Fig. 1.

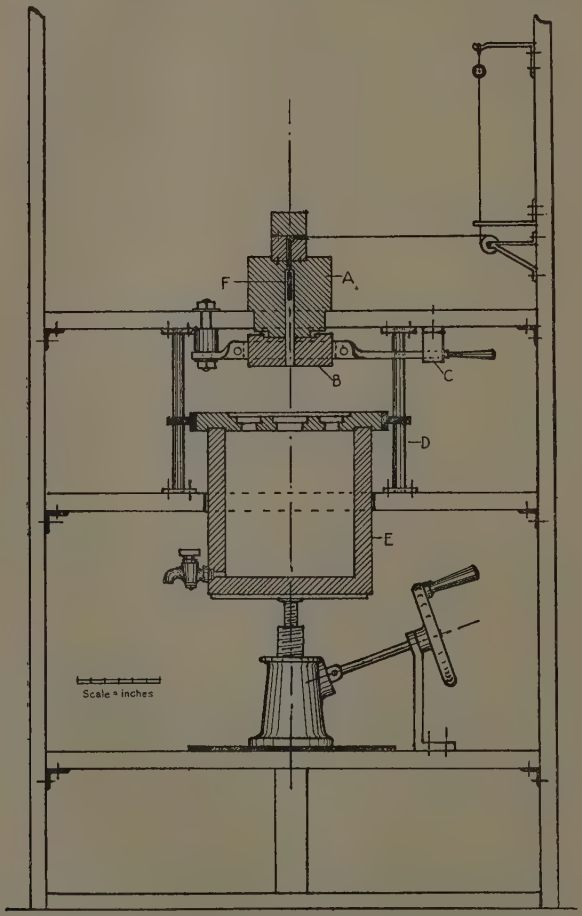

A, lead block ; B, sliding lead block ; C, bracket ; D, steel guides ; E, lead bucket ; F, radium " bomb."

in the lead cap on the top of A, and thence over a pulley, the end being fastened to a ball and hook which determine

the position of the bomb. The bomb is lowered by unhooking the line from the top eyelet and allowing the ball to rest on the bottom bracket. The ball consists of two wooden hemispheres screwed together, and by slackening the screws the position of the ball on the cord can be varied; in this way the distance through which the bomb is lowered can be adjusted. The drop is calibrated, using a dummy bomb. The top of the lead cap is detachable, to facilitate threading the cord. When not in use the bomb is kept in A, as shown in fig. 1.

The sliding block B, $2\frac{1}{2}$ inches thick, with a $\frac{1}{2}$-inch hole drilled through, is carried by an iron clip with two arms, one of which is fixed and the other able to move laterally in the bracket C. When this arm is at one end of this bracket the holes in B and A register, and when at the other end the hole in A is closed. The operator is thus protected by at least $2\frac{1}{2}$ inches of lead in every direction while the bomb is in A. The top of B is recessed $\frac{1}{4}$ inch deep to within $1\frac{1}{2}$ inch of the edge, to receive the reduced part of A.

A lead bucket, approximately 12 inches diameter by 12 inches deep with $1\frac{1}{4}$ inch walls, filled with distilled water, is supported on an iron plate riveted to a double throw Shelley Jack operated by a hand-wheel, with an extended shaft carried by a stout supporting bearing. The jack is bolted to a metal plate fixed to the lower shelf to distribute the weight. The small tap at the base of the bucket is used when cleaning out, and also when it is required to carry out experiments without water in the bucket, viz., bombardment by fast neutrons.

The lid of the bucket is $1\frac{1}{4}$ inch thick, and an iron clip, with two welded lugs diametrically opposed, was clamped around its circumference. Two polished steel rods fixed between the shelves and passing through these lugs respectively keep the bucket steady and in its true relative position whilst being raised and lowered. The lid is recessed $\frac{1}{4}$ inch deep to within 2 inches of its edge, and is drilled with one central hole and four holes around it, each hole being recessed, as shown in fig. 2.

All the lead components were cast in closed moulds with large "risers" to avoid "blow holes" which would reduce their protective efficiency, and machined all over to the required size.

Mode of Operating.

To use the apparatus the hole in A is closed and the bucket lowered as far as possible. The substance, liquid or solid, to be irradiated is placed in the annular space between the tubes shown in fig. 2. This tube is made of soft glass, which is more transparent to neutrons than Pyrex, and placed in the central hole in the lid of the bucket; the bucket is then raised so that the lid just touches the base of B. The arm in the bracket C is now

Fig. 2.

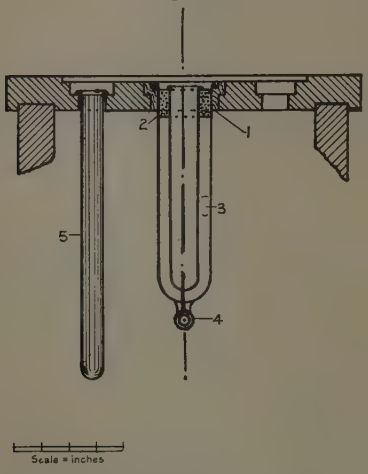

1, wood bush; 2, rubber bung; 3, annular space; 4, sinker attached here; 5, glass tube.

moved into the position where A and B register, and the apparatus is constructed so that the central glass tube now registers with the holes in A and B. The bomb is then lowered into the central tube.

After the substance has been sufficiently exposed to neutrons (irradiation for six times the length of the half-life of the radio-element concerned gives 98·5 per cent. of the activity produced by exposure for a relatively infinite time) the radium is drawn up into the block A, and B moved across. The bucket is now lowered

and the irradiated substance removed, the whole operation taking about 20 seconds.

It will be seen that by using recessed lead blocks the operator is always protected by at least 1 inch of lead, and is never exposed to direct radiation even during the time the radium bomb is being transferred from A to the bucket or *vice versâ*.

With the above procedure the substance is exposed to a mixture of fast neutrons direct from the source, and ones which have been slowed down by collision with the water molecules and have found their way back to the region of the central tube. By draining off the water from the bucket this latter effect can be eliminated and the substance irradiated with fast neutrons only. If the bucket is filled with water and the liquid to be irradiated placed in four soft glass tubes, supported in the four outer holes provided in the lid, the annular space in the central tube being empty, the liquid is exposed almost entirely to slow neutrons.

When radio-iodine was produced by exposure of aqueous solutions of sodium iodide the greatest activity was obtained by placing the solution as near as possible to the source of neutrons, which was adjusted to hang halfway down the bucket. The bomb rested on the bottom of the central tube during the exposure, and the solution was therefore made up so that its level in the annular space came 2 inches above the top of the bomb. Solubility considerations made it sometimes necessary to increase the size of the annular space.

A method invented by Szillard [2] enables radio-halogens to be produced with large activities by means of quite small neutron sources. The principle of the method depends upon the fact that when a halogen atom in an organic molecule captures a neutron the molecule disintegrates and the radio-halogen atom is set free. When the organic liquid is subsequently shaken with an aqueous solution of alkali halide the free atoms are concentrated in the latter. A large percentage of the active atoms produced in the organic liquid are thus transferred to the aqueous layer, and the smaller the quantity of alkali halide used the greater its activity per gram. Not all the neutrons are absorbed by the organic halide in the central tube, and an increased activity can be obtained by placing around it tubes

filled with the same liquid, supported in the four holes provided in the lid. The number of radioactive atoms liberated in the central tube is thereby somewhat diminished, because some slow neutrons which otherwise would have found their way back to it are absorbed by the outer tubes. The total activity is, however, increased, since a greater number of neutrons are absorbed by the five tubes together than by the central tube alone, and could be further increased, up to a certain limit, by using additional tubes.

This method can be used to prepare radio-iodine, using ethyl iodide, radio-bromine, using ethylene dibromide, and radio-chlorine, using carbon tetrachloride. In the latter case the method is especially important, as the activity produced in chlorine is relatively feeble.

This apparatus was constructed preliminary to an investigation on the use of radio-elements in chemical problems under the supervision of Dr. C. H. Johnson [3]. We are indebted to the Colston Society of Bristol for part of the cost.

References.

(1) Fermi et al., Proc. Roy. Soc., A, cxlvi. p. 483 (1934), and cxlix. p. 522 (1935).
(2) Szillard and Chalmers, ' Nature', cxxxiv. p. 462 (1934).
(3) Johnson and Hamblin, ' Nature,' cxxxviii. p. 504 (1936).

Department of Physical and Inorganic Chemistry,
University of Bristol.

LVI. *The Temperature Distribution within the Auroral Region of the Atmosphere.* *By* L. Vegard, *Dr.Phil., Professor of Physics at the University, Oslo* *.

[Plates III. & IV.]

1. THE spectral analysis of the auroral luminescence combined with measurements of the height and light distribution along the auroral ray-streamers showed that in the auroral region—from say 80 km. upwards to 600–1000 km.—the density of matter decreases at a very much slower rate than in the lower part of the atmosphere.

This result, which was found and discussed in 1923 †,

* Communicated by the Author.

† L. Vegard, Phil. Mag. xlvi. pp. 193 & 577 (1923); *Zs. f. Phys.* xvi. p. 367 (1923).

was the more remarkable as the analysis of the auroral spectrum had revealed the fact that no atmospheric layer of light gases existed on the top of the atmosphere ; but the fairly heavy nitrogen was shown to be predominant throughout the whole auroral region, to the very top of auroral rays reaching altitudes of say 600–800 km.

In the papers referred to the writer discussed two possible ways of explaining the peculiar distribution of matter in the auroral region. The one possibility would be to assume that the temperature in the auroral region increased rapidly upwards, and the second possibility was that matter was in a highly ionized state and was driven towards higher altitudes through the effect of electric forces.

The primary cause for this " electric lifting of atmospheric matter " was found in the action of sunlight of very short wave-length resulting in the expulsion of high speed electrons according to the Einstein photo-electric equation, and matter will be driven upwards by any process which causes high speed electrons to be expelled from the atmosphere.

A state similar to that of the solar corona should be formed round the earth, and especially on the side facing the sun. During the night the emission of high speed electrons will be essentially reduced, except perhaps on areas exposed to the precipitations of electric rays which accompany magnetic disturbances and auroras. As a general rule the " coronal " structure will be much reduced on the night side. After sunset a shrinkage or depression in the auroral region will take place. But auroral height measurements show that even during the night the density of matter decreases very much more slowly in the auroral region than in the lower part.

As shown by the writer this " night distribution " or " night corona " may be accounted for without assuming that it is essentially due to a rapid increase of temperature as we pass upwards, for in the very highest regions the negative electricity in the highly ionized matter to a large degree consists in the form of free electrons.

On account of the rapid motion of the electrons they will try to get away from the atmosphere, and on account

of the electric fields the positive ions and the ordinary atmospheric matter will be forced upwards. *The presence of free electrons will have a similar effect as if the average molecular weight of the gas had been largely reduced.*

The results obtained through auroral investigations regarding the state of the upper atmosphere has been confirmed in a most striking way by radio-echo measurements. They have revealed the existence of layers (F-layers) of high altitude, which corresponds to the electronic layer which from the auroral studies were found to result from the photoelectric expulsions of electrons towards higher altitudes.

The researches of Appleton and his collaborators have shown that the reflexion from the F-layer is mostly due to electrons and that the F-layer persists throughout the night. From measurements of the coefficients of the absorption and reflexion of radio-waves Farmer and Ratcliffe * find, in accordance with previous results from auroral studies, that above say 80 or 100 km. the density of matter decreases at a much lower rate than in the region below. As already mentioned this peculiar distribution might formally at any rate be interpreted by assuming a rapidly increasing temperature as we pass upwards in the auroral region.

Assuming the increase to take place according to a linear law, Martyn and Pulley † find that in the height interval from 100 to 250 km. the temperature should increase from say 300° K. to 1200° K.

Theoretical considerations of Appleton and Naismith ‡ would, according to Martyn and Pulley, lead to summer temperatures in the F-layer of about 3000° K.

To account for the enormous temperature changes, Martyn and Pulley have to assume the presence of a considerable percentage of water vapour in the auroral region. Now, in the auroral spectrum—which has now been fairly completely explored—there is no trace of the spectrum of water vapour.

In the spectrum of the night sky certain observers (*e. g.*, Sommer § and Cabannes ‖ give a large number

* F. T. Farmer and J. A. Ratcliffe, Proc. Roy. Soc. cli. p. 370 (1935).
† D. F. Martyn and O. O. Pulley, Proc. Roy. Soc. cliv. p. 455 (1936).
‡ E. V. Appleton and R. Naismith, Proc. Roy. Soc. cl. p. 685 (1935).
§ L. A. Sommer, *Zs. f. Phys.* lxxvii. p. 374 (1932).
‖ J. Cabannes, *Journ. de Phys. et le Radium*, v. p. 601 (1934).

of bands which they interpret as due to water vapour; but, as pointed out in previous papers *, a large number of the bands they give are not proved to be really existing, and the spectrum of the night sky, as far as it is known, can be interpreted as consisting of nitrogen bands and the oxygen lines ($^1S_0 - {}^1D_2$) and ($^1D_2 - {}^3P_{012}$).

For this and other reasons the interpretation of the distribution of matter by assuming increasing temperatures therefore meets with great difficulties, and I think we have to fall back on the view taken by the writer, that the coronal structure is essentially due to the presence of free electrons which, on account of electric forces, will have the effect of lifting the matter towards higher altitudes.

The electron gas will have a tendency to assume a distribution with altitude as if it consisted of neutral particles of mass 1/1800 of that of a hydrogen atom, but on account of the charge an electric field will set up which will act on the positively charged atmospheric matter and produce reduction in the gravitational attraction.

2. *On the Solution of the Temperature Problem.*

The question regarding the night temperature within the auroral region can probably be settled by taking advantage of the auroral spectrum.

The writer has shown that the temperature of the auroral luminescence can be measured fairly accurately by means of the energy distribution within the R-branches of the negative nitrogen bands.

The temperature has been measured by the writer † partly in collaboration with Mr. Tönsberg ‡ for a considerable number of spectrograms, and all spectrograms lead to temperatures between 220–250° K. or between −50 and −20° C.

These measurements require fairly large dispersion and therefore long exposures during several nights, therefore the temperature obtained in this way corresponds to the height interval in which the aurora on an average appear with maximum intensity, or an interval between 100–125 km.

* L. Vegard and E. Tönsberg, *Zs. f. Phys.* xciv. p. 413 (1935).

† L. Vegard, Geofys. Publ. ix. no. 11 (1932); Terrestr. Magn. p. 389 (1932).

‡ L. Vegard and E. Tönsberg, Geofys. Publ. xi. no. 2 (1935).

Our temperature measurements from auroral bands thus fix the average night temperature in the height interval 100–125 km. to the interval T = 220°–250° K.

In order to determine the temperature at higher altitudes by means of the band spectra we should have to take spectra solely from the upper limit of very long auroral rays, but as such rays are fairly weak and comparatively rare we should require a spectrograph of much higher light power; but such an instrument will ordinarily have a smaller dispersion, which will make the temperature determinations less reliable. Still we hope to construct suitable spectrographs which will enable us to measure the " band temperatures " for the upper part of long rays.

In the present paper we are going to deal with another method which, by fairly simple experimental equipments, enables us to study the possible temperature variations with altitude by means of the luminescence from long auroral rays, and certain important results already obtained will be briefly dealt with.

3. *Method and Procedure.*

As is well known the width of a spectral line will increase with temperature on account of Doppler effect produced by the thermal motion of the emitting particles. In the auroral luminescence we have two sharp atomic lines, 5577 and 6300, which might be utilized for temperature studies.

Now the width of these lines may be studied by means of interferometer methods. Such interferometers have been used by Babcock * to obtain an accurate value of the green line from the night sky luminescence, and the writer, in collaboration with Mr. Harang, has used a similar interferometer method for precision measurements of the wave-lengths of the lines 5577 and 6300 from the auroral luminescence.

In a paper dealing with the green auroral line † we have discussed the possibility of determining the temperature by means of the width of the interference fringes, and we came to the conclusion that, at any rate with the fairly lightly silvered interferometer plates used by

* H. D. Babcock, Contrib. from Mount Wilson Obs. no. 259 (1923).
† L. Vegard and L. Harang, Geofys. Publ. xi. no. 1 (1934).

our observations, an accurate, absolute temperature determination would not be possible, because the temperature broadening would be partly masked by the width of the fringes due to the small reflexion coefficient of the metallic layers of the interferometer plate; but, although an absolute determination of the temperature is difficult, the sharpness of the interference fringes may be used as an indication for variations in temperature.

If, *e. g.*, the temperature from 100 km. to say 250 km. increased from 240° to 1200°, or, perhaps, 2000°, then such an enormous temperature increase should produce a marked broadening of the fringes.

The application of the interferometer for temperature measurements has the advantage that only a fairly short time of exposure is wanted. In the case of the strong green line an exposure of a few minutes may be sufficient, and even in the case of the red line we have obtained good pictures of fringe systems with exposures down to 40 minutes.

In addition to the interferometer used at the Auroral Observatory at Tromsö, the writer built another one principally for use at Oslo, and this instrument was provided with two etalons with a fairly dense aluminium coating, which gave a higher reflexion coefficient than those used at Tromsö.

The instrument is described in a paper recently published *, giving results of precision measurements undertaken on the basis of observations from Oslo. Regarding details we may refer to this paper; in this connexion we merely wish to state a few facts.

The instrument consists of a camera with a Fabry-Perot plate of quartz in front of the lens. Before reaching the Fabry-Perot etalon the light has to pass coloured filters suitably selected for the line to be investigated. We used two etalons made by Hilger with thicknesses of about 2·5 and 1·5 mm.

As regards results the paper referred to only deals with the problem of measuring the wave-length of the red line 6300 with the highest possible precision, but, as will be shown in the present paper, the observations also give valuable information regarding the temperature within the auroral region.

The interference pictures were taken at Oslo during

* L. Vegard and L. Harang, Geofys. Publ. xi. no. 15, iii. (1937).

an auroral display, which lasted during the whole night, Oct. 16–17, 1936.

Five interference pictures of the red line 6300 were obtained with the 1·5 mm. etalon; and combining the wave-length values obtained with this etalon with those previously obtained at Tromsö with 2·5 and 5·0 mm. etalons, it was possible for the first time to obtain without ambiguity a high precision value of the wave-length of the red auroral line which we knew to be situated near 6300. The mean wave-length obtained from the Oslo observations was found to be

$$\lambda = 6300{\cdot}286\ (+0{\cdot}006)\ \text{I.U.}$$

The wave-length of the oxygen line ($^1D_2 - {}^3P_2$), as found from laboratory experiments, is $\lambda = 6300{\cdot}279$. These measurements have thus proved that the red auroral line which *e. g.* produces the red auroræ of type A is identical with the oxygen line OI ($^1D_2 - 3P_2$). In order to investigate the possible temperature variations with altitude by means of the interferometer we may adopt two different ways of procedure.

We may take two pictures of ring systems preferably on the same plate. In taking one of the pictures we point the axis of the instrument solely towards parts of the auroræ near the lower limit of the streamers. By the second picture the instrument when in function is always to be directed towards regions near the upper limits of very long rays.

By the second procedure we make use of the fact that all rays coming from the same part of the auroræ or a bundle of parallel rays will unite in a point on the photographic plate. If we direct the instrument towards an auroral drapery or a bundle of auroral rays at a considerable distance from the spot of observation the lower limit will be situated near the horizon.

As we pass upwards the luminescence will correspond to continually increasing altitudes, and at the upper limit of somewhat long streamers the altitude may be several hundred kilometres.

At the lower part of the fringe picture the light has been emitted from high altitudes, while at the lower part the fringes are due to light from parts near the lower limit with altitudes near 100 km. An interferometer ring system photographed under such conditions

would give us a means of studying possible temperature variations with altitude within the auroral region.

If there was a rapid increase of temperature upwards, as maintained by Appleton, Naismith, Martyn and Pulley, we should expect the fringes to become broader and more diffuse as we passed from the upper towards the lower part of the interference picture.

4. *Results of Observations of the Red Line* 6300.

The auroral display observed at Oslo, 16–17 Oct., 1936, had just the proper structure and position relative to the spot of observation to give favourable conditions for the study of the temperature variation with altitude from a single interference picture.

The auroræ were situated far north, so the bottom edges were found a few degrees above the horizon, and they usually consisted of draperies and ray bundles which often had a length of several hundred kilometres.

Under these conditions the upper and lower part of the fringe system correspond to a fairly large average difference of altitude probably amounting to 200 km. or more.

As already mentioned, we obtained five interferometer pictures ; but all of them showed ring systems with the same sharpness of the fringes in all directions. Two enlarged interference pictures of the red line are shown on Pl. III. *We notice that there is no indication that the fringes corresponding to luminescence from the highest altitudes are less sharp and distinct than those corresponding to regions near the bottom edge.*

When we are taking interference pictures of the red line a number of nitrogen bands will also pass through the filter and produce a ground fog on the plate. For this reason interference pictures of the red line are not well suited for absolute temperature measurements ; but the fringe system ought to indicate temperature variations with altitude of the magnitude mentioned, if they existed.

5. *Interference Pictures of the Green Line from Varying Altitudes.*

As the green auroral line usually is much stronger than the red one, and as no lines or bands of noticeable strength appear in its nearest surroundings, the green

line will be more suitable for temperature measurements than the red one, and the writer intends to continue these temperature measurements by means of interferometer pictures from the green line. On account of the considerable intensity of this line it will be possible to use interferometer etalons with sufficient dense metallic coating to give very sharp fringes, which will show up any real broadening of the spectral line ; and it may perhaps also be possible to obtain interferometer pictures which may be utilized for absolute temperature measurements.

By these investigations I intend to adopt both the procedures previously mentioned. According to conditions, we may either take pictures of distant auroræ with pronounced ray structure, or we may take two pictures preferably on one plate, one corresponding to places near the lower edge and the second corresponding to parts near the upper edges of long auroral rays.

During an auroral display observed at Oslo, 4–5 May this year, we were already able to take some interference pictures of the green auroral line with the 1·5 mm. etalon. The apparatus was the same as the one which was used for the red line, and which was described in the previous paper referred to *. The only difference was that the red filter was interchanged with a yellow one (Wratten 15 G.), and that we used an orthochromatic plate (Gevaert, Ultra-Press ortho). The auroræ appeared on the northern sky, and they were not particularly strong.

At this time of the year at Oslo the auroral region on the northern sky will be exposed to sunlight, and therefore not only light from the green line but also some scattered sunlight will pass into the instrument and produce some ground-blackening on the plate.

Reproductions of the three pictures obtained are shown on Pl. IV., and we notice that in spite of the somewhat unfavourable circumstances we obtained quite distinct interference fringes.

The picture (Pl. IV., *a*) (exposure 23^{45} to 0^{30}) was obtained by directing the axis of the instrument towards the lower border of the auroræ.

During the exposure of picture *b* (Pl. IV.), which lasted from 0^{30} to 1^{15}, the instrument was directed towards the upper half of the auroral luminescence ; and the last picture

* L. Vegard and L. Harang, Geofys. Publ. xi. no. 15, iii. (1937).

(Pl. IV., *c*) (exposure 1^{16} to 2^{05}) corresponds to the upper limits.

The pictures *a*, *b*, and *c*, therefore, should correspond to luminescence of increasing altitude. The luminescence of *c* is mainly emitted from regions which are probably about 100 km. higher than that of picture *a*.

Looking at the pictures we see *that the interference fringes of picture c are equally sharp as those of a, and the upper part of the same picture is equally sharp as the lower part.*

In connexion with our precision measurements of the wave-length of the green line from the aurora a large number of successful interferometer pictures was obtained at the Auroral Observatory, Tromsö ; some of these were obtained by keeping the axis of the instrument in a nearly horizontal direction, and for these pictures the lower fringes should correspond to a considerably larger altitude than those in the upper part.

Reproductions of a large number of interference ring systems of the green auroral line are given in a paper previously published *. The writer has carefully examined all the fringe systems on the original plates and on the reproductions, but none of the pictures give indication of any broadening of the fringes in those parts which correspond to auroral light emitted from the greatest altitudes.—

From the observations made at Oslo, which have been confirmed by the Tromsö material, we may draw the following conclusions :—

If the temperature is at all sufficiently high to influence the sharpness of the interference ring system, the change of temperature within a height interval from say 100 *to* 200 *km. must be small as compared with* 250° *K., which is about the mean temperature at* 100 *km. Thus the interferometer pictures for different height intervals give no indication of such a large increase of temperature with altitude as that maintained by Appleton, Naismith, Martyn and Pulley.*

The slow rate with which the density of matter decreases upwards must therefore be explained in the way proposed by the writer in 1923, as effected by the cloud of rapidly moving electrons forming the limiting aspect of our atmosphere and by the resulting electric fields. It must be remembered that the electron cloud

* L. Vegard and L. Harang, Geofys. Publ. xi. no. 1 (1934).

on the night side may be continually fed by the rapidly moving electrons expelled on the day side, as the result of high energy photons contained in the sun's radiation. The power of the electrons to lift the ionized atmosphere increases with their kinetic energy.

Physical Institute, University, Oslo.

LVII. *A Note on the Calculation of the Peltier Heat.* *By* G. P. Dube, *M.Sc., Cambridge University* *.

THE object of this note is to derive the expression for the Peltier heat directly from its definition. When a current passes along a circuit consisting of two dissimilar materials at the same temperature, there is an absorption or evolution of heat at the junction. This is called the Peltier effect. The Peltier coefficient π_{12} is defined as the heat absorbed per second when unit current flows from the first conductor to the second. The usual method of calculation assumes that the composition varies continuously from one conductor to the other. If there be an electric field **F** and a temperature gradient parallel to the x-axis, and if (u, v, w) is the velocity and E the total energy of an electron, the electric and the heat currents at a point x are †

$$J=-\epsilon\int uf\,du\,dv\,dw=K_1\left\{\epsilon^2F+\epsilon T\frac{\partial}{\partial x}\left(\frac{\zeta}{T}\right)\right\}+\frac{K_2\epsilon}{T}\frac{\partial T}{\partial x}, \quad . \quad . \quad . \quad (1)$$

$$W=\int Euf\,du\,dv\,dw=K_2\left\{-\epsilon F-T\frac{\partial}{\partial x}\left(\frac{\zeta}{T}\right)\right\}-K_3\cdot\frac{1}{T}\frac{\partial T}{\partial x}, \quad . \quad . \quad . \quad (2)$$

where $-\epsilon$ is the charge of the electron, f is the velocity distribution function, ζ is the Fermi energy of the conduction electrons, and K_1, K_2, K_3 are certain integrals. The heat Q produced per second in unit volume is

$$Q=JF-\frac{\partial W}{\partial x}. \quad . \quad . \quad . \quad . \quad . \quad . \quad . \quad (3)$$

Therefore

$$Q=\frac{J^2}{\sigma}+\frac{J}{\epsilon}T\frac{\partial}{\partial x}\frac{K_2-\zeta K_1}{K_1T}+\frac{\partial}{\partial x}\left(K\frac{\partial T}{\partial x}\right), \quad . \quad (4)$$

* Communicated by Prof. R. H. Fowler, M.A.

† ' Theory of Metals,' by A. H. Wilson (Cambridge University Press, 1936), p. 174.

since $\partial J/\partial x=0$, the first and the last terms being the Joule heat and the heat due to thermal conduction, while the second term is the thermoelectric heat. When T is constant, the thermoelectric heat is an exact differential, and the total heat absorbed between two points only depends on the composition at those points, and not on whether the change is continuous or abrupt. We therefore have

$$\pi_{12}=-\frac{1}{\epsilon}\left[\left(\frac{K_2-\zeta K_1}{K_1 T}\right)_{\text{Conductor 2}}-\left(\frac{K_2-\zeta K_1}{K_1 T}\right)_{\text{Conductor 1}}\right]. \quad . \quad . \quad . \quad (5)$$

It is obvious from the definition that we must be able to derive this expression for π_{12} more straightforwardly from the difference in the energy fluxes at the two points considered. When two conductors are in contact in equilibrium, the value for ζ is the same * for both. Taking ζ to be the energy zero in both conductors, and taking T to be constant, the energy flux from one side is

$$\int (E-\zeta)uf\,du\,dv\,dw=W+\frac{\zeta J}{\epsilon}\text{, from (1) and (2),}$$

$$=-\frac{J}{\epsilon}\frac{K_2-\zeta K_1}{K_1} \quad . \quad . \quad . \quad . \quad . \quad (6)$$

The difference of two such terms, depending on the nature of the two materials, gives the usual expression for π_{12}, since the heat absorbed from (or given to) the surroundings to keep the temperature constant must be equal to the net flux of energy out of (or in) the region considered. It is to be noted that it is not necessary that the composition should be constant at the two points considered. The current density is constant throughout the circuit, and, if $\partial\zeta/\partial x\neq 0$, the electric field F must adjust itself so as to make J constant. In the formula (6) both F and $\partial\zeta/\partial x$ have been eliminated by the help of the relations (1) and (2), and $\partial J/\partial x$ is the only condition necessary for the validity of the theory.

My thanks are due to Prof. R. H. Fowler, for suggesting this problem to me.

* The ζ is known as the thermo-dynamic potential, and it is obvious that this must be the same for the two materials in contact to satisfy the equilibrium conditions. See ' Theory of Metals ' (Wilson), p. 257.

LVIII. *The Determination of Specific Heats by an Eddy-current Method.*—Part I. *Theoretical.* *By* R. M. Davies, *D.Sc., F.Inst.P., and* W. J. Thomas, *B.Sc., Ph.D., University College of Wales, Aberystwyth* *.

Contents.

Section 1.

Introduction.

THE aim of the present work has been to investigate theoretically and experimentally a new electrical method of determining the specific heats of metals and alloys, employing alternating current. In this method the specimen is heated by eddy-currents produced in it when placed in an alternating magnetic field; amongst other things, this eliminates the disadvantage, common to other electrical methods, of having to insert a heating coil in the specimen.

Let an alternating current of pulsatance ω flow in a coil which does not contain a metallic core; let the conditions be such that the current is distributed uniformly across each cross-section of the wire of the coil. Under these conditions the resistance R_0 and the inductance L_0 of the coil will be identical with the values for direct current.

Let $i=\hat{i}\,.\,e^{j\omega t}$ be the instantaneous value of the current in the coil, $\hat{i}$ being its peak value, and $j=\sqrt{-1}$; let I be the virtual value of i. Let v be the instantaneous value of the p.d. across the coil, and ϕ_0 the instantaneous value of the flux of induction through the coil. Then

$$\phi_0=L_0 i$$

and ϕ_0 and i are in the same phase.
Now

$$v=R_0 i+\frac{\partial \phi_0}{\partial t}=R_0 i+L_0\frac{\partial i}{\partial t}=(R_0+j\omega L_0)i, \qquad (1.1)$$

* Communicated by the Authors.

and the power W_0 expended in the coil is given by

$$W_0 = R_0 I^2. \quad . \quad . \quad . \quad . \quad . \quad . \quad . \quad (1.2)$$

Let a non-magnetic conducting core be inserted in the coil, the current I through the coil being kept constant. Eddy currents will be induced in the core, and these will, in general, modify the magnitude and phase of the flux of inductance through the coil. If the core be ferro-magnetic as well as conducting, there will be further changes in the magnitude and phase of the flux of induction. Thus, in general, the flux of induction, ϕ, with the core inserted, may be written

$$\phi = (A - jB) \, . \, i, \quad . \quad . \quad . \quad . \quad . \quad . \quad . \quad (1.3)$$

where A and B are functions of ω, I, the dimensions of the coil and the core, and the permeability and resistivity of the core material. Generally the flux ϕ lags behind the current i, so that B is usually positive.

In this case v, the instantaneous value of the p.d. across the coil, is given by

$$\left.\begin{aligned} v = R_0 i + \frac{\partial \phi}{\partial t} &= R_0 i + j\omega(A - jB) \, . \, i \\ &= (R_0 + \omega B) . i + j\omega A i \\ &\equiv (R + j\omega L) . i, \end{aligned}\right\} \quad . \quad . \quad (1.4)$$

where $R(\equiv R_0 + \omega B)$ is the effective resistance of the coil and $L(\equiv A)$ is the effective inductance of the coil.

Thus the insertion of the core has increased the effective resistance of the coil by an amount ωB, and the effective inductance of the coil has changed from L_0 to A. For non-magnetic core materials A is generally less than L_0, since the induced currents in the core will flow in the opposite direction to the coil-current, and thus the total flux in phase with the current will be decreased by the insertion of the core. With ferro-magnetic core materials A is generally greater than L_0, since the increase of flux in phase with the current, due to the increased permeability of the core, will exceed the decrease of flux caused by eddy-currents.

The power W expended in the coil when the core is inserted is

$$W = I^2(R_0 + \omega B) = I^2 R, \quad . \quad . \quad . \quad . \quad (1.5)$$

and thus the change P in the power expended in the coil due to the insertion of the core is

$$P=W-W_0=I^2(R-R_0)=\omega BI^2. \quad . \quad . \quad (1.6)$$

P will also be equal to the power expended in the core, and if dt be an infinitesimal time-interval, the energy Q dissipated in the core in the time-interval from 0 to t will be

$$Q=\int_0^t (W-W_0)\,dt=\int_0^t I^2(R-R_0)\,dt. \quad . \quad (1.7)$$

The energy Q will be equal to the heat-energy produced in the core, provided that the core does not gain or lose heat by radiation, etc. Let M be the mass of the core, s its specific heat, Θ_c the rise in temperature (corrected for radiation losses, etc.) in the time-interval 0 to t; then

$$Q=JMs\Theta_c=\int_0^t P\,dt=\int_0^t (W-W_0)\,dt=\int_0^t I^2(R-R_0)\,dt, \quad . \quad . \quad . \quad (1.8)$$

where J is the electrical equivalent of heat, and if $\dot{\theta}$ be the rate of rise of temperature of the core at any instant,

$$\dot{\theta}=\frac{P}{JMs}=\frac{W-W_0}{JMs}=\frac{I^2(R-R_0)}{JMs}. \quad . \quad . \quad (1.9)$$

If W_0, W, I, R_0, and R are constant, then equation (1.8) becomes

$$Q=JMs\Theta_c=Pt=(W-W_0)\,.\,t=I^2(R-R_0)\,.\,t. \quad (1.10)$$

Thus the specific heat s of the core can be determined if the following quantities are determined :—

(*a*) the mass M of the core ;
(*b*) the corrected temperature rise Θ_c in time t ;
(*c*) the change in power, $(W-W_0)$, or the product, $I^2(R-R_0)$.

For reasons given in Section 2 of Part II. of this work it is more convenient to measure I and the change in the resistance, $(R-R_0)$, rather than to measure the change in power, $(W-W_0)$, directly.

Preliminary experiments showed that care would be required in the design of an apparatus to be used for the determination of specific heat by this method. It was soon found that it was desirable that the rate of rise of temperature, $\dot{\theta}$, and the change in resistance, $(R-R_0)$, should be as large as possible, and the parameters which determine the value of these quantities are

(*a*) the magnitude of the alternating magnetic field in which the core is situated ;
(*b*) the frequency of the current ;
(*c*) the size and shape of the core, its density, specific heat, permeability, and resistivity.

It is possible to determine approximately the optimum values of these parameters from the theory of eddy-current and hysteresis losses. In practice the desired rapid rate of rise of temperature and the large change in resistance is very easily obtained with ferro-magnetic substances, and for the present purpose there is little point in investigating this case theoretically. In the sequel it will be assumed that there are no hysteresis losses, although in the formulæ for eddy-current losses the permeability will be retained for the sake of generality.

This theory of eddy-current losses has attracted much attention on account of its application to the calculation of losses in transformer and choke-coil cores, and, more recently, on account of its bearing on high-frequency induction furnaces.

From the theoretical standpoint the simplest cases are those in which the core is either a rectangular plate of infinite length and breadth or an infinitely long rectangular circular cylinder ; the plate or cylinder is assumed to be placed in an alternating magnetic field whose peak value is assumed constant at the surface of the plate or cylinder. The direction of the field is parallel to the length of the plate or to the axis of the cylinder. Under these circumstances the currents induced in the cores will flow in planes perpendicular to the direction of the field. It is convenient to regard the field as being produced by an alternating current flowing in an infinitely long solenoid whose axis is parallel to the length of the plate or to the axis of the cylinder.

The case of the losses in plates was first discussed by

Thomson [1], and Ewing [2], and the case of the cylinder by Heaviside [3]. A discussion of the theory for plates and cylinders is given by Russell [4], and a discussion of the cylinder problem is given by McLachlan [5]. The application of the theory to induction furnaces has been discussed by Burch and Davis [6], and by Strutt [7]. Strutt has also generalized and extended the theory—first to the case of elliptic cylinders, and finally to the case of a core of any arbitrary form [8].

In the elementary theory relating to plates and cylinders which is discussed in the following sections, in addition to the above assumptions it is assumed that

(*a*) the magnetic fields inside and outside the core are everywhere parallel to the axis of the solenoid ;

(*b*) the magnetic field outside the core is uniform over a cross-section of the solenoid ;

(*c*) the wave-length of the alternating current is large in comparison with the dimensions of the solenoid and its core ; this implies that displacement currents are negligible in comparison with conduction currents, and that the problem may be treated as a quasi-static problem.

It follows that the results given by this theory can only be regarded as approximate; but they are, nevertheless, of value in indicating points of importance in the design of the apparatus.

It should be noticed that the particular aspects of the theory required for the present purpose differ from the aspects which are of importance in ordinary eddy-current loss theory and induction furnace calculations. In the present work it is essential to make $\dot{\theta}$ as large as possible, using frequencies within the range of audio-frequency alternating current bridges, *i. e.*, frequencies in the range 500 to 2500 (*vide* Section 2 (vi.)). In eddy-current loss theory the aim is usually to make $\dot{\theta}$ as small as possible, using currents of power frequency, say 50 cycles/second. In induction furnace calculations the aim is again to make $\dot{\theta}$ as large as possible, but the frequencies used are generally higher than 2500 cycles/second—the upper limit in the present work.

Section 2.

Eddy-current Losses in Plates.

(a) *Notation.*

The origin, O (fig. 1), is taken at the centre of the plate. The axis of the solenoid and the direction of the length

Fig. 1.

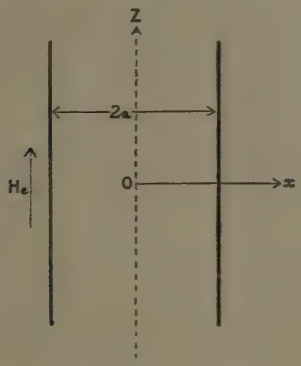

of the plate are taken as the Oz axis, and the direction of the thickness of the plate is taken as the Ox axis.

n = number of turns per unit length of solenoid ;

μ = permeability of core ;

ρ = specific resistance of core in e.m.u. cm. ;

f = frequency of coil-current ;

$\omega = 2\pi f$ = pulsatance of coil-current ;

p = eddy-current parameter, defined by $p^2 = 2\pi\mu\omega/\rho = 4\pi^2\mu f/\rho$;

$2a$ = thickness of the core ;

d = density of the core ;

M = mass of the core ;

V = volume of the core ;

s = specific heat of the core ;

θ = temperature of the core at any instant ;

$\dot{\theta}$ = rate of rise of temperature of the core at any instant ;

U = virtual value of the current density in the core (in e.m.u.) at a distance x from the median plane ;

I = virtual value of the coil-current (in e.m.u.) ;

$\hat{h}_e$, H_e = peak and virtual values of the magnetic field outside the core ;

R_0 = effective resistance of the coil in absence of core ;

R = effective resistance of the coil with core inserted ;

P = power dissipated in the core (ergs/second).

All alternating quantities are assumed to vary harmonically according to the law

$$(\text{instantaneous value}) = (\text{peak value}) \times e^{j\omega t}.$$

(b) *Eddy-current Losses in the Core.*

(i.) *General Results.*

As shown by Russell (*op. cit.*, p. 497, equation (12)), the total power, P, dissipated in the core is given by the equation

$$P = \frac{\rho p V H_e^2}{16\pi^2 a} \cdot \frac{\sinh 2pa - \sin 2pa}{\cosh 2pa + \cos 2pa} \cdot \quad . \quad . \quad (2.1)$$

Since the mass, M, of the core is equal to Vd, it follows from equation (1.9) that the rate of rise of temperature, $\dot{\theta}$, is given by

$$\dot{\theta} = \frac{P}{JVsd} = \frac{\rho p H_e^2}{16\pi^2 Jasd} \cdot \frac{\sinh 2pa - \sin 2pa}{\cosh 2pa + \cos 2pa}, \quad (2.2)$$

or, substituting for p,

$$\dot{\theta} = \frac{\mu H_e^2}{2Jsd} \cdot \frac{f}{2pa} \cdot \frac{\sinh 2pa - \sin 2pa}{\cosh 2pa + \cos 2pa} \cdot \quad . \quad . \quad (2.2)$$

Thus, apart from the density d and the specific heat s of the core, the rate of rise of temperature $\dot{\theta}$ depends on H_e, f, μ, ρ, and s. It is interesting to note that $\dot{\theta}$ is independent of the length, the breadth, and the mass of the core. This is due to the fact that the eddy-current loss (P) and the thermal capacity (Ms) of the core are both proportional to the length, the breadth, and the mass of the core ; if the length, breadth, or mass be

increased or decreased, the eddy-current loss and the thermal capacity will both increase or decrease in the same proportion, so that the rate of rise of temperature remains unaltered. The change, $(R-R_0)$, in the resistance of the coil, according to equations (1.9) and (2.2), is given by

$$(R-R_0)=\frac{JMs\dot{\theta}}{I^2}=\frac{\mu H_e^2}{2I^2}.V.\frac{f}{2pa}.\frac{\sinh 2pa-\sin 2pa}{\cosh 2pa+\cos 2pa},$$

or . . . (2.3)

$$(R-R_0)=8\pi^2n^2\mu V.\frac{f}{2pa}.\frac{\sinh 2pa-\sin 2pa}{\cosh 2pa+\cos 2pa}, \quad . \quad (2.4)$$

since $H_e=4\pi nI.$

Thus $(R-R_0)$ depends on n, V, μ, ρ, a, and f; it is interesting to note that $(R-R_0)$ is independent of the density of the core, depending only on its volume V when n, μ, ρ, a, and f are constant.

Let

$$N(2pa)=N=\frac{1}{2pa}.\frac{\sinh 2pa-\sin 2pa}{\cosh 2pa+\cos 2pa}. \quad . \quad (2.5)$$

In terms of N, $\dot{\theta}$ becomes

$$\dot{\theta}=\frac{\mu H_e^2}{2Jsd}.f.N. \quad . \quad . \quad . \quad . \quad . \quad . \quad (2.2a)$$

and $$(R-R_0)=8\pi^2n^2\mu V.f.N. \quad . \quad . \quad . \quad (2.4a)$$

(ii.) *Variation of* $\dot{\theta}$ *and* $(R-R_0)$ *with* H_e.

From equation (2.2) it is clear that H_e should be large in order to make $\dot{\theta}$ large; since H_e is equal to $4\pi nI$, this implies that the product nI should be large. From equation (2.4) it is seen that n should be large in order that $(R-R_0)$ should be large. Thus, in order that both $\dot{\theta}$ and $(R-R_0)$ should be large, it is essential to make n as large as possible, at a sacrifice, if necessary, of a large value of I. The optimum values of n and I are determined mainly by the characteristics of the alternating-current generator; for this reason further discussion of this point will be deferred until the appropriate section (Section 2(*b*)) of Part II. of this work, and, in the sequel, H_e, n, and I will be regarded as constant. In the

following discussion it will also be convenient to regard μ, s, and d as constant, and thus equations (2.2 a) and (2.4 a) may be written

$$\dot{\theta}=\mathrm{C}\,.f\,.\,\mathrm{N}, \quad . \quad . \quad . \quad . \quad . \quad (2.2\,b)$$

where

$$\mathrm{C}=\mu\mathrm{H}_e{}^2/2\mathrm{J}sd,$$

and

$$(\mathrm{R}-\mathrm{R}_0)=\mathrm{D}.f.\mathrm{N}.\mathrm{V}, \quad . \quad . \quad . \quad . \quad (2.4\,b)$$

where

$$\mathrm{D}=8\pi^2n^2\mu.$$

(iii.) *Particular Cases of the General Results.*

In considering the variation of $\dot{\theta}$ and $(\mathrm{R}-\mathrm{R}_0)$ with a, f, μ, and ρ, since p is a function of f, μ, and ρ, it follows that the variation of $\dot{\theta}$ with these quantities is somewhat complicated. The function N simplifies, however, in two extreme cases—(a) when $2pa$ is small, and (b) when $2pa$ is large.

In this connexion it is useful to know the value of the parameter p in certain typical cases. Taking iron first, as typical of a ferro-magnetic substance, μ is of the order of 2500, whilst ρ is of the order of 10 microhm cm., *i. e.*, 10^4 e.m.u. cm.; these values give $p=3{\cdot}141\sqrt{f}$. Taking copper as an example of a good non-magnetic conductor, μ is unity, and ρ is 1·721 microhm cm., *i. e.*, $1{\cdot}721\times10^3$ e.m.u. cm.; these figures give $p=0{\cdot}1515\sqrt{f}$. Taking bismuth as a typical poor non-magnetic conductor, ρ is 119·0 microhm cm., *i. e.*, $1{\cdot}190\times10^5$ e.m.u. cm., and μ is unity; these values give $p=0{\cdot}01822\sqrt{f}$ for bismuth. Finally, considering an aqueous solution of a salt such as potassium chloride, the permeability is unity and the resistivity for a concentration of about 20 per cent. is of the order of 3·9 ohm cm., *i. e.*, $3{\cdot}9\times10^9$ e.m.u. cm.; these values give $p=10^{-4}\sqrt{f}$ approximately.

Case (a). 2 *pa small.*

If $2pa$ be small, then expansion of the trigonometric and hyperbolic functions in series gives

$$\sinh 2pa-\sin 2pa=2\left\{\frac{(2pa)^3}{3\,!}+\frac{(2pa)^7}{7\,!}\ldots\right\},$$

$$\cosh 2pa+\cos 2pa=2\left\{1+\frac{(2pa)^4}{4\,!}\ldots\right\}.$$

Thus, if fourth and higher powers of $2pa$ be neglected in comparison with unity,

$$N = \frac{2p^2a^2}{3} = \frac{8\pi^2\mu f a^2}{3\rho},$$

and from equations (2.2 *a*) and (2.4 *a*)

$$\dot{\theta} = \frac{4\pi^2}{3} \cdot \frac{H_e^2}{Jsd} \cdot \frac{\mu^2 a^2}{\rho} \cdot f^2, \quad . \quad . \quad . \quad . \quad (2.6)$$

$$(R - R_0) = \frac{64\pi^4}{3} n^2 V \cdot \frac{\mu^2 a^2}{\rho} \cdot f^2. \quad . \quad . \quad . \quad . \quad (2.7)$$

The approximate value of N is accurate to at least 0·1 per cent. when $\frac{(2pa)^4}{4} \leqslant 10^{-3}$, *i. e.*, when $2pa \leqslant 0{\cdot}4$; similarly, the accuracy is at least 1 per cent. when $2pa \leqslant 0{\cdot}7$. Assuming a strip 1 cm. thick, *i. e.*, $a = 0{\cdot}5$ cm., the condition for 1 per cent. accuracy implies that $f \leqslant 0{\cdot}05$ for iron, $f \leqslant 21{\cdot}3$ for copper, $f \leqslant 1477$ for bismuth, $f \leqslant 4{\cdot}84 \times 10^7$ for the aqueous solution. In this region it is seen that $\dot{\theta}$ and $(R - R_0)$ are proportional to μ^2, a^2, f^2, and $1/\rho$.

Case (b). $2pa$ *large.*

If $2pa$ be large, the values of the hyperbolic functions are very large in comparison with the values of the trigonometrical functions; the latter may therefore be neglected. At the same time, cosh $2pa$ is equal to sinh $2pa$, and, therefore,

$$N = \frac{1}{2pa}.$$

Thus, from equations (2.2 *a*) and (2.4 *a*),

$$\dot{\theta} = \frac{H_e^2}{8\pi Jsd} \cdot \frac{1}{a} \cdot \sqrt{(\rho\mu f)}, \quad . \quad . \quad . \quad (2.8)$$

$$(R - R_0) = 2\pi n^2 V \cdot \frac{1}{a} \sqrt{(\rho\mu f)}. \quad . \quad . \quad . \quad . \quad (2.9)$$

The approximate expression for N is accurate to at least 0·1 per cent. when $2pa \geqslant 8$, and to at least 1 per cent. when $2pa \geqslant 5$. Assuming again a strip 1 cm. thick,

the conditions for 1 per cent. accuracy implies that $f \geqslant 2{\cdot}53$ for iron, $f \geqslant 1090$ for copper, $f \geqslant 75320$ for bismuth, and $f \geqslant 2{\cdot}5 \times 10^9$ for the aqueous solution.

In connexion with equations (2.8) and (2.9) it is interesting to note that, in this region, $\dot{\theta}$ and $(R-R_0)$ are proportional to $1/a$, $\sqrt{f}$, $\sqrt{\rho}$, and $\sqrt{\mu}$.

(iv.) *Variation of* $\dot{\theta}$ *and* $(R-R_0)$ *with* a—H_e, f, μ, *and* ρ *constant.*

Under these conditions, if $2pa$ be small, $\dot{\theta}$ is proportional to a^2 according to equation (2.6), and thus $\dot{\theta}$ increases rapidly when a increases. On the other hand, according

Fig. 2.

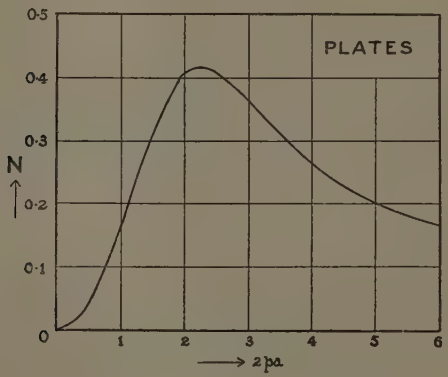

Graph of the function N against $2pa$.

to equation (2.8), when $2pa$ is large, $\dot{\theta}$ is inversely proportional to a, and $\dot{\theta}$ decreases when a increases. For given values of H_e and f, and for a given material, there must therefore exist an optimum value a_0 of a, the rate of rise of temperature, $\dot{\theta}$, being a maximum when $a=a_0$.

Under the conditions stated above, $\dot{\theta}$ is proportional to N, and thus the variation of $\dot{\theta}$ with a will be shown by the curve showing the relation between N and $2pa$. This curve is given in fig. 2, in which N is plotted as ordinate and $2pa$ as abscissa. From this curve it is clear that N increases rapidly with $2pa$ for small values

of $2pa$; N then reaches a maximum value N_0, and finally decreases with increasing $2pa$, in agreement with the general result deduced above. The maximum value of N is seen to be in the neighbourhood of $2pa=2{\cdot}25$; the numerical value of N_0, the maximum value of N, is 0·4172.

The optimum value of a, i. e., a_0, is thus given by the equation

$$a_0 = \frac{2{\cdot}25}{2p} = 0{\cdot}1790\sqrt{(\rho/\mu f)}. \quad . \quad . \quad . \quad (2.10)$$

Fig. 3.

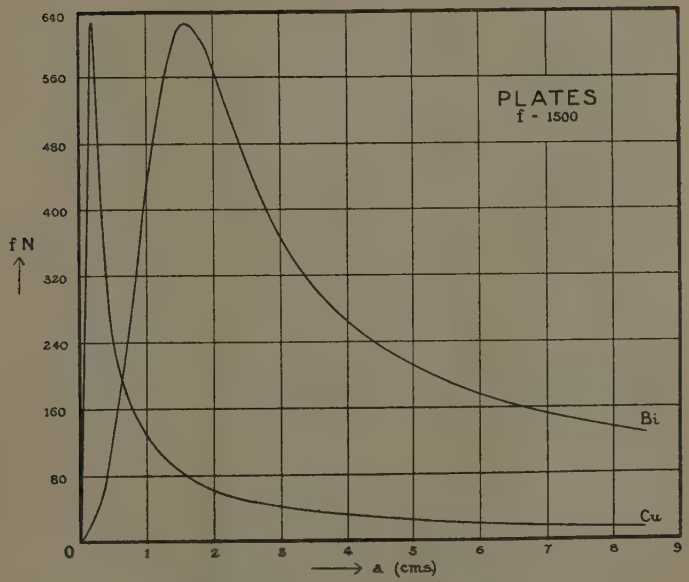

Graph of fN (proportional to $\dot{\theta}$) against a.

Thus a_0 is proportional to $\sqrt{\rho}$ and inversely proportional to $\sqrt{\mu}$ and $\sqrt{f}$. Using the values given previously, for iron $a_0=0{\cdot}3580/\sqrt{f}$; for copper $a_0=7{\cdot}425/\sqrt{f}$; for bismuth $a_0=61{\cdot}73/\sqrt{f}$; for the aqueous solution, $a_0=1{\cdot}118\times10^4/\sqrt{f}$. At a frequency of 1500, for example, the optimum thickness $(2a_0)$ is 0·0185 cm. for iron, 0·3834 cm. for copper, 3·19 cm. for bismuth, and 577·3 cm. for the aqueous solution. These figures show

clearly how an increase in resistivity brings about an increase in a_0.

This may be illustrated with reference to fig. 3, which refers to specimens of copper (Cu) and bismuth (Bi) at a frequency of 1500. In this figure the semi-thickness a (in cm.) is plotted as abscissa and fN as ordinate; the ordinate is thus proportional to the rate of rise of temperature $\dot{\theta}$. Both curves are seen to be of the same general form as the curve of fig. 2.

Turning next to the variation of $(R-R_0)$ with a when H_e, f, μ, and ρ are constant, it is seen from equation (2.4*b*) that $(R-R_0)$ is proportional to the product of the volume V of the core and the function N. If it is assumed that the length and breadth of the core are kept constant, V is proportional to a, and in this case $(R-R_0)$ is to be regarded as proportional to aN, and $(R-R_0)$ will therefore not be a maximum when N is a maximum. It is, however, clear that fulfilling the condition for maximum $\dot{\theta}$ is more important than fulfilling the condition for maximum $(R-R_0)$, since it is easy to compensate for any deviation from the condition for maximum $(R-R_0)$ by varying the length and the breadth of the core. In fact, $(R-R_0)$ can be made as large as is desired by varying the length and breadth of the core, whereas the rate of rise of temperature will be unchanged by this variation. For this reason it is unnecessary to consider the conditions for maximum $(R-R_0)$ in this case or in any case considered in the sequel.

(v.) *Variation of $\dot{\theta}$ with f*—H , a, μ, *and* ρ *constant.*

Under these conditions, if $2pa$ is small, $\dot{\theta}$ is proportional to f^2 (see equation (2·6)); if $2pa$ be large, $\dot{\theta}$ is proportional to $\sqrt{f}$ (see equation (2.8)). Thus $\dot{\theta}$ increases with increasing frequency, the rate of increase of $\dot{\theta}$ with f being greater for small values of $2pa$. This can be seen by reference to fig. 4, which relates to two plates, one of copper and one of bismuth, each plate being 1 cm. thick. In this figure the function fN (proportional to $\dot{\theta}$) is plotted as ordinate and the frequency f as abscissa. In the case of copper $2pa$ is small for frequencies less than 25, whilst $2pa$ is large for frequencies exceeding 1000; this curve shows clearly the rapid initial increase of

$\dot{\theta}$ with f, and also the slower increase for large values of f. In the case of bismuth $2pa$ is small for frequencies less than 1500, and the major part of the curve thus falls within the region of rapid increase of $\dot{\theta}$ with f. It should be added that the values of fN for the aqueous solution are very much smaller than the corresponding values for copper and bismuth; for a semi-thickness, a, of 0·5 cm. and for a frequency of 3600 the value of fN for the aqueous solution is, for example, only 0·0216, as compared with about 395 for copper and about 650 for bismuth.

Fig. 4.

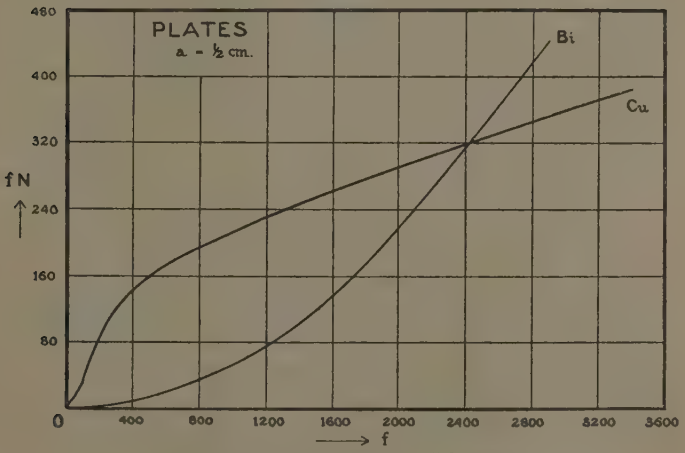

Graph of fN (proportional to $\dot{\theta}$) against f.

(vi.) *Variation of $\dot{\theta}$ with a, f, and ρ—H_e and μ constant.*

It is often stated that the eddy-current loss in a material increases as the resistivity ρ of the material decreases. As equations (2.6) and (2.8) show, this statement is only true for small values of $2pa$, i. e., speaking generally, for low frequencies, small thicknesses, and high resistivities. For large values of $2pa$, $\dot{\theta}$ and the eddy-current loss is actually proportional to $\sqrt{\rho}$, other quantities being constant (see equation (2.8)). This point is clearly

brought out in fig. 4. For a thickness of 1 cm. and for frequencies less than 2470, $\dot{\theta}$ for the copper plate ($\rho=1{\cdot}721$ microhm cm.) exceeds $\dot{\theta}$ for the bismuth plate ($\rho=119$ microhm cm.), but for frequencies greater than 2470, $\dot{\theta}$ for the bismuth plate exceeds $\dot{\theta}$ for the copper plate. Another aspect of this fact is brought out in fig. 3 ; from this figure it is clear that, at a given frequency for small thicknesses, $\dot{\theta}$ for copper exceeds $\dot{\theta}$ for bismuth ; for large thicknesses the reverse is true.

It is therefore clear that, by suitable choice of thickness and frequency, the rate of rise of temperature of a bad conductor can be made to equal or to exceed the rate of rise of temperature of a good conductor.

Another point of interest relates to plates of optimum thickness ; when the condition for optimum thickness ($2pa_0=2{\cdot}25$) is satisfied, the value of N is $N_0=0{\cdot}4172$. Under these conditions, from equations (2.2 *b*) and (2.4 *b*), if $\dot{\theta}_p$ be the rate of rise of temperature at optimum thickness,

$$\left.\begin{aligned}\dot{\theta}_p&=0{\cdot}4172\ \mathrm{C}.f,\\ (\mathrm{R}-\mathrm{R}_0)&=0{\cdot}4172\ \mathrm{D}.\mathrm{V}.f.\end{aligned}\right\} \quad . \quad . \quad . \quad (2.11)$$

This equation shows that for plates of optimum thickness the rate of rise of temperature is independent of the resistivity of the plate, and is a function of f only. In order therefore to obtain large values of $\dot{\theta}$ the two conditions to be satisfied are

(i.) the frequency should be as high as possible ;
(ii.) the plate should be of optimum thickness.

Fig. 5 is of interest in this connexion ; it shows the variation of fN (proportional to $\dot{\theta}$) with a for plates of copper, fN being plotted as ordinate and a as abscissa. The upper curve shows the relation between the two quantities when the frequency is 2000 the second curve relates to a frequency of 1750 the third to a frequency of 1500 the fourth to a frequency of 1000, and the lower curve to a frequency of 750. For a material of high resistivity such as bismuth the curves would be of similar form ; the curves would, however, be displaced in the direction of larger values of a (*cf.* fig. 3).

The curves of fig. 5 show clearly the necessity of

satisfying the two conditions stated above. They show, for example, that $\dot{\theta}$ decreases very rapidly on either side of $a=a_0$. They show also that the value of $\dot{\theta}$ at the optimum thickness increases with increasing frequency. Finally, they show that $\dot{\theta}$ for a plate of non-optimum thickness at a high frequency can exceed $\dot{\theta}$ for a plate of optimum thickness at a lower frequency.

Fig. 5.

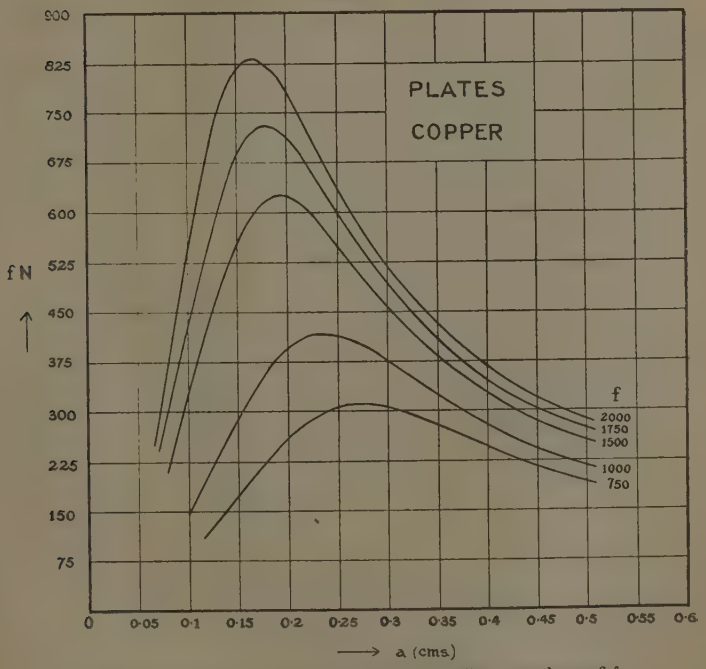

Family of (fN, a) curves for copper, for different values of f.

The importance of using as high a frequency as possible is obvious, and in practice the upper limit is determined by the accuracy required in the measurement of the change in power, $(W-W_0)$, or the quantity $I^2(R-R_0)$ of equations (1.8) (1.9), and (1.10). It is difficult to measure these quantities accurately in the radio-frequency range, but as shown in Part II. (Section 2 (*d*)) of this work,

accurate measurements are possible in the audio-frequency range, *i. e.*, with frequencies up to about 2500 ; for this reason it was decided to use frequencies within this range in the present work. It should be noticed that, as shown in the next Section, even with this restriction as to frequency the method can be used with practically any metallic conductor. The method, however, will not be applicable to substances of very high resistivities such as aqueous solutions, since, as shown above, the optimum thickness for an aqueous solution at a frequency of 1500 is about 580·8 cm., whilst the rate of rise of temperature for a " plate " of aqueous solution 1 cm. thick at a frequency of 3600 is only about 5×10^{-5} that of a similar plate of copper at the same frequency. It may be added that for the aqueous solution the frequency corresponding to an optimum " plate " thickness of 1 cm. is about 5×10^{8} ; this frequency corresponds to electromagnetic waves whose wave-length is 0·6 metre.

(vii.) *Numerical Examples.*

The orders of magnitude of $\dot{\theta}$ and $(R-R_0)$ may be estimated as follows. In the experiments described in Part II. of this work the number of turns per cm. of the coil was approximately 56, the coil-current was of the order of 0·2 ampere ; hence H_e was approximately 14·1 oersted and H_e^2 about 200 (oersted)^2. Hence, from equations (2.2 *b*) and (2.4 *b*),

$$C=\frac{\mu H^2}{2Jsd}=\frac{2\cdot392\times10^{-6}\times\mu}{sd},$$

$$D=8\pi^2n^2\mu=2\cdot477\times10^{5}\mu.$$

Assuming that the plates are of optimum thickness,

$$N=N_0=0\cdot4172.$$

Hence from the same equations

$$\left.\begin{aligned}\dot{\theta}\equiv\dot{\theta}_p&=C.f.N=9\cdot979\times10^{-7}\mu f/sd,\\(R-R_0)&=D.V.f.N=1\cdot033\times10^{5}\mu f.V.\end{aligned}\right\}. \quad (2.12)$$

In the case of copper

$$s=0\cdot092,\quad d=8\cdot9\text{ gm./cm.}^3,\quad \dot{\theta}_p=1\cdot219\,f\times10^{-6}.$$

If $f=2000$,

$$\dot{\theta}_p=2{\cdot}438\times10^{-3}\ ^\circ\text{C./sec.}=0{\cdot}1463\ ^\circ\text{C./minute},$$

which is a reasonable figure from the experimental standpoint. At the same frequency

$$(\text{R}-\text{R}_0)=2{\cdot}066\text{V}\times10^8\ \text{e.m.u.}=0{\cdot}2066\text{V ohm};$$

if $(\text{R}-\text{R}_0)$ is less than about 1·5 ohm the electrical measurements become inaccurate; this implies that V should exceed 7·26 c.c.

(c) *Rate of Generation of Heat at Various Points in the Core.*

In connexion with the measurement of the rise in temperature of the core in the present experiments, it is of interest to examine how $\dot{\text{Q}}$, the rate of generation of heat per unit volume of the core, varies with the distance x from the median plane of the plate. In order to be able to compare results for plates of different thicknesses it is advantageous to take x/a, the fractional distance from the median plane, as the independent variable rather than the actual distance, x. If U be the virtual value of the current-density in the core at a distance x from the median plane, then $\dot{\text{Q}}$ is equal to ρU^2. For a plate of given dimensions and material it is known that U is a function of x, the value of U being zero at the median plane and a maximum at the surface, and it follows that $\dot{\text{Q}}$ will vary in a somewhat similar manner.

According to Russell (*op. cit.* p. 497, and equation (7), p. 494)

$$\text{U}^2=\frac{(\text{A}^2+\text{B}^2)\,.\,p^2}{8\pi^2}\,.\,(\cosh 2px-\cos 2px),$$

where

$$\text{A}=\hat{h}_e\,.\,\frac{\cosh pa\,.\cos pa}{\cosh 2pa+\cos 2pa};$$

$$\text{B}=\hat{h}_e\,.\,\frac{\sinh pa\,.\sin pa}{\sinh 2pa+\sin 2pa}.$$

From the values of A and B it is found that

$$\text{A}^2+\text{B}^2=\frac{\text{H}_e^2}{\cosh 2pa+\cos 2pa},$$

and finally,

$$\dot{Q}=E.f\left\{\frac{\cosh 2px-\cos 2px}{\cosh 2pa+\cos 2pa}\right\}, \quad . \quad . \quad (2.13)$$

where

$$E=\mu H_e^2.$$

It follows that $\dot{Q}$ is zero at the medium plane, and that $\dot{Q}$ is a maximum at $x=a$. The maximum value, $\dot{Q}_a$, of $\dot{Q}$ is given by the equation

$$\dot{Q}_a=E.f\left\{\frac{\cosh 2pa-\cos 2pa}{\cosh 2pa+\cos 2pa}\right\}. \quad . \quad (2.14)$$

Let $S_a=\dot{Q}/\dot{Q}_a$; S_a is thus the rate of generation of heat at a distance from the median plane when the rate of generation of heat at the surface is unity It is desirable to consider S_a, rather than $\dot{Q}$, as dependent variable when comparing plates of different thicknesses, or when comparing the same plate at different frequencies.

From equations (2.13) and (2.14) it follows that

$$S_a=\frac{\cosh 2px-\cos 2px}{\cosh 2pa-\cos 2pa}=\frac{\cosh (cx/a)-\cos (cx/a)}{\cosh c-\cos c}, \quad (2.15)$$

where $$c=2pa.$$

S_a may thus be regarded as a function of c and the fractional distance (x/a) from the median plane.

When c is small equation (2.15) simplifies, since

$$\cosh c-\cos c=2\left[\frac{c^2}{2!}+\frac{c^6}{6!}+\ldots\right]$$

$$=c^2\left[1+\frac{c^4}{360}+\ldots\right].$$

Hence, if $c^4/360$ is small in comparison with unity,

$$S_a=\frac{x^2}{a^2}\left[1-\frac{c^4}{360}\left(1-\frac{x^4}{a^4}\right)\ldots\right], \quad . \quad . \quad (2.16)$$

and when $c^4/360$ is negligibly small

$$S_a=\frac{x^2}{a^2}.$$

The approximate value, (x^2/a^2), for S_a is accurate to at least 1 per cent. when $c^4\leqslant 3{\cdot}6$, *i. e.*, when $c\leqslant 1{\cdot}37$, and

under this condition the relation between S_a and (x/a) is parabolic.

If (x/a) be supposed to remain constant, and if c be supposed to increase, then the c^4 term in the equation (2.16) will increase numerically and S_a will decrease. Thus, in a family of curves showing the relation between S_a and (x/a) for different values of c, the parabola of equation (2.16) will represent the upper limiting curve; the curves for higher values of c lie between this limiting parabola and the (x/a) and S_a axes.

It is thus clear that the rate of generation of heat is far from uniform across the cross-section; the major part of the heat generated in any particular case is generated near the surface of the plate, and, as c increases, the concentration of heat-generation near the surface increases correspondingly.

These considerations are illustrated in the curves of fig. 6, which show S_a as ordinate plotted against (x/a) as abscissa for various values of c. In this diagram curve (i) shows the parabolic variation of S_a with (x/a) when $c \leqslant 1{\cdot}37$ approximately; curve (ii) relates to $c=2{\cdot}25$; curve (iii) to $c=4{\cdot}5$; and curve (iv) to $c=9{\cdot}0$. These curves clearly show the points mentioned above.

Assuming first that the frequency is kept constant, c will be proportional to the semi-thickness, a; curve (ii) shows the relation between S_a and (x/a) for a plate of optimum thickness; curve (i) relates to plates whose thickness is less than 0·6 of the optimum thickness; whilst curves (iii) and (iv) relate to plates whose thicknesses are respectively twice and four times the optimum thickness. As the thickness of the plate increases, the frequency remaining constant, the heat generated becomes more concentrated near the surface.

Similarly, if the thickness be constant, and if the frequency, f, be varied, c will be proportional to $\sqrt{f}$, and the curves show that the concentration of heat-generation in the neighbourhood of the surface increases with increasing frequency.

Two points of interest are clear from the above discussion :—

(1) If a thermocouple be used to measure the rise in temperature of the core, and if the thermocouple be inserted in a hole in the centre of the plate, then no heat will be generated directly in the thermocouple by

the coil-current. The temperature rise registered by the thermocouple will thus be due to the heat generated in the core.

(2) Since the heat generated in the central portion of the core is small, and since the mass of this portion contributes to the total thermal capacity of the core,

Fig. 6.

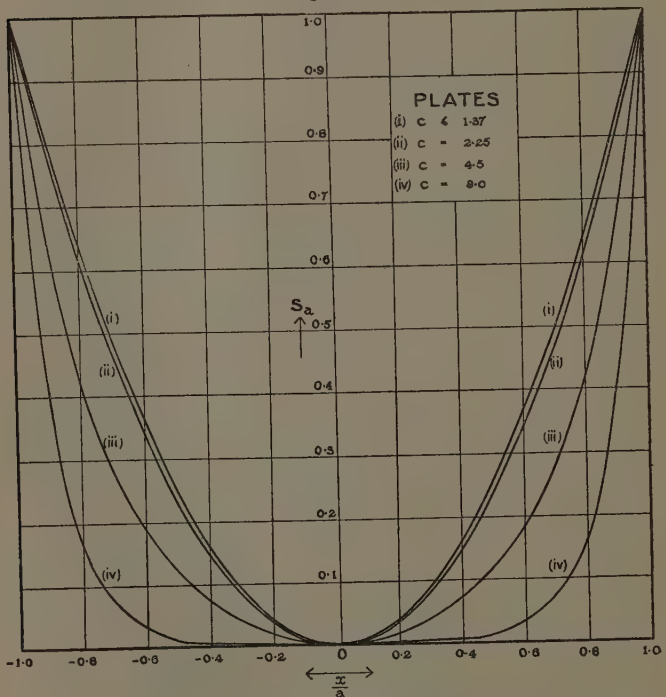

Graph of S_a against x/a for different values of c.

it follows that an increased rate of rise of temperature could be obtained by removing the central portions of the cores, *i. e.*, by using cores with hollow centres. Such a procedure was found to be unnecessary, since it would also increase the radiation correction by increasing the area exposed, and thus it was not adopted.

Since the rate of generation of heat is not uniform across a cross-section, it follows that the temperature of the core will not become uniform immediately the coil-current is switched off. In an actual experiment this will be shown by a lag between the instant of switching off the coil-current and the instant of maximum temperature of the thermocouple (inserted in the centre of the core). In practice this lag is very small even in the case of a bad conductor of heat such as bismuth or antimony.

Section 3.

Eddy-current Losses in Cylinders.

(a) *Notation.*

The cylinder and solenoids are supposed to be coaxial and infinitely long; this common axis is taken as the Oz axis. The symbols n, μ, ρ, f, ω, d, M, V, s, θ, $\dot{\theta}$, I, H_e, $\hat{h}_e$, R_0, R, and P have the significance defined above (Section 2 (a)) in the case of a rectangular plate. In addition, let

m = eddy-current parameter, defined by $m^2 = 4\pi\mu\omega/\rho = 8\pi^2\mu f/\rho = 2p^2$;

b = radius of the core;

U = virtual value of the current density in the core (in e.m.u.) at a perpendicular distance r from the Oz axis.

l = length of the core.

(b) *Eddy-current Losses in the Core.*

(i.) *General Results.*

As shown by Russell (*op. cit.* p. 506) and McLachlan (*op. cit.* p. 144), the total power P dissipated in the length l of the core is given by the equation

$$P = \frac{\rho l H_e^2}{8\pi} \cdot mb \cdot \frac{Z(mb)}{X(mb)}, \quad . \quad . \quad . \quad . \quad (3.1)$$

where $Z(mb)$ and $X(mb)$ are functions of the modified Bessel functions ber and bei and their derivatives ber′ and bei′; Z and X are defined by the equations

$$\left.\begin{aligned} Z(x) &= \mathrm{ber}\, x\, \mathrm{ber}'\, x + \mathrm{bei}\, x\, \mathrm{bei}'\, x, \\ X(x) &= \mathrm{ber}^2 x + \mathrm{bei}^2 x. \end{aligned}\right\} \quad . \quad . \quad (3.2)$$

Tables of these functions are to be found in the British Association Report for 1916, p. 118.

Since the volume V of the core is equal to $\pi b^2 l$, the rate of rise of temperature, $\dot{\theta}$, according to equation (1.9), is given by

$$\dot{\theta} = \frac{P}{JVsd} = \frac{\rho m H_e^2}{8\pi^2 b J sd} \cdot \frac{Z(mb)}{X(mb)},$$

or, substituting for m,

$$\dot{\theta} = \frac{\mu H_e^2}{Jsd} \cdot \frac{f}{mb} \cdot \frac{Z(mb)}{X(mb)} \quad . \quad . \quad . \quad . \quad . \quad (3.3)$$

It is seen that this equation is essentially of the same form as the corresponding equation (2.2) for a plate, the main difference being that the hyperbolic and trigonometric functions of equation (2.2) are replaced by the functions Z and X. In the case of the cylinder $\dot{\theta}$ is independent of the length l of the core.

According to equations (1.9) and (3.3), the change, $(R-R_0)$, in the resistance of the coil is given by

$$(R-R_0) = \frac{JMs\dot{\theta}}{I^2} = \frac{\mu H_e^2}{I^2} \cdot V \cdot \frac{f}{mb} \cdot \frac{Z(mb)}{X(mb)},$$

or, in terms of n, the number of turns per unit length of the solenoid,

$$(R-R_0) = 16\pi^2 n^2 \mu V \cdot \frac{f}{mb} \cdot \frac{Z(mb)}{X(mb)} \quad . \quad . \quad (3.4)$$

and, as in the case of the plate, $(R-R_0)$ is proportional to the volume V of the core, but is independent of its density.

Let

$$T = \frac{1}{mb} \cdot \frac{Z(mb)}{X(mb)} \quad . \quad . \quad . \quad . \quad . \quad . \quad (3.5)$$

The function T is analogous to the function N of the equation (2.5), and in terms of T

$$\left.\begin{aligned} \dot{\theta} &= \frac{\mu H_e^2}{Jsd} \cdot f \cdot T, \\ (R-R_0) &= 16\pi^2 n^2 \mu V \cdot f \cdot T. \end{aligned}\right\} \quad . \quad . \quad . \quad (3.6)$$

In view of the close analogy between the above equations and the corresponding equations for a plate, a detailed

discussion of the equations for a cylinder will be unnecessary, and it will often be sufficient to refer to the results already derived for a plate.

Omitting the discussion of the variation of $\dot{\theta}$ and $(R-R_0)$ with n and I (see Section 2 (*b*) (ii.)), H_e, n, I, μ, s, and d will be regarded as constants, and equations (3.6) may be written

$$\left.\begin{aligned}\dot{\theta} &= 2C\,.\,f\,.\,T,\\ (R-R_0) &= 2D\,.\,V\,.\,f\,.\,T,\end{aligned}\right\} \quad . \quad . \quad . \quad (3.7)$$

where C and D are defined, as in Section 2 (*b*) (ii.), as

$$C=\mu H_e^2/2Jsd\,; \qquad D=8\pi^2n^2\mu.$$

(ii.) *Particular Cases of the General Results.*

In the extreme cases when mb is small on the one hand and large on the other hand, the function T simplifies. In this connexion the values of the parameter m may be calculated using the data given in Section 2 (*b*) (iii.). For iron $m=4{\cdot}441\sqrt{f}$; for copper $m=0{\cdot}2142\sqrt{f}$; for bismuth $m=0{\cdot}02577\sqrt{f}$; for the aqueous solution $m=1{\cdot}414\times10^{-4}\sqrt{f}$ approximately.

Case (a). *mb small.*

If mb be small, then (see Russell, *op. cit.* p. 211, equation (29))

$$\frac{Z(mb)}{X(mb)}=\frac{(mb)^3}{16}\left\{1-\frac{11}{24}\left(\frac{mb}{2}\right)^4+\ldots\right\}, \quad . \quad (3.8)$$

and, neglecting fourth and higher powers of mb in comparison with unity,

$$T=\frac{(mb)^2}{16},$$

$$\dot{\theta}=\frac{\mu H_e^{\,2}}{16Jsd}\,.\,f\,.\,(mb)^2=\frac{\pi^2}{2}\cdot\frac{H_e^2}{Jsd}\cdot\frac{\mu^2b^2}{\rho}\,.\,f^2, \quad . \quad (3.9)$$

and

$$(R-R_0)=\pi^2n^2\mu V\,.\,f\,.\,(mb)^2=8\pi^4n^2V\,.\,\frac{\mu^2b^2}{\rho}\,.\,f^2, \quad (3.10)$$

from equations (3.3) and (3.4).

These approximations are correct to at least 1 per cent. when

$$\frac{11}{24}\left(\frac{mb}{2}\right)^4 \leqslant 10^{-2},$$

i. e., when $mb \leqslant 0{\cdot}77$.

Assuming a cylinder 1 cm. in diameter, this condition implies that $f \leqslant 0{\cdot}12$ for iron, $f \leqslant 51{\cdot}6$ for copper, $f \leqslant 3573$ for bismuth, and $f \leqslant 1{\cdot}17 \times 10^8$ for the aqueous solution.

As in the case of the plate, in this region $\dot{\theta}$ and $(\mathrm{R}-\mathrm{R}_0)$ are proportional to μ^2, f^2, b^2, and $1/\rho$.

Case (b). *mb large.*

In this case (Russell, *op. cit.* p. 212, equation (35))

$$\frac{\mathrm{Z}(mb)}{\mathrm{X}(mb)} = \frac{1}{\sqrt{2}} - \frac{1}{2mb} - \ldots \quad . \quad . \quad (3.11)$$

and, if mb is large enough to allow $\left(\frac{1}{2mb}\right)$ to be neglected in comparison with $1/\sqrt{2}$,

$$\mathrm{Z}/\mathrm{X} = 1/\sqrt{2},$$

and

$$\mathrm{T} = 1/mb\sqrt{2}.$$

Hence, from equations (3.3) and (3.4)

$$\dot{\theta} = \frac{\mathrm{H}_e^2}{4\pi \mathrm{J} sd} \cdot \frac{1}{b} \sqrt{(\rho\mu f)} \quad . \quad . \quad . \quad . \quad (3.12)$$

and

$$(\mathrm{R}-\mathrm{R}_0) = 4\pi n^2 \frac{\mathrm{V}}{b} \cdot \sqrt{(\rho\mu f)}. \quad . \quad . \quad (3.12)$$

The accuracy of this approximation does not become 1 per cent. until mb is approximately 70·7, and for values of mb less than about 70·7 it is necessary to take terms in $(mb)^{-1}$ and $(mb)^{-2}$ into account. Considering a cylinder 1 cm. in diameter, the condition for 1 per cent. accuracy implies that $f \geqslant 1013$ for iron, $f \geqslant 4{\cdot}36 \times 10^5$ for copper, $f \geqslant 3 \times 10^7$ for bismuth, and $f \geqslant 10^{12}$ for the aqueous solution.

As in the case of the plate, $\dot{\theta}$ and $(\mathrm{R}-\mathrm{R}_0)$ are proportional to $1/b$, $\sqrt{f}$, $\sqrt{\rho}$, $\sqrt{\mu}$ when mb is large. It is, however, interesting to note that the asymptotic expressions (3.12) do not become valid until mb reaches the comparatively high value of about 70·7, whereas the

corresponding expressions for the case of the plate become valid when $2pa$ reaches a comparatively small value, about 5.

(iii.) *Variation of* θ *and* $(R-R_0)$ *with* b—H_e, f, μ, *and* ρ *constant.*

As in the case of a plate, if H_e, f, μ, and ρ be constant there must exist an optimum value b_0 of b at which $\dot{\theta}$ is a maximum. This can be found by plotting T against mb; a curve showing the relation between 2T and mb is given by McLachlan (*op. cit.* fig. 24, p. 145), and from this curve it is seen that T reaches a maximum value T_0 of 0·1887 when $mb=2{\cdot}5$. The optimum radius, b_0, is thus given by

$$b_0=2{\cdot}5/m=0{\cdot}2813\sqrt{(\rho/\mu f)}. \quad . \quad . \quad . \quad (3.13)$$

This equation is similar in form to the corresponding equation for a plate; it is interesting to notice that the numerical coefficient for the cylinder is about 1·57 times as large as the coefficient for the plate.

For iron $b_0=0{\cdot}5626/\sqrt{f}$; for copper $b_0=11{\cdot}67/\sqrt{f}$; for bismuth $b_0=97{\cdot}03/\sqrt{f}$; and for the aqueous solution $b_0=1{\cdot}757\times10^4/\sqrt{f}$. At a frequency of 1500, $b_0=0{\cdot}01452$ cm. for iron, $b_0=0{\cdot}3014$ cm. for copper, $b_0=2{\cdot}505$ cm. for bismuth, and $b_0=453{\cdot}6$ cm. for the aqueous solution.

Fig. 7, referring to specimens of copper and bismuth at a frequency of 1500, illustrates this point. In this figure, the radius b (in cm.) is plotted as abscissa and fT (proportional to $\dot{\theta}$) as ordinate. These curves should be compared with the corresponding curves for a plate (fig. 3). The curves of figs. 3 and 7 are seen to be of the same general form—an initial rapid increase of fT (or fN) with increasing b (or a), followed by a maximum value, and finally, a slow decrease of fT (or fN) with increasing b (or a).

Comparison of figs. 3 and 7 brings out clearly the fact that, for a given material at a given frequency, the optimum radius for a cylindrical core is about 60 per cent. greater than the optimum semi-thickness for a core in the form of a plate.

With regard to the condition for maximum change in resistance due to insertion of the core, the remarks concerning the case of a plate apply also to the case of

a cylinder, and for the reasons given in Section 2 (*b*) (iv.), it is unnecessary to consider the conditions for maximum $(R-R_0)$.

(iv.) *Variation of $\dot{\theta}$ with f—H_e, b, μ, and ρ constant.*

As for a plate, $\dot{\theta}$ is proportional to f^2 for small values of mb (see equation (3.9)), whilst $\dot{\theta}$ is proportional to $\sqrt{f}$

Fig. 7.

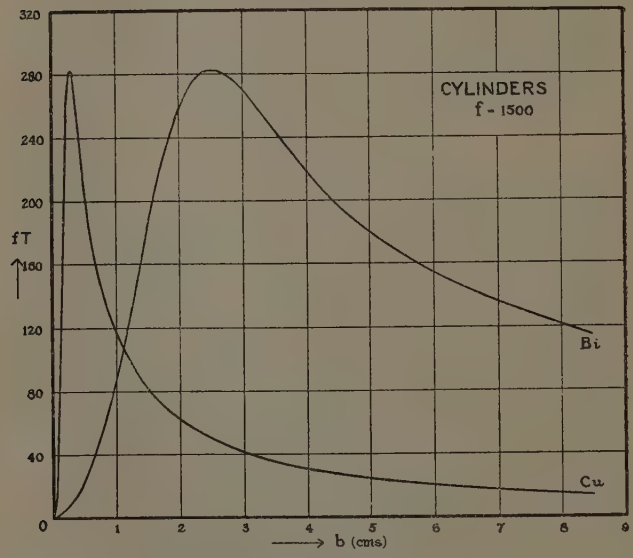

Graph of fT (proportional to $\dot{\theta}$) against b.

for large values of mb (see equation (3.12)); $\dot{\theta}$ thus increases with f, the rate of increase of $\dot{\theta}$ with f being greater for small values of mb. This is illustrated by fig. 8, which shows the variation of fT (proportional to $\dot{\theta}$) with f for a copper and a bismuth cylinder each 1 cm. diameter; in this diagram fT is plotted as ordinate and f as abscissa. In the case of copper mb is small, in the meaning of Section 3 (*b*) (ii.), for frequencies less than about 50, and large for frequencies greater than

about $4{\cdot}36 \times 10^5$; in the case of bismuth mb is small up to a frequency of about 3600, and the major part of the bismuth curve thus falls within the region of small mb. In the case of copper the curve does not reach the range of large mb within the frequency range shown in the figure, but the curve does, nevertheless, show a flattening at the larger values of f.

Fig. 8.

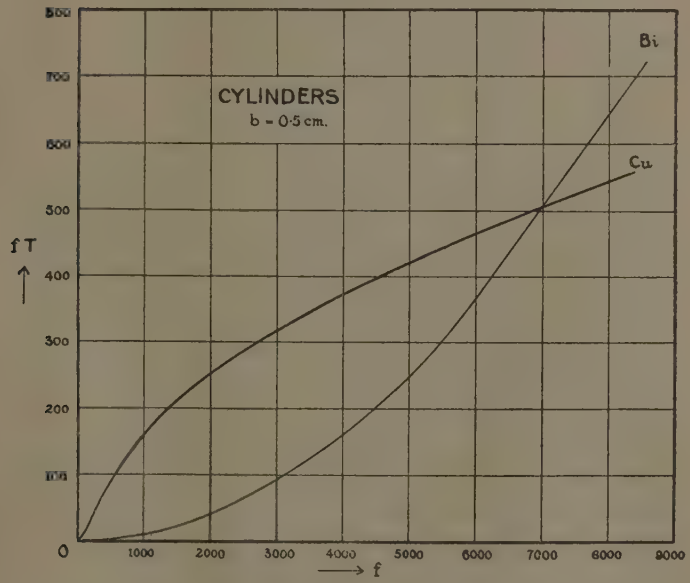

Graph of fT (proportional to $\dot{\theta}$) against f.

(v.) *Variation of* $\dot{\theta}$ *with* b, f, *and* ρ—H *and* μ *constant.*

The conclusions derived in Section 2 (*b*) (vi.) for the case of a plate clearly hold also in the case of a cylinder. The fact that the rate of rise of temperature in a badly-conducting cylinder (such as a bismuth cylinder) can exceed that in a good-conducting cylinder (such as a copper cylinder) is clearly shown in fig. 8. In the case here considered the critical frequency is about 7000; below this frequency $\dot{\theta}$ for the copper cylinder

exceeds that for the bismuth cylinder, whilst the reverse is true for frequencies above 7000. It is interesting to notice that this critical frequency is much higher for the cylinders considered here than for the plates considered in Section 2(*b*) (vi.), even though the thickness of the plates is equal to the diameter of the cylinders.

For cylinders of optimum radius, b_0, ($mb_0=2{\cdot}5$), from equations (3·7), the rate of rise of temperature $\dot{\theta}_c$ and $(R-R_0)$ are given by

$$\left.\begin{aligned}\dot{\theta} &= 0{\cdot}3774\,C.f,\\ (R-R_0) &= 0{\cdot}3774\,D.V.f,\end{aligned}\right\} \quad . \quad . \quad (3.14)$$

since, for cylinders of optimum thickness,

$$T=T_0=0{\cdot}1887.$$

Fig. 9 shows the variation of fT (proportional to $\dot{\theta}$) as ordinate with b as abscissa for cylinders of copper ; the upper curve relates to a frequency of 2000, the second to a frequency of 1750, the third to a frequency of 1500, the fourth to a frequency 1000, and the lower curve to a frequency of 750. These curves are very similar in form to the analogous curves of fig. 5, which show the relationship between fN and a for plates of copper at the same frequencies.

(vi.) *Numerical Examples.*

In order to estimate the magnitude of $\dot{\theta}$ and $(R-R_0)$, the values of the various constants given in Section 2(*b*) (vii.) may be used. Thus

$$C=\frac{2{\cdot}392\,\mu\times10^{-6}}{sd}; \quad D=2{\cdot}477\,\mu\times10^{5}.$$

Assuming that the cylinders are of optimum radius from equation (3.14),

$$\left.\begin{aligned}\dot{\theta}_c\equiv\dot{\theta} &= 0{\cdot}3774\,C.f=9{\cdot}028\times10^{-7}\,\mu f/sd,\\ (R-R_0) &= 0{\cdot}3774\,V.D.f=9{\cdot}348\times10^{4}\,\mu f.V.\end{aligned}\right\} \quad (3.15)$$

In the case of copper

$$s=0{\cdot}092, \quad d=8{\cdot}9\ \text{gm./cm.}^3,$$

and hence

$$\dot{\theta}_c=1{\cdot}103f\times10^{-6};$$

if $f=2000$,

$$\dot{\theta}_c=2{\cdot}206\times10^{-3}\ ^\circ\text{C./sec.}=0{\cdot}1324\ ^\circ\text{C./minute.}$$

At the same frequency

$$(R-R_0)=1{\cdot}870\ V\times10^8\ \text{e.m.u.}=0{\cdot}1870\ V\ \text{ohm};$$

it is necessary that $(R-R_0)$ should be at least 1·5 ohm, and hence V should exceed 8·02 c.c.

Fig. 9.

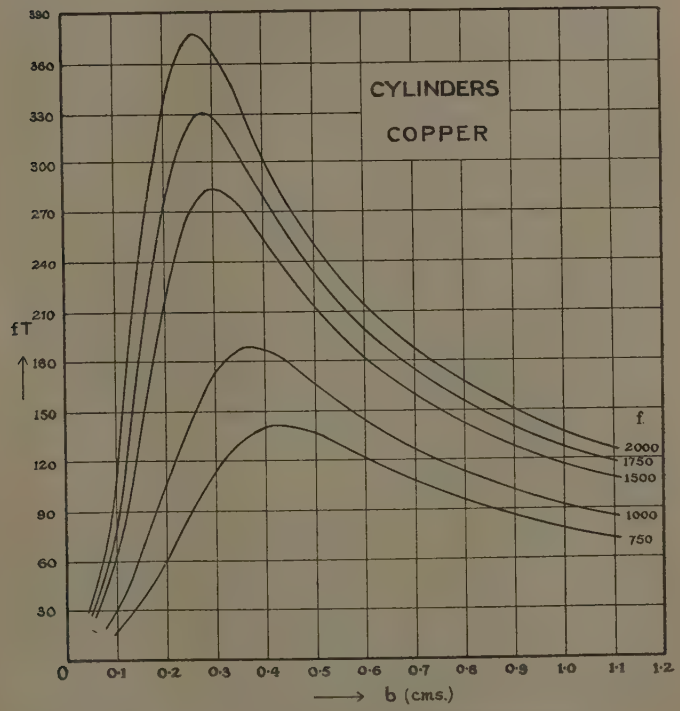

Family of (fT, b) curves for copper for different values of f.

(vii.) *Comparison of Cylinders and Plates.*

It is interesting to compare the relative advantages of cylinders and plates from the standpoint of the present work.

Taking first the optimum lateràl dimensions of specimens, it has been shown in Section 3 (*b*) (iii.) that the diameter of the optimum cylinder is about 60 per cent. greater than the thickness of the optimum plate; thus,

when dealing with metals or alloys which are difficult to procure or prepare, it is advantageous to use a plate rather than a cylinder. Further, when dealing with high-resistivity metals or alloys, the diameter of an optimum cylinder may become too large for use with coils of reasonable dimensions ; with bismuth, for example, at a frequency of 1500 the optimum diameter of a cylinder is over 5 cm., whereas the optimum thickness of a plate is about 3·2 cm. It is therefore possible to utilize plates of optimum thicknessunder circumstances which do not allow the use of cylinders of optimum diameter.

Another comparison of importance is the comparison of the rate of rise of temperature $\dot{\theta}_p$ for a plate of optimum thickness and the rate of rise of temperature $\dot{\theta}_c$ at the same frequency for a cylinder of optimum diameter and of the same material. From equations (2.11) and (3.14) $\dot{\theta}_p/\dot{\theta}_c=1{\cdot}105$, and thus, under these conditions, a plate gives a rate of rise of temperature approximately 10 per cent. greater than the cylinder. The ratio of the change in the resistance of the coil, $(R-R_0)$, in the two cases is also equal to 1·105, provided that the volumes of the cylinder and the plate are equal. From the standpoint of rate of rise of temperature and change in coil resistance there is thus little to choose between a cylinder and a plate.

In connexion with these conclusions it should again be emphasized that the theory on which they are based is only approximate (see Section 1). The results for the cylinder are, however, likely to be more accurate than those for the plate ; in the case of a plate it has been assumed that both the length and breadth are very large in comparison with the thickness, whereas in the case of a cylinder it has been assumed that the length is very large in comparison with the radius.

(c) *Rate of Generation of Heat at Various points in the Core.*

If U be the virtual value of the current density in the core, at distance r from the axis, then (see Russell, *op. cit.* p. 505)

$$U^2=\frac{\mu H_e^2}{2\rho}.f.\frac{V(mr)}{X(mb)}, \quad . \quad . \quad . \quad (3.16)$$

where

$$V(mr)=\mathrm{ber}'^2\, mr+\mathrm{bei}'^2\, mr.$$

The rate of generation of heat, $\dot{Q}$, at distance r from the axis is ρU^2, and thus

$$\dot{Q} = F.f\frac{V(mr)}{X(mb)}, \quad . \quad . \quad . \quad . \quad (3.17)$$

where $F=\mu H_e^2/2$.

Since $X(mb)$ is finite for finite values of the argument, $V(0)=0$, and since $V(mr)$ increases from $mr=0$ to $mr=1$, it follows that $\dot{Q}$ is zero at the axis and a maximum at the surface of the cylinder. If $\dot{Q}_b$ be the value of $\dot{Q}$ at the surface, then

$$\dot{Q}_b = F.f.\frac{V(mb)}{X(mb)}. \quad . \quad . \quad . \quad . \quad (3.18)$$

Hence, if $S_b=\dot{Q}/\dot{Q}_b$,

$$S_b = \frac{V(mr)}{V(mb)} = \frac{V(c'r/b)}{V(c')}, \quad . \quad . \quad . \quad . \quad (3.19)$$

where $c'=mb$.

S_b is clearly the rate of generation of heat at a fractional distance (r/b) from the axis when the rate of generation of heat at the surface is unity. S_b may be regarded as a function of c' and the fractional distance (r/b).

For small values of the argument, $V(x)$ becomes

$$V(x) = \frac{x^2}{4}\left\{1+\frac{1}{2}\left(\frac{1}{1!}\right)^2\cdot\frac{1}{3!}\left(\frac{x}{2}\right)^4+\cdots\right\}$$

$$= \frac{x^2}{4}\left\{1+\frac{x^4}{192}+\cdots\right\}$$

(see Russell, *op. cit.* p. 211).

Hence, if $(c'^4/192)$ is small in comparison with unity,

$$S_b = \frac{r^2}{b^2}\left\{1-\frac{c'^4}{192}(1-r^4/b^4)-\cdots\right\} \quad . \quad (3.20)$$

and, if $c'^4/192$ may be neglected in comparison with unity,

$$S_b = \frac{r^2}{b^2}. \quad . \quad . \quad . \quad . \quad . \quad . \quad (3.21)$$

Equation (3.21) is accurate to at least 1 per cent. when $c'^4 \leqslant 1{\cdot}92$, *i. e.*, when $c' \leqslant 1{\cdot}18$; under these conditions the relation between S_b and (r/b) is parabolic. Equations (3.20) and (3.21) are of the same form as equation (2.16) of Section 2 (*c*), and it is thus unnecessary to discuss

in detail the variation of S_b with (r/b), since it is very similar to the variation of S_a with (x/a) in the case of plates.

Fig. 10 shows the variation of S_b (as ordinate) with (r/b) (as abscissa) ; in this diagram curve (i) shows the parabolic variation of S_b with (r/b) when $c' \leqslant 1{\cdot}18$;

Fig. 10.

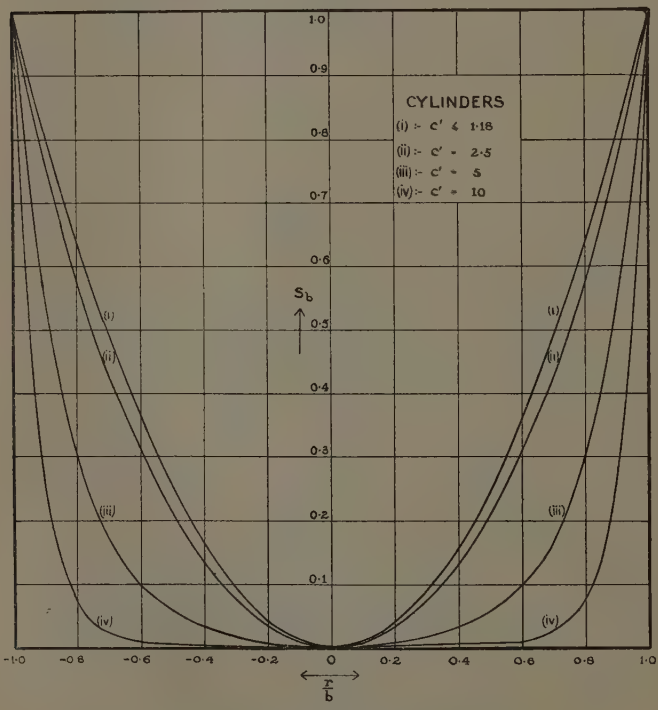

Graph of S_b against r/b for different values of c'.

curve (ii) relates to a cylinder of optimum radius $(c' = 2{\cdot}50)$ whilst curves (iii) and (iv) relate to c' equal to 5 and 1 ; respectively.

As in the case of a plate, the rate of generation of heat across the cross-section is not uniform ; the main part of the heat generated is concentrated near the surface, and the concentration near the surface increases as the

frequency increases and as the thickness of the plate increases beyond the optimum thickness. This implies that an increased rate of heating could be obtained by using specimens in the form of hollow cylinders ; but, as in the case of plates, this was not found to be necessary. The non-uniformity of generation of heat does, however, suggest an alternative method of determining the specific heats of materials of high resistivity, whether solids such as antimony or bismuth, or liquids such as aqueous solutions or organic liquids ; as shown above, for this class of material, at audio-frequencies, the optimum diameter of a cylinder or the optimum thickness of a plate is large for a metal of high resistivity and impracticably large for a liquid (see Sections 2 (*b*) (iv.), and 3 (*b*) (iii.).

The suggested method consists in using a hollow cylinder (or plate) of material of low resistivity such as copper, the external diameter of the cylinder (or the thickness of the plate) being approximately equal to the optimum diameter ; with a metal of high resistivity a cylindrical core of appropriate diameter of this metal is driven tightly into the hollow cylinder (or plate), whilst for use with a liquid the hollow cylinder is closed at its lower end, and the liquid is placed in the vessel thus formed. In a composite cylinder formed in this way, the generation of heat occurs in the outer portion, and the central portion is heated by conduction and convection from the outer portion. From a knowledge of the thermal capacity of the composite cylinder and the thermal capacity of the hollow cylinder and the mass of the core the specific heat of the core can be calculated. This method has been successfully used with bismuth which was cast in the form of cylinders of approximately 0·6 cm. radius, but was found to be less accurate in the case of liquids (see Sections 5 and 6 of Part II. of this work).

4. *References.*

(1) Thomson, ' The Electrician,' xxviii. p. 599 (1891).
(2) Ewing, ' The Electrician,' xxviii. p. 631 (1891).
(3) Heaviside, ' The Electrician,' xiii. p. 583 (1884).
(4) Russell, ' Alternating Currents,' vol. i. Chapter xx. (Cambridge, 1914).
(5) McLachlan, ' Bessel Functions for Engineers,' Chapter ix. (Oxford, 1934).
(6) Burch and Davis, Phil. Mag. i. p. 768 (1926); and ' Theory of Eddy-current Heating ' (London, 1928).
(7) Strutt, *Ann. d. Physik*, lxxxii. p. 605 (1927).
(8) Strutt, *Ann. d. Physik*, viii. p. 777 (1931).

LIX. *Heat Loss by Natural Convection from Vertical Cylinders.* *By* J. B. Carne, *B.Sc.* (*London*), *Assistant in the Physical Laboratory, South Metropolitan Gas Company* *.

Introduction.

THE subject of heat loss by convection has been a most fertile one for investigations both theoretical and experimental. That such is the case is only to be expected when the numerous technical applications of data of this subject are considered. It is therefore surprising to find that no reliable data of a systematic investigation of the dependence upon diameter and length of the natural heat loss by convection from a vertical cylinder of dimensions met in practice are available [1]. The frequency with which such data are required prompted the author into undertaking the investigations herein described. It was also thought that such an investigation would provide material for testing the theories of the mechanism of heat transfer by convection and the various mathematical relations deduced from them. Experimental investigations most closely resembling that of the author are those of Péclet [1a] and Hughes [1b].

Péclet describes his determinations of the rate of cooling of cylinders of various lengths and diameters filled with water and with mercury. He was greatly troubled with the effect of the ends, and as a consequence, expressed dissatisfaction with the accuracy of the results he obtained. In spite of this his general conclusions have been substantially confirmed indirectly by later workers. The law of variation with diameter which he deduced was based on determinations made on cylinders only 20 cm. high, and since extrapolation in this region is unjustified the law has only very limited applications. Furthermore, convection and radiation were not separated.

Hughes [1b], in his account of experiments on the heat loss from steam-heated cylinders when subjected to forced convection, also provides results of the loss by

* Communicated by J. S. G. Thomas, D.Sc.

natural convection from cylinders of various diameters. The conditions under which the heat loss occurred were peculiar to the arrangement of the apparatus he used, and from inspection these results are so inconsistent that they appear to be of little value. Hughes himself ignored them except as corrections to his major determinations. Further references to work indirectly relevant to the present investigation are made later in the discussion of the experimental results of this investigation.

Experimental Method.

The relation between the heat loss by natural convection from a body and its excess temperature over that of the incident air is well established [2] as being $h_c \propto \theta^{(4/5)}$; consequently determinations at one value only of θ are necessary. This fact and the simplicity of the apparatus required resulted in the steam condensation method being used. The radiation correction to be applied was minimized by using highly polished aluminium tubes, the emissivity of which is small and well known. This correction was calculated. Corrections for the loss of heat from the ends of the cylinders and for the loss of water by evaporation from the condensed water were both determined by experiments.

Apparatus.

All the experiments except those on cylinders longer than 7 feet were made in a room $12 \times 8 \times 10$ feet high. Exchange of air between the room and its exterior was naturally effected through an air brick at floor level and a hole 18 in. diameter in the ceiling. Cylinders longer than 7 feet were set up in the main Physical Laboratory of the South Metropolitan Gas Company. Absence of draughts was indicated by the vertical drift of steam or smoke in the locality of the cylinder. Fig. 1 shows diagrammatically the arrangement of the apparatus. All the tubes leading to and from the cylinder and the water-trap were well lagged with cotton wool. The ends of all tubes of $\frac{3}{4}$ in. and more in diameter were closed with 1 in. thick cork bungs, through which passed the steam supply and exhaust tubes. The outer end of the bung was fitted flush with the end of the tube. In the case of smaller diameter tubes the connexions with the tubes

S and E were made with rubber tube. Radiation from the steam generator to the cylinder was prevented by the double shield shown, and excess steam escaping

Fig. 1.

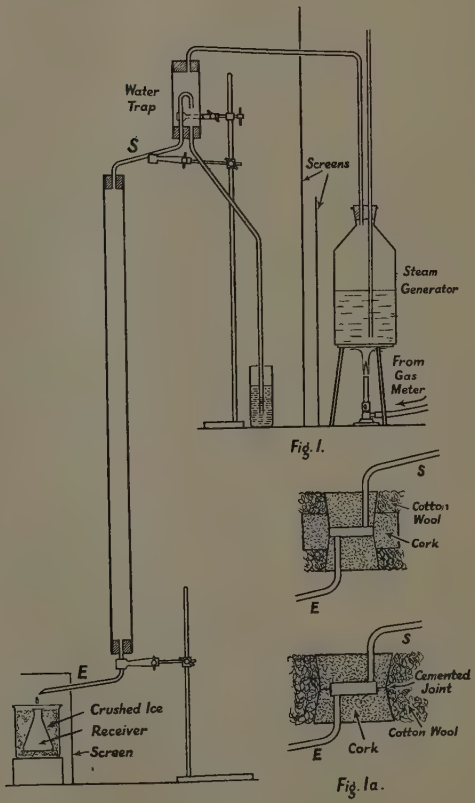

from the exhaust tube was prevented from drifting near to the cylinder by another shield also indicated in the diagram. The receiver for the water of condensation was a 100 c.c. conical glass flask, immersed to the mouth in crushed ice, and carefully placed with

the mouth $\frac{1}{2}$ inch below the end of the tube E, so that no steam impinged on the flask. The average temperature of the enclosure walls was obtained from three thermometers, the bulbs of which were plastered to the wall of the room at suitable positions. The temperature of the air at a point about 18 inches from the lower end of the cylinder was measured with an N.P.L. certified thermometer, which was shielded and over which the air was aspirated in order to avoid error due to radiation.

Experimental Procedure.

Preliminary experiments showed that a steady thermal state was established between the heated cylinder and its surroundings at approximately 15 minutes after steam had commenced passing through the cylinder, and that the rate of absorption of water by a cork bung $1\frac{1}{2}$ in. diameter after steam had passed through the cylinder for 30 minutes was less than 0·3 grm. per hour. It was also shown by experiment that so long as steam issued from the exhaust tube the quantity of condensation was constant to within 2 per cent. when the rate of gas consumption of the steam generator burner was varied from 1950 B.Th.U./hr. to 4600 B.Th.U./hr. The rate of gas consumption of the generator burner was throughout the experiments within these limits.

Collection of condensate was commenced after steam had passed continuously for at least 30 minutes. The period of collection varied from 10 minutes for the largest tubes to 60 minutes for the smallest.

It was obvious that an accurate determination of the heat loss from the tubes S and E and the cork ends of the cylinders was necessary, especially in the case of the short cylinders. In order to reproduce the conditions of experiment closely for this determination the cork bungs and the tubes were arranged as shown in fig. 1 *a*.

Collection of condensate was commenced after steam had passed through the tubes for 30 minutes. In this method of procedure the same thermal conditions were realized and the same quantity of water was absorbed by the cork as when fitted in the cylinder. The small error due to the latter was thus eliminated, since it occurred in both determinations.

During the time that drops of condensation were forming on the end of the tube E and while they were falling into the receiver evaporation from them took place. The apparatus and method devised to determine the quantity lost by evaporation at various rates of dropping are described in the appendix to this paper.

Calculations.

Total Heat Loss from the Cylinder Surface.

$$H_T = \{(W+E)-(w+e)\}\ 539{\cdot}3 \text{ calories per hour}$$
$$= W_c\ 539{\cdot}3 \text{ calories/hr.},$$

where

H_T = total heat lost from cylinder surface per hour,

W = weight of condensate from cylinder, the supply and exhaust tubes, and the cylinder ends per hour,

w = weight of condensate from the supply and exhaust tubes and the cylinder ends per hour,

E = water lost by evaporation from the quantity W per hour,

e = water lost by evaporation from the quantity w per hour,

539·3 = the latent heat of steam at 100° C.

The quantities W and w were obtained in the manner described and the quantities E and e were read from the graph in the appendix.

Heat lost by Radiation from the Cylinder.

$$H_R = 0{\cdot}053 \times 1{\cdot}36 \times 10^{-12}\ (373^4 - T_W^4) \times 3600\ A.$$
calories per hr.,

where

0·053 = emissivity (relative to black) of polished aluminium,

T_W = average temperature of enclosure walls (° A.),

A = area of cylindrical surface.

Heat lost by Convection.

$H_c = H_T - H_R$, where H_c = heat lost from the cylinder by convection per hour.

The heat lost per unit area per second is obviously given by

$$h_c = \frac{H_c}{\text{convecting area} \times 3600}.$$

The wall thickness of the tubes was 0·102 cm., and consequently the edges of the ends of the tubes appreciably increased the convecting area in the cases of the shortest two tubes approximately 8 cm. and 15 cm. long. In these cases, therefore, the areas of the edges were added to those of the cylindrical surfaces in calculating the values of h_c.

It is assumed that for all sizes the heat loss by convection is proportional to $\theta^{5/4}$, where θ = the difference between the temperature of the surface of the cylinder and that of air remote from the surface.

Hence $h_c = \alpha\theta^{5/4}$, where $\alpha = f(\mathrm{L})\, f_1(d)$ and $f(\mathrm{L})$ and $f_1(d)$ are functions of the length and diameter of the cylinder.

Approximations have been made in assigning values to the surface temperature of the cylinder. Firstly, it was assumed that the temperature of the outer surface of the cylinder was that of the steam inside. This latter temperature was taken as the boiling-point of water at the average pressure of the steam in the cylinder, which was taken as the mean of the barometric pressure and the absolute pressure of the steam in the water-trap. Also the radial temperature gradient in the wall of the tube has been neglected, since it can be easily shown that in the case of the maximum heat loss measured the difference in temperature between the tube surfaces was less than 0·02° C. At the ends of the cylinder walls there is a longitudinal temperature gradient due to the inside of the cylinder being protected by the cork bung from steam heating. This can be shown to be approximately 0·6° C./cm., and since it extended over not more than 2·5 cm. at each end the error in the case of even the shortest cylinders was only of the order of 0·5 per cent.

Representative experimental results are set out in Tables I. and II., and on graph A are plotted all the values obtained by experiment.

In graph B, in which values of α are plotted against the lengths of the cylinders of various diameters, the character of the curves apparently indicates that there is no simple relation connecting the three factors (α, L, and d) over the complete range. Since in practice

TABLE I.

Results of Cylinders. Height 61 cm. (Polished Aluminium.)

Date.	D (cm.).	L (cm.).	W (gm.).	E (gm.).	w (gm.).	e (gm.).	W_c (gm.).	Wall temp. °C.	Air temp. °C.	Steam temp. °C.	H_T calories per hr.	H_R calories per hr.	H_c calories per hr.	θ °C.	$\frac{H_c}{\theta^{5/4}}$	α.
16.10.36..	0·475	60·5	28·44	1·0	10·71	0·5	18·23	18·5	19·0	100·2	9815	284	9530	81·2	39·4	121·3 $\times 10^{-6}$
13.10.36..	0·635	60·0	29·94	1·05	10·71	0·5	19·78	16·6	17·5	100·2	10,720	383	10,340	82·7	415	96·2
7.10.36..	1·905	61·0	48·68	1·5	10·12	0·5	39·6	15·0	15·5	100·2	21,350	1180	20,170	84·7	78·5	59·7
7.10.36..	1·905	61·0	47·04	1·45	10·12	0·5	37·9	16·0	16·4	100·2	20,440	1170	19,270	83·8	76·0	57·9
13.10.36..	3·81	60·5	71·59	1·77	14·65	0·7	57·98	17·2	18·0	100·2	31,270	2310	28,960	82·2	117·0	44·9
14.10.36..	3·81	60·5	70·63	1·75	14·65	0·7	57·0	16·6	17·4	99·9	30,740	2320	28,420	82·5	114·3	43·9
10.10.36..	5·71	60·7	98·55	2·1	15·14	0·7	84·81	15·3	16·1	100·2	45,780	3520	42,260	84·1	166	42·3
10.10.36..	5·71	60·7	102·0	2·12	15·14	0·7	88·28	15·4	16·6	100·2	47,620	3520	44,100	83·6	175	44·5
14.10.36..	7·62	61·0	121·64	2·32	15·0	0·7	108·3	17·9	18·8	99·9	58,390	4620	53,800	81·1	221	42·1
14.10.36..	7·62	61·0	119·4	2·3	15·0	0·7	106·0	18·5	19·3	99·9	57,220	4600	52,600	80·6	218	41·4
14.10.36..	7·62	61·0	127·1	2·37	19·1	0·8	109·6	18·5	19·8	99·9	59,100	4600	54,500	80·1	228	43·4
15.10.36..	7·62	61·0	127·7	2·37	19·1	0·8	110·2	17·5	18·7	99·8	59,430	4620	54,800	81·1	225	42·9

Table II.

Results. Diameter of cylinders 3·81 cm. (Polished Aluminium.)

Date.	L (cm.).	W (gm.).	E (gm.).	w (gm.).	e (gm.).	W_c (gm.).	Wall temp. °C.	Air temp. °C.	Steam temp. °C.	H_T calories per hr.	H_R calories per hr.	H_c calories per hr.	θ °C.	$\frac{Hc}{\theta^{5/4}}$	α.
27.10.36..	7·62	29·37	1·02	18·75	0·8	10·84	17·2	17·6	99·8	5850	290	5560	82·2	22·5	66·2 $\times 10^{-6}$
27.10.36..	7·62	28·96	1·02	18·75	0·8	10·43	14·5	14·6	99·8	5620	296	5320	85·2	20·6	60·5
27.10.36..	7·62	29·26	1·02	18·75	0·8	10·73	14·7	14·5	99·8	5790	296	5490	85·3	21·2	62·5
23.10.36..	15·24	34·66	1·15	18·75	0·8	16·26	18·7	19·9	100·2	8770	574	8200	80·3	34·1	51·1
23.10.36..	15·24	34·74	1·15	18·75	0·8	16·34	18·7	19·9	100·2	8810	574	8240	80·3	34·3	51·3
26.10.36..	15·24	35·20	1·2	18·75	0·8	16·85	16·0	16·7	99·7	9086	586	8500	83·0	33·9	50·8
26.10.36..	30·48	47·85	1·4	18·75	0·8	29·7	16·0	17·5	99·7	16,020	1170	14,850	82·2	60·0	45·3
26.10.36..	30.48	48·45	1·43	18·75	0·8	30·33	15·5	17·4	99·7	16,350	1180	15,170	82·3	61·2	46·2
6.11.36..	36·8	54·2	1·5	17·64	0·75	37·31	15·3	16·4	99·3	20,120	1420	18,700	82·9	74·7	47·1
6.11.36..	36·8	52·7	1·5	17·64	0·75	35·8	15·8	17·3	99·2	19,310	1420	17,890	81·9	72·6	45·8
13.10.36..	60·5	71·59	1·77	14·65	0·7	57·98	17·2	18·0	100·2	31,270	2310	28,960	82·2	117·0	44·9
14.10.36..	60·5	70·63	1·75	14·65	0·7	57·0	16·6	17·4	99·9	30,740	2320	28,420	82·5	114·3	43·9
6.11.36..	80·3	98·64	2·1	17·64	0·75	82·35	16·5	17·6	99·2	44,410	3080	41,330	81·6	168·6	48·7
7.11.36..	80·3	101·3	2·1	17·64	0·75	85·01	14·6	14·7	99·2	45,840	3070	42,770	84·5	166·9	48·2
6.11.36..	91·4	110·6	2·2	17·64	0·75	94·41	16·3	17·0	99·2	50,910	3510	47,400	82·2	191·5	48·6
6.11.36..	91·4	110·5	2·2	17·64	0·75	94·31	16·4	17·0	99·2	50,860	3500	47,360	82·2	191·4	48·6
19.10.36..	91·4	114·9	2·25	18·75	0·8	97·65	16·0	16·5	99·8	52,640	3520	49,120	83·3	195·2	49·6
7.11.36..	213·8	288·0	3·6	17·64	0·75	273·21	15·0	15·3	99·2	147,300	8300	139,000	83·9	547·4	59·4
7.11.36..	213·8	286·2	3·6	17·64	0·75	271·41	15·1	15·3	99·2	146,300	8300	138,000	83·9	543·6	59·0
8.11.36..	331	461·4	4·65	17·64	0·75	447·7	13·8	13·3	99·2	246,800	12,900	228,500	85·9	873·8	61·3
8.11.36..	331	455·5	4·6	17·64	0·75	441·7	13·8	13·3	99·2	238,200	12,900	225,300	85·9	864·0	60·5
8.11.36..	331	460·4	4·65	17·64	0·75	446·7	13·8	13·3	99·2	240,800	12,900	227,900	85·9	871·4	61·1

almost all cylinders are more than 12 in. high, as far as correlation of the variables is concerned, attention has been paid only to such cylinders.

The graphs C and D show that an expression of the type $\alpha = k_1 + \frac{k_2}{d}$ connects α and d and that k_1 is a

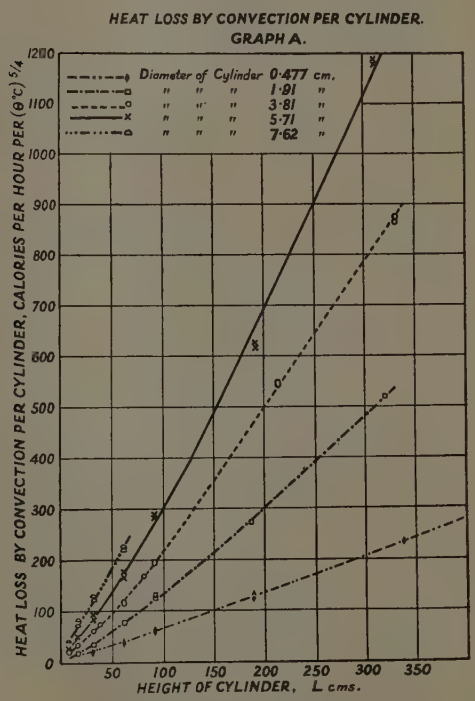

function of L. It is obvious that k_1 is the value of α when $d = \infty$, and is the value of α for a vertical plane. The small change in slope of the curves in graph D indicates that k_2 is also a function of L. However, the accuracy of the data does not justify formulating any law for this small variation.

The plot of log α for $d = \infty$ against log L in graph E, together with graph D,

show that

$$\alpha \times 10^6 = 15{\cdot}24\ L^{0{\cdot}212} + \frac{42{\cdot}7}{d},$$

is an equation which satisfactorily correlates the experimental results over the range

$$\begin{cases} L > 59 \text{ cm.} < 360 \text{ cm.} \\ d > 0{\cdot}6 \text{ cm.} < 8 \text{ cm.} \end{cases}$$

GRAPH 8.
VARIATION OF α WITH L.

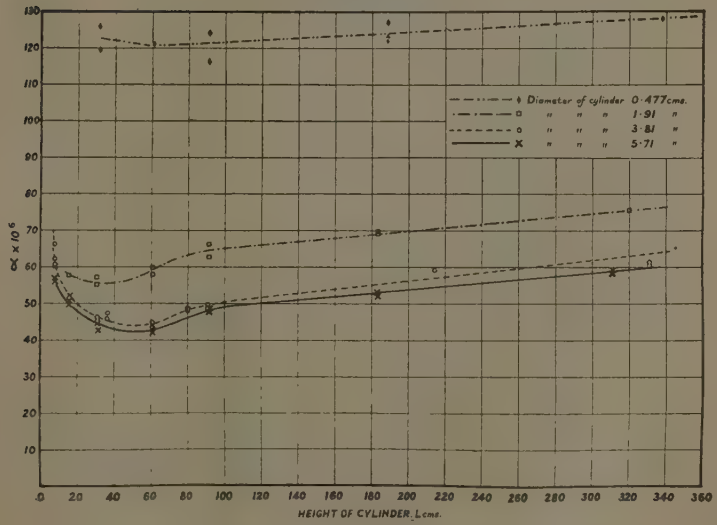

Discussion of Results.

The relation obtained for the dependence of α on d is of the same type as that found by Péclet [3] and Petavel and Lander [5] for horizontal cylinders, and by Ayrton and Kilgour [4] for horizontal wires. Although it might be anticipated from the dissimilarity of the character of the convection currents in the neighbourhood of a vertical cylinder and those near a horizontal cylinder that this relation would differ considerably for the two cases, it is to be observed that experimenters [6], [7], [8], [9], using cylinders varying in diameter from fine wires to

6 in. diam. have found that the difference of the heat loss in the two cases is of the order of only a few per cent. Each investigator found that the heat loss from a cylinder was greater in the horizontal position than in the vertical *. The results obtained, therefore, in this investigation are in general agreement with those of other workers in so far as the effect of diameter is concerned.

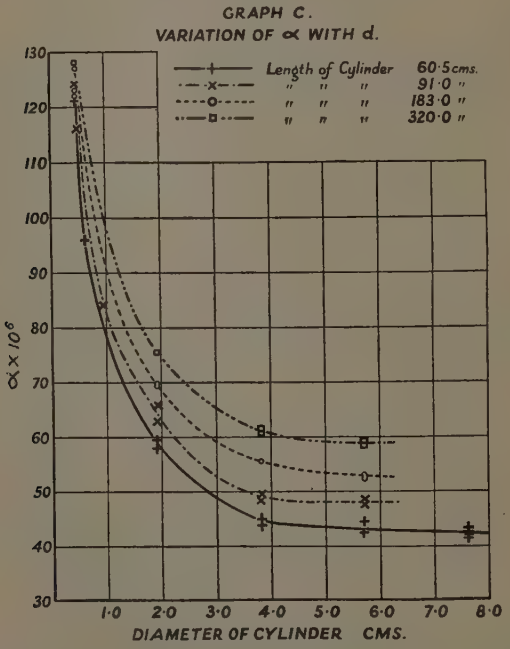

To explain the hyperbolic variation of α with d the following simple theory is suggested.

The atmosphere in the immediate neighbourhood of the hot cylindrical surface will be composed of "cold" gas molecules, the kinetic energy of which corresponds to that of gas remote from the surface, and "hot"

* In 'The Calculation of Heat Transmission' Fishenden and Saunders quote Petavel incorrectly on this point.

molecules, which have acquired an additional amount of kinetic energy as a result of impact with the hot surface. The "hot" molecules in their path away from the surface will lose their acquired K.E. by molecular impacts in a distance which will be independent of the curvature of the surface but dependent on the nature and state of the gas.

Let "a" be the distance from the hot surface at which the "hot" molecules still retain a definite large fraction of their acquired K.E.

GRAPH D.

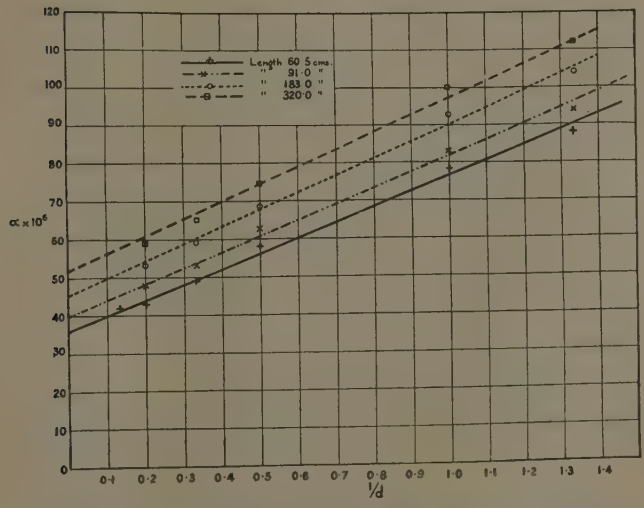

Now the magnitude of the heat transfer coefficient is assumed proportional to the density of the cold molecules in the immediate neighbourhood of the surface,

i. e., $$\alpha = K(\rho_1 - \rho_2),$$

where

ρ_1 = density of the surrounding gas,

ρ_2 = density of the "hot" molecules.

No $$\rho_2 \propto \frac{n}{v},$$

where

v=volume in which the hot molecules are distributed,

n=number of hot molecules in vol. v,

and n will be proportional to both the rate of heat loss and the area of the hot surface. For unit length of cylinder

$$n=k\alpha 2\pi r,$$

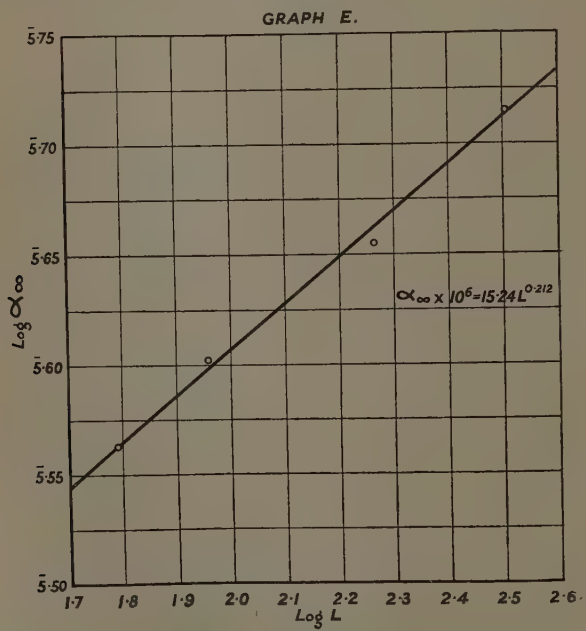

and $$v=\pi\left[(a+r)^2-r^2\right].$$

Hence $$\rho_2=\frac{k\alpha 2\pi r}{\pi(2ar+a^2)};$$

$$\therefore \quad \alpha=\mathrm{K}\left[\rho_1-\frac{2kr}{a^2+2\,ar}\right],$$

$$\alpha r(2k+2a)+a^2\alpha-2a\mathrm{K}\rho_1-a^2k\rho_1=0,$$

which is the equation of a rectangular hyperbola whose axes are

$$r = \left[\frac{-a^2}{2(k+a)}\right]; \quad \alpha = \left[\frac{a\mathrm{K}\rho_1}{k+a}\right].$$

With regard to the variation of α with L the results differ somewhat from those obtained by Griffiths and Davis [10] in respect to both the magnitude of α and its variation with L. It appears from the nature of the curves of graph C justifiable to extrapolate the results obtained to cylinders of the diameter used by these workers. When this is done it is found that α for a cylinder 6 in. diam. and 24 in. long is 40×10^{-6}, whereas the corresponding value found by Griffiths and Davis is 50×10^{-6}. This difference is probably partly accounted for by the difference in degree of roughness of the convecting surfaces with which the two sets of results were obtained. The lower value was found with a highly polished surface, whereas the higher value was found with the rough surface of an ordinary gas-pipe.

The results agree, so far as the length at which the minimum value of α occurs, but the rate of increase of α with decrease of L, for short cylinders, is less than that found by Griffiths and Davis. Clearly an erroneous allowance for the heat loss from the ends of the cylinders would result in relatively large errors in the values of α for short cylinders. In the experiments described the end losses have been determined experimentally, and it is improbable that these determinations err consistently in the same direction for each size tube.

Accepting the present conclusions as being correct, it would appear that the end corrections calculated by Griffiths and Davis are too small. Saunders [11], as a result of measurements of the heat loss from a vertical plate in air at various pressures, has also suggested that these corrections are erroneous.

Another probable explanation, however, is that in Griffiths and Davis's experiments the convection currents near the heated cylinder were considerably modified by the presence of the insulating caps, and thereby the effective length of the cylinders was altered.

The increase of h_c with L for plane surfaces of more than 2 feet high, as obtained by extrapolation, is in conflict with the mathematical deduction of Lorenz [12] that

α proportional L $^{\frac{1}{4}}$, and the conclusions based on experimental data of Griffiths and Davis [10] and Montsinger [13] that α is independent of L.

In the experiments described it is evident that the determinations are consistent among themselves to within 5 per cent., and that the corrections applied are relatively small quantities. For cylinders 2 feet and more high by far the largest correction applied is that for the heat loss from the tubes S and E and the ends of the cylinder, a correction which at the most is approximately 20 per cent. of the total heat loss. A relatively large error in this determination would obviously have little effect on the deduced value of α. Again, the correction for radiation does not exceed 8 per cent. of the total heat loss from the cylinder, and hence errors as a result of assumptions made in the calculation of this quantity also have a negligible effect on the magnitude of α.

Summary.

(1) The heat loss by natural convection from vertical cylinders of diameters from 0·5 to 7·6 cm. and heights from 7·6 to 330 cm. has been determined for temperature excesses of approximately 80° C. by the steam condensation method. The radiation correction was kept below 8 per cent. of the total heat loss, and other corrections were determined experimentally.

(2) A formula satisfying the results for the heat loss coefficient of $\theta^{5\cdot4}$ for cylinders of greater height than 30 cm. is found to be

$$\alpha \times 10^6 = 15{\cdot}24 L^{0{\cdot}212} + \frac{127}{d},$$

where $\alpha\theta^{5\cdot4}$ is the heat loss per unit area per °C., difference of temperature for a cylinder of diameter d cm., and of length L cm. in calories/sec.

(3) The variation of α with d is in general agreement with that found by previous workers, but the dependence of α on L for planes, obtained by extrapolation, is in marked disagreement with previous determinations.

Appendix.

Determination of the Loss by Evaporation from Water Drops.

For the determination of the quantity of water which evaporated from the drops the conditions under which

they were collected in the heat loss experiments were reproduced as far as possible in the experiments now described.

From experience gained by preliminary experiments

Fig. 2.

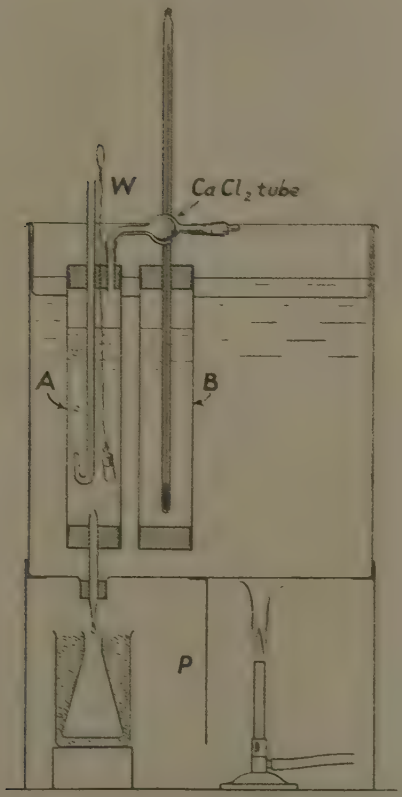

on this determination the apparatus as shown in fig. 2 was evolved. The tube A, called the container, consisted of a glass tube, approximately 1 in. diameter and 5 in. long, closed at each end by a rubber bung. Through the upper bung passed a glass vent tube, to which was connected a small bulb containing calcium chloride, for the purpose

of preventing the escape of water vapour. As in the Mariotte bottle a constant head of water was virtually maintained in the container during efflux of water by a glass tube which passed through the upper bung and admitted air at a point below the surface of the contained water. Both this tube and the calcium chloride tube were closed by a small glass plug and rubber tube. The dropping tube passed through the lower bung and was constricted at both ends. The upper end of this tube was drawn down to a fine orifice in order to restrict the flow of water, and thus the formation of drops, to the desired rate, whilst the lower end was of the diameter required for the formation of drops of the desired weight.

A glass plug which closed the upper end of this tube could be removed by a wire which was attached to the plug and which passed through the upper bung.

The plate P shown in the diagram was soldered to the tank in order to keep the products of combustion of the heating burner from the neighbourhood of the dropping tube.

In carrying out a determination the container was almost filled with distilled water, weighed and placed in the copper tank shown in the diagram, with the dropping tube projecting a few millimetres through the rubber bung in the floor of the tank. A duplicate container B, similarly filled with water and containing a thermometer, was placed in the tank close to the container A, and the tank was filledwith water so that the containers were almost completely immersed.

The receiver used in the heat loss experiments was immersed to its mouth in crushed ice contained in a beaker, and was placed with the mouth half an inch below the end of the dropping tube. The plug on the $CaCl_2$ tube was removed and the water bath heated to boiling-point and vigorous ebullition was maintained. When the thermometer in the container B indicated a temperature of approximately 98° C. the vent plug on the $CaCl_2$ was replaced, and the plug on the dropping tube was removed by pulling the wire attached to it. The plug on the Mariotte tube was also removed, and thereby air was admitted to the container. Drops then formed on the end of the dropping tube at a rate determined by the effective height of water in the container, and the dimensions of the ends of the dropping tube, assuming

other factors remained constant. When sufficient water had collected in the receiver the efflux was terminated by replacing the plug on the end of the Mariotte tube and emptying the tank. The period of efflux was observed. After removing and drying the container it was weighed. The difference between the weights of the water lost from the container and that collected in the receiver was taken as the quantity of water lost by evaporation.

The weight of the drops used in these determinations was the same as the average of those formed in the heat loss experiments.

To ascertain whether any appreciable cooling occurred during the passage of the water through the part of the dropping tube outside of the water bath experiments were made in which the tube projected in one case 3 mm. and in another case 10 mm. through the bung in the tank. The results of these experiments, which are typical of all those made, are as follows :—

Average weight of the drops 0·0224 grm.

Length of dropping tube outside the bath.	3 mm.	10 mm.
Weight of container before experiment.	93·246 grm.	94·375 grm.
After experiment	85·055 „	82·332 „
Weight of water dropped from container.	8·191 „	12·043 „
Time of efflux	15 minutes.	22 minutes.
Average temperature of duplicate container.	97·6° C.	97·5° C.
Weight of water collected in receiver.	7·925 grm.	11·657 grm.
Weight of water lost by evaporation.	0·266 „	0·386 „
Dry bulb temperature of surrounding air.	71·7° F.	68·5° F.
Wet bulb temperature of surrounding air.	58·5°	57·0°
Relative humidity	48·5 per cent.	48 per cent.
Absolute „	3·75 grains/C.ft.	3·65 grains/C.ft
Rate of dropping	32·76 grm./hr.	32·85 grm./hr.
Rate of evaporation	1·06 „	1·05 „

As the results are in agreement to within approximately 1 per cent., it was concluded that in the determinations made there was no appreciable cooling of the water during its passage to the end of the dropping tube.

Determinations were made in which the distance of

the end of the dropping tube from the mouth of the receiver differed. These showed that small variations in this distance had little influence on the quantity lost by evaporation. The drops used in these experiments were approximately 0·054 grm. in weight, and the results obtained were as follows :—

Distance of fall above mouth of receiver.	1·25 cm.	5·1 cm.
Rate of dropping	66·5 grm./hr.	70·3 grm./hr.
Rate of evaporation	2·39 „	2·55 „

Experiments in which the humidity of the air in the neighbourhood of the drops differed showed that, as far as natural variations of this condition were concerned, their effect was also negligible in these determinations. These experiments were made with drops 0·0224 grm. in weight, and gave the results :—

Absolute humidity	6·5 grains/cu.ft.	3·65 grains/cu.ft.
Relative humidity	62 per cent.	48 per cent.
Rate of dropping	32·6 grm./hr.	32·85 grm./hr.
Rate of evaporation	1·08 „	1·05 „

The final results obtained with drops of the same weight as the average of those formed in the heat loss experiments are set out in the following table and plotted on the accompanying graph :—

Rate of dropping grm./hr.	Rate of evaporation grm./hr.
6·95	0·44
32·6	1·08
32·8	1·06
32·85	1·05
37·0	1·14
50·5	1·51
53·2	1·66
54·2	1·65
90·6	2·00
99·6	2·01
161·2	2·64
229·8	3·36
252·2	3·24
443·8	4·66
561	5·07

Graph F.

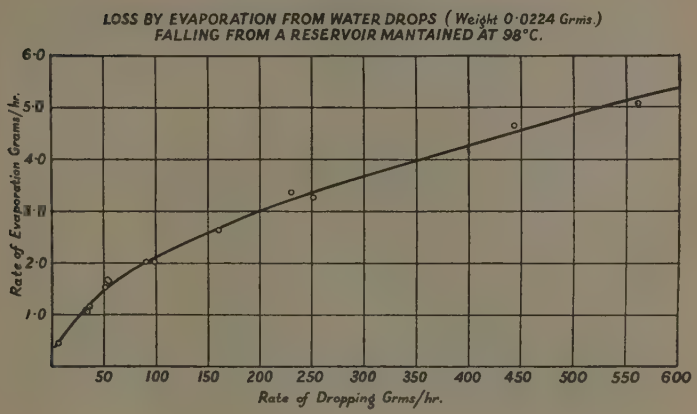

The work described above was done in the Physical Laboratory of the South Metropolitan Gas Company, and I wish to express my thanks to Dr. J. S. G. Thomas, Senior Physicist, for his kind interest during its progress, and to Mr. E. V. Evans, F.I.C., General Manager of the Company, by whose permission the results are available for publication.

References.

(1) International Critical Tables, vol. v. p. 235.
(1 *a*) ' Traité de Chaleur ' (1860), Péclet.
(1 *b*) Phil. Mag. xxxi. p. 118 (1916).
(2) R. Nelson, Phys. Rev. xxiii. p. 94 (1924).
(3) *Loc. cit.*
(4) Phil. Trans. Roy. Soc. vol. clxxxiii. p. 371 (1892).
(5) Elec. Review, vol. ii. p. 530 (1912).
(6) Petavel, Trans. Roy. Soc. vol. cxci. p. 501.
(7) Langmuir, Phys. Rev. 1912, vol. xxix. p. 403.
(8) Thomas, Phil. Mag. vol. xl. p. 640 (1920).
(9) Barratt and Scott, Proc. Phys. Soc. Journal, 1920.
(10) S.R. No. 9 D.S.I.R. Food Investigation Board.
(11) Proc. Roy. Soc. Nov. 1936 (A, vol. clvii. p. 283).
(12) Lorenz, *Ann. der Phys.* 1881, xiii. p. 582.
(13) Montsinger, American Inst. Elec. Eng. vol. xxxv. p. 599.

Physical Laboratory,
South Metropolitan Gas Company,
709 Old Kent Road,
London, S.E. 15.
November, 1936.

LX. *An Effect of X-radiation on Colloidal Carbon.* *By* J. A. Crowther, *M.A., Sc.D., Professor of Physics in the University of Reading,* H. Liebmann, *Ph.D., and* T. B. Lane, *M.Sc.**

Introduction.

IN a previous communication on the "Action of X-rays on Ferric Hydroxide Sol" [1] we reported that the effect produced by the radiation—an increase in the sensitivity of the sol towards electrolytes—did not vary monotonically with the exposure, but showed a series of maxima and minima as the exposure was uniformly increased. The phenomenon was entirely unexpected, though we have since found that a similar effect has been reported for ultra-violet light [2] [3]. These authors do not appear to have followed up the work, and their results seem to have been entirely ignored.

The effect seemed to justify further investigation, firstly because it occurred with doses of X-rays far smaller than any which had hitherto been reported as producing any chemical effect, secondly because of the difficulty of imagining any rational explanation of the form of the relation, and lastly because of its possible bearing on the problem of X-ray dosage in therapeutical work. The ferric hydroxide sol, however, was not very well suited to the work, partly because of its complex nature, but mainly because the chemical method used for determining the sensitivity of the sol was not capable of the degree of accuracy which would obviously be necessary to establish a phenomenon of this kind, nor was it capable of yielding sufficient information as to the precise nature of the effect. It was thought that direct measurement of the electrophoretic velocity of the colloid particles might give results of greater accuracy and at the same time yield more exact information as to what the effect of the radiation on the colloidal particles actually was. This has proved to be the case.

In preliminary experiments, however, we found that the measurements of electrophoretic velocities by the slit ultra microscope when used with a cell of the type first designed by Tuorila [4] were subject to considerable

* Communicated by the Authors.

variations. A theoretical investigation of the method, undertaken at our request by Dr. P. White [5], ultimately revealed unequal electrosmosis on the walls of the cell as the source of these discrepancies, and a technique was evolved by which results could be obtained which were, for any given observer, reproducible to an accuracy of the order of 2 per cent. [6]. This technique is fully described in the reference just quoted, and has been scrupulously adhered to throughout the present work.

Preparation of Sols.

For the majority of the experiments described in the present communication we have employed dilutions of aquadag in conductivity water. Aquadag is supplied in paste form, and consists of artificially prepared colloidal graphite, which, after being steeped for some time in a weak solution of tannic acid, is finally taken up with water containing a trace of ammonia. The particles are very easy to observe in the ultra-microscope, and the sol appears to contain no amicrons, so that the only particles which can be affected by the radiation are the particles actually observed. The specific conductivity of the sol is low, showing a small electrolyte content, and the sol can be preserved, under proper conditions, for months without suffering any perceptible change in properties. On the theoretical side carbon has the advantage that its absorption towards X-rays is very similar to that of water, so that it is unnecessary to consider the possibility of selective absorption effects, while its inertness and its elementary nature makes it improbable that any effects observed should be ascribed to a direct chemical action on the particles.

Some observations have also been made on an interesting sample of sugar carbon prepared by Professor Kruyt. We are indebted to Dr. Kruyt for supplying us with this material both in its negatively and positively charged form. This material, which reached us as a powder, was taken up in conductivity water, and centrifuged to remove the heavier particles. Unfortunately the sample of the positive sol proved to be unstable, the particle gradually acquiring negative charge, and only rough observations could be made on it. Details of the sols used are contained in Table I.

TABLE I.

Data of Sols Investigated.

	Graphite A.	Graphite B.	Negative sugar carbon.
Concentration gm. per litre	1·66	2·63	—
Particle number per litre	$5{\cdot}3 \times 10^{13}$	$8{\cdot}0 \times 10^{13}$	10^{11}
Spec. conductivity cm.$^{-1}$ ohm^{-1}.....	$6{\cdot}6 \times 10^{-5}$	$14{\cdot}1 \times 10^{-5}$	$1{\cdot}1 \times 10^{-5}$
Mobility: cm./sec./volt/cm. .	$1{\cdot}72 \times 10^{-4}$	$2{\cdot}21 \times 10^{-4}$	$2{\cdot}08 \times 10^{-4}$
ζ potential volts ..	$-2{\cdot}61 \times 10^{-2}$	$-3{\cdot}36 \times 10^{-2}$	$-3{\cdot}16 \times 10^{-2}$

Experimental Details.

The source of radiation was a demountable X-ray tube fitted with a palladium anticathode and excited from an A.C. high tension transformer at a peak potential of 60,000 volts. The tube was regulated so as to deliver as nearly as possible a constant output of radiation of about 0·86 r. per sec. The output was measured by an air-wall ionization chamber of the type described by Treloar [7], the ionization current being measured by a radiation integrator of the type described by Lane [8]. The sol was irradiated in a quartz dish, the position of which was adjusted so that the X-ray beam just covered its surface. The depth of the sol in the dish was 2·3 mm.; the variation of the intensity of the radiation with the depth owing to absorption in the sol was therefore relatively unimportant. In these circumstances it was considered unnecessary to stir the sol during exposure. An equal volume of the sol was measured into a similar quartz dish, and placed as close as possible to the irradiated sample during exposure (but outside the actual beam of radiation) to serve as control. In practice, however, the electrophoretic velocities of the controls did not differ appreciably from those obtained with samples taken directly from the stock. After exposure the irradiated specimens were stored in quartz test-tubes, and for measurement a sample of 0·02 c.c. was withdrawn by a micro-pipette, and diluted with 100 c.c. of conductivity water..

Experimental Results.

The results obtained are summarized in the accompanying graphs. Fig. 1 contains the results for the two dispersions of graphite for exposures between 0 and 200 r. The crosses refer to sol A, the circles are the results obtained by a different observer for sol B. The points for the maxima and minima have been frequently repeated. Their probable error is shown in Table III. The intermediate points are single observation having a standard

Fig. 1.

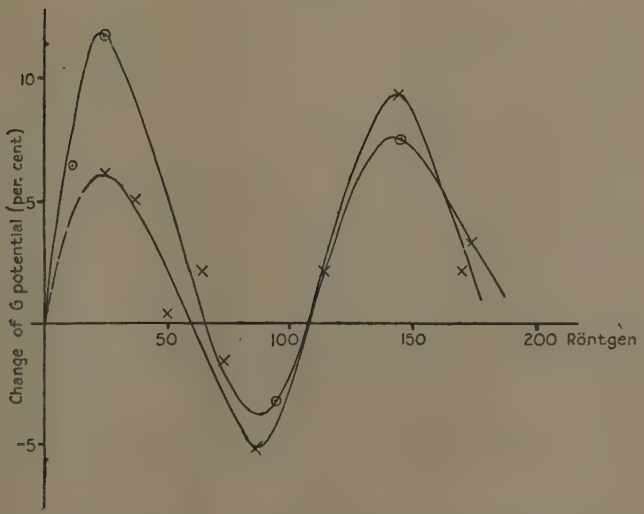

error of 2 per cent. Fig. 2 contains the observations on sol B for exposures between 1200 and 1800 r., the crosses and circles here particularizing observations made on the same sol by different observers. The points represented by circles are again the mean of several determinations. Fig. 3 contains the measurements on sugar carbon, the full curve relating to the negative sol, the dotted line to the positive one. In this figure all the points have been duplicated. The ordinates represent in all cases the percentage change in ζ potential produced by the corresponding dose of radiation measured in röntgen.

It will be seen that all the curves are of the same type. A small exposure to radiation produces an increase in the numerical value of the ζ potential which attains a maximum value for some definite dose. This dose appears to vary with the material, but is the same for different preparations of the same material. With further exposure the ζ potential gradually resumes its normal value and then falls below it, only to return to its original value if the exposure is still further increased.

Fig. 2.

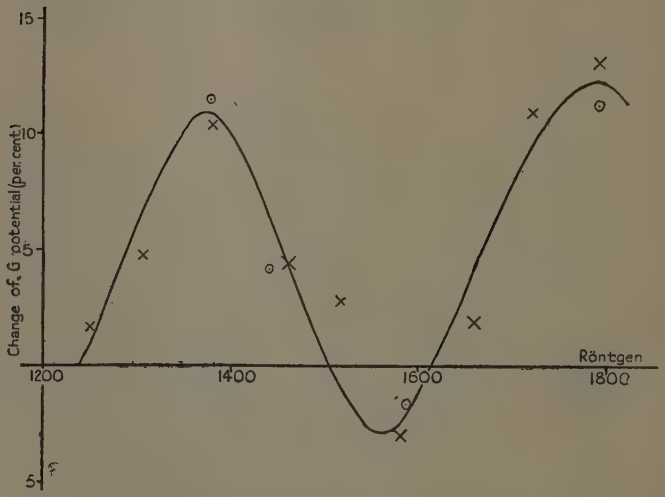

The ζ potential apparently continues to describe this cycle of changes with increasing exposure, as is shown in fig. 2, the amplitude remaining nearly constant, although the wave-length, if we may call it so, increases as the total exposure is increased. The maximum change produced in the ζ potential is of the order of 10 per cent.

Discussion of the Data.

The peculiar nature of the phenomenon described and the comparative smallness of the observed departures from the mean value of the ζ potential naturally raise the

question as to the objective reality of the effect described above. No one who has had to deal with masses of experimental observations can have failed to realize the way in which a series of quite random errors may simulate curves of the type shown in figs. 1–3. The proof of the genuineness or otherwise of the apparent

Fig. 3.

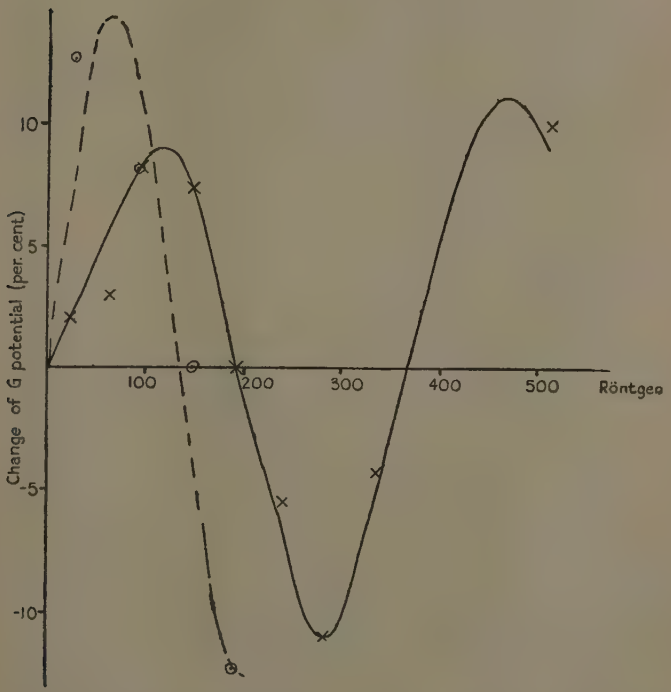

variations produced by the radiation in the ζ potential of the particles was obviously of vital importance, and we have concentrated almost exclusively on this point.

The evidence falls into three categories, which we propose to deal with separately :—(1) the accuracy of the observations, (2) the persistence of the effect, (3) the reproducibility of the effect.

(1) *Accuracy of Observation.*—This was discussed in some detail by Lane and White [6], who showed that the probable error of a single observation was of the order of 2 per cent. We have thought it proper, however, in view of the importance of the subject, to make further tests on the matter with our actual experimental data. In a complete determination of the electrophoretic velocity (from which the ζ potential is deduced) five measurements of the velocities of different particles under the electric field are made at one Smoluchowski level and repeated with the field reversed. The whole measurement is then repeated at the second Smoluchowski level. Each mobility measurement is thus the mean of measurements on twenty particles, and is automatically compensated for convection, drift, and unequal electrosmosis of the medium. The data are reduced to a standard temperature of 17° C.

The measured mobilities of individual particles differ appreciably, owing no doubt to lack of uniformity of the particles themselves. The standard deviations of the mobilities of the particles can be determined, and hence the mean standard error of the mean of twenty readings can be deduced. If no random errors are introduced by the processes of dilution of the sol and pouring it into the cataphoretic cell this should also be the standard deviation of a complete measurement of mobility. A similar test can also be applied to the irradiated sol to determine whether the operations necessary for irradiation introduce random errors into the measurements. The results of one complete test are reproduced in Table II. The measurements quoted are reciprocals of the time taken by the particle to travel a fixed distance (5×10^{-3} cm.) under a field of 8 volts per cm. It will be seen that there is no significant difference between the standard deviations calculated from the experimental values obtained for the stock and the irradiated sol and the theoretical values deduced from the mobilities of the individual particles. It seems clear, therefore, that the various operations through which the sol passes introduce no random errors of any appreciable magnitude, and that the standard error of a single complete measurement, whether of the irradiated or the unirradiated sol is not appreciably greater than 2 per cent. We are indebted to Dr. P. White for this analysis.

Analysis of the observations on the stock and controls were in agreement with this estimate of the standard error. On the other hand, measurements on the mobility of the irradiated sol near the maximum or minimum of the curve differ from the mean stock value by from three to six times the standard error. These differences are therefore statistically significant.

(2) *Persistence of the Effect.*—The experimental data for the first two maxima and the intervening minimum

TABLE II.

Statistical Test of Consistency of Observations.

	Separate fillings of stock sol.		Separate fillings of irrad. sol.	
	Dil. 1.	Dil. 2.	Dil. 1.	Dil. 2.
	350	355	406	403
	351	349	397	409
	357	353	385	396
	365	365	399	389
		357		
Mean	355·8	355·8	396·7	399·2
Standard deviation	6·9	5·9	8·7	8·7
Standard deviation of all individual particle mobilities	..	31·35	34·71	
∴ Calculated mean standard error of mean of twenty readings	..	7·0	7·7	
Observed standard error	..	6·4	8·7	
Standard error of one complete mobility measurement.	..	1·9 p. c.	2·2 p. c.	

of the curve for stock A in fig. 1 are given in Table III. The first column gives the date of the observation, the second the difference between the mobility of the irradiated sol and that of the control in the units employed in the previous table. The mean value for the control was 275. It will be seen that there is no significant change in the response of the sol throughout the month during which it was kept under observation. The scatter of the individual readings agrees with the estimate of the standard error of a single reading given in the previous section.

It may be mentioned that on 16. 2 the stock was accidentally contaminated with a small quantity of surface

active material. The sensitivity of the sol to X-rays was completely destroyed, and though measurements were made on it for some time in no case did we obtain a value for the mobility after irradiation which was significantly different from that of the unirradiated stock. As a result of this incident it was necessary to continue the experiments with a fresh preparation of aquadag, sol B.

(3) *Reproducibility of the Effect.*—The results represented by crosses in fig. 2 for exposures of sol B to doses of

TABLE III.

Data on the Persistence and Uniformity of the Effect.

Dose 26 r.		86 r.		146 r.	
Date.	I—S.	Date.	I—S.	Date.	I—S.
13.1	18	15.1	—17	25.1	16
25.1	20	19.1	—22	26.1	38
2.2	21	25.1	—11	28.1	23
4.2	12	26.1	—16	29.1	30
12.2	17	28.1	—12	30.1	28
	—		——	1.2	11
					—
Mean	18	..	—16	..	24
Percentage change..	6·5 p. c.		— 5·8 p. c.		8·7 p. c.
Standard error ...	0·7 p. c.		0·7 p. c.		1·1 p. c.

X-rays between 1200 and 1800 r. were obtained by T. B. L. between 18. 2. 37 and 4. 3. 37. As the stock was still available and showed no change in its electrophoretic mobility it was decided to have this portion of the curve investigated again by an independent observer (H. L.). His results are shown by the small circles in the graph, each point being a mean of two completely independent experiments and having a standard error of 1·5 per cent. It will be seen that the new measurements, which were made between 25. 5. 37 and 2. 6. 37, some three months after the original measurements, are in close agreement with the earlier data.

Further Discussion of Results.

With a view to investigate the genuineness of the effect attention has been concentrated mainly on neighbourhood of the maxima and minima of the graphs. For the intervening portions of the curve the observations are as yet not sufficiently numerous to fix its exact shape with any accuracy. However, in the cases where exposures between a maximum and a minimum were made points were obtained which show that the curve is continuous.

Different solutions of the same colloid, aquadag, give maxima and minima at the same points in the exposure scale, though there is some evidence that the effects produced in sol B were rather greater than those in sol A. The interval between successive maxima appears to increase with the total exposure, being some 120 r. for the first portion of the curve and about 500 r. for the portion between 1200 and 1800 r. It should be mentioned that the changes produced in the ζ potential by irradiation appear to be permanent so long as the sol is not subjected to further radiation. Irradiated sols which have been kept for a week before measurement give values of the mobility which are identical with those measured immediately after irradiation.

The negative sugar carbon (fig. 3) behaved in a similar way to the graphite sols, but required nearly three times the exposure to produce the first maximum. The experiments with the positive carbon are unfortunately incomplete as the sol appears to be unstable. The observations, however, seem to show that the effect is not confined to negative sols. Preliminary experiments which are now in progress with gold sols also show a similar oscillatory effect of the radiation on the potential. In this case, however, the initial effect of the radiation is to produce a decrease in the potential. We hope to report further on this point in the near future.

Conclusion.

The results recorded in the previous sections seem to establish the fact that quite small exposures to X-rays produce a significant change in the ζ potential of a colloid particle, and that the potential shows alternate maxima and minima as the exposure is uniformly increased. We have at present no explanation to offer for the phenomenon.

It has, however, been possible to test whether the effect is due to a large change in ζ potential of a few particles or whether all the particles are more or less equally affected by the radiation. If the change in the average mobility is due to the presence of a small number of particles with excessively high or low mobilities the scatter of the individual mobility readings should be greater for the irradiated sol than for the stock. To test this point a graphite sol was given an exposure of 27 r. (for which the effect is a maximum) and nine complete sets of twenty individual readings were made. The coefficient of variation of these 180 readings was calculated and compared with that of a similar set of readings for the unexposed sol, with the following result :—

Coefficient of variation of stock ..... $7{\cdot}98 \pm 0{\cdot}84$ (S.E.).
Coefficient of variation of irradiated ..... $8{\cdot}671 \pm 0{\cdot}6$ (S.E.).

There is a small difference between the two estimates, but it is not significant. It would appear that all the particles are more or less equally affected by the radiation.

Acknowledgments.

We are indebted to the British Empire Cancer Campaign for their generosity in defraying the expenses of this research. One of us (T. B. L.) has been in receipt of a training grant from the Department of Scientific and Industrial Research, and takes this opportunity of expressing his thanks to the Department. We have to thank the Research Board of the University of Reading for a grant covering the cost of the slit ultra microscope used in the experiments.

References.

(1) Crowther, Liebmann, and Mill, British Journ. of Radiology, ix. (new series) p. 631 (1936).
(2) Beaver and Muller, Journ. Am. Chem. Soc. l. p. 304 (1928).
(3) Schnitzler, ' Dissertation' (Cologne).
(4) Tuorila, *Kolloid Zeitschrift*, xliv. p. 15 (1928).
(5) White, Phil. Mag. xxiii. p. 811 (1937).
(6) Lane and White, Phil. Mag. xxiii. p. 824 (1937).
(7) Treloar, British Journ. of Radiology, ii. (new series) p. 188 (1929).
(8) Lane, Journ. of Scientific Instruments, xiii. p. 364 (1936).

The University of Reading.
August 20th, 1937.

LXI. *Acoustical Experiments with Telephone Receivers.*—Part I. *By* E. Tyler, *D.Sc., M.Sc., F.Inst.P., A.F.R.Ae.S., Department of Physics, Leicester College of Technology* *.

Summary.

Descriptions of various non-aural electrical methods for the measurement of the velocity of sound in air contained in various pipe systems and free air are given.

An electrically maintained telephone earpiece, energized by either a valve oscillator or oscillating neon tube is employed as the source of sound, and its frequency determined stroboscopically by the standardized A.C. mains supply at 50 cycles/sec.

Computation of the wave-length of the sound vibrations is effected by either measuring the variable reactive effects at the source (Part I.), or employing a second telephone earpiece and a two-valve amplifier as a detector of the aerial vibrations (Part II.). In each case the effects are recorded electrically and examined in terms of the resulting rectified currents. Graphical representation of such results permitted interpolation of the wave-length and final deduction of the speed of sound in air.

A further adaptation of the pipe results is mentioned whereby the natural frequency of vibration of a clamped telephone diaphragm may be ascertained.

A critical review of the various techniques usually employed in the examination of aerial vibrations within pipes is also included.

Introduction.

When an electrically maintained telephone earpiece functions as a source of sound the acoustical reaction exerted by the surrounding medium upon the diaphragm has certain repercussions upon both the mechanical impedance of the vibrator and the electrical impedance of the energizing circuit, in addition to modifying the natural frequency of vibration of the diaphragm. Such reactive effects depend upon the nature of the surrounding medium and the configuration of the space into which

* Communicated by the Author.

the sound waves are propagated. Kennelly and Pierce *, utilizing this change in electrical impedance for measuring purposes, have successfully examined the vibrational and electrical characteristics of a telephone diaphragm excited at different frequencies.

If external means are available for supplying to the vibrating diaphragm periodic acoustic damping of varying degree (*e. g.*, by means of a tunable resonating air column attached to the earpiece) the resulting effects are readily examined in terms of the small oscillating currents induced in the energizing circuit. In this direction the experiments of Mallet and Dutton †, West ‡, and Kaye and Sherratt § are particularly interesting. Mallet and Dutton, employing a Rayleigh disk, confined their attention to the measurement of the resonant frequency and decay factor of a telephone receiver under varying conditions as regards diaphragm clamping and air cavity in front and behind the diaphragm. Kaye and Sherratt, in endeavouring to complete some earlier work of Sherratt and Awbery ||, have made precision measurements over a moderate temperature range and wide frequency range (500–27,000 cycles/sec.) of the velocity of sound waves in a gas using resonating tubes of different length and diameter. The sources of sound comprised either a maintained telephone or a quartz oscillating crystal and the successive resonant lengths of air column detected electrically by observing the reactive effects at the source. This permitted computation of the wave-length, and hence, finally, the velocity of sound.

The utilization of an electrically maintained telephone receiver as a steady source of sound of controlled but variable frequency is well known, and many beautiful and instructive experiments illustrating the properties of sound waves in pipes and free air are possible, particularly those of Humby ¶ and Andrade **. Furthermore the employment of a telephone receiver purely as a detector of aerial vibrations has also many applications.

* Amer. Acad. Proc. xlviii. p. 113 (1912).
† Journ. I. E. E. lxiii. pp. 502–516 (1925).
‡ Journ. I. E. E. lxvii. p. 1137 (1929).
§ Proc. Roy. Soc. Series A, cxli. (July 1933).
|| Proc. Phys. Soc. xliii. p. 242 (1931).
¶ Proc. Phys. Soc. xxxix. part 5 (Aug. 1927).
** Proc. Roy. Soc. Series A, cxxxiv. (Dec. 1931); Phil. Trans. A, ccxxx. p. 413 (1932). Also Andrade and Lewer, 'Nature' (Nov. 9th, 1929), and Journ. Sci. Inst. p. 52 (Feb. 1930).

The desirability of adapting as recognized laboratory methods simplified experimental arrangements for the measurement of the velocity of sound in a gas has led me to investigate the possibilities of certain methods employing telephone receivers in pipes and free air, the results of which appear herein.

In aural methods of determining the speed of sound in a gas the ear is used as a detector for locating the maximum and minimum pressure variations in a sound wave. Any electrical method of recording such variations possesses distinct advantages, since not only is the personnel error eliminated but the method becomes suitable for operation by a deaf person. In the experiments described herein electrical devices are employed for computing the wave-length of the sound in free air or in pipe systems, either by measuring the reactive effects at the source due to variable air damping (Part I.), or at a second telephone receiver functioning as a detector of aerial vibrations (Part II.).

Part I.

Measurement of the Velocity of Sound in Air contained in Pipes by observing the Reaction Effects at the Source.

(a) *Pipe Systems used.*

In the first series of experiments in which the reactive effects upon the source due to variable air damping are measured three different pipe systems were used, viz. :— (1) The ordinary resonance tube (fig. 1 (*a*)), (2) Kundt's tube (fig. 1 (*b*), and (3) sliding pipes, either open or closed at remote end from the source (fig. 1 (*c*)).

Since the object of the experiments was to test their relative merits from the point of view of electrically recording the reactive effects at the source it was considered sufficient to use only air in the pipes, so that modifications in the apparatus are necessary for investigations with gases at different temperatures, and pipes of varying size *.

* Partington and Shilling, Trans. Faraday Soc. xviii. p. 386 (1923); Roberts, 'Heat and Thermodynamics,' p. 133; Parker, Proc. Phys. Soc. xlix. no. 271 (March, 1937); Dixon, Proc. Roy. Soc. A, c. p. 1 (1921); Dixon and Greenwood, Proc. Roy. Soc. A, cv. p. 199 (1924).

When fixing the maintained earpiece at one end of the pipe provision was made by means of a rubber washer

Fig. 1.

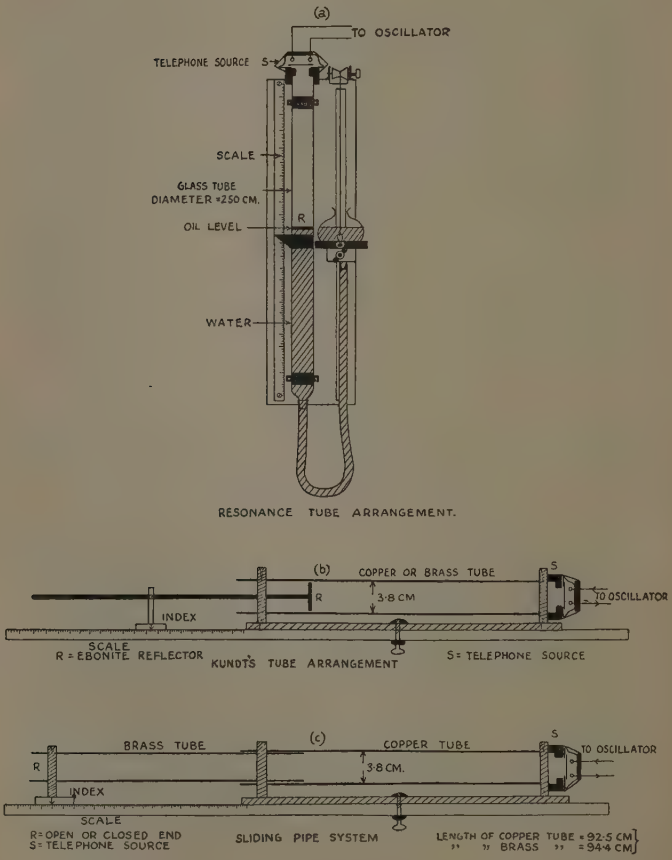

for insulating the pipe from any direct vibration that may be transmitted along its walls owing to possible direct contact between its free end and the casing of the earpiece.

(b) *Methods of Operating Source of Sound.*

The source comprised an ordinary telephone earpiece with an aperture (2·50 cm.), and was operated electrically by either a valve oscillator or oscillating neon tube. By suitable choice of inductances and capacities a wide range

Fig. 2.

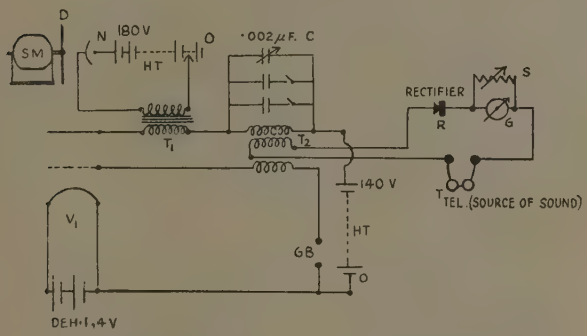

SM = Synchronous motor.
D = Stroboscopic disk.
N = Neon lamp.
R = Rectifier (photronic cell).
G = Reflecting galvo.
T = Source of sound.
T_1, T_2 = Transformers.
V_1 = DEH ·1, 4 V valve.

Fig. 3.

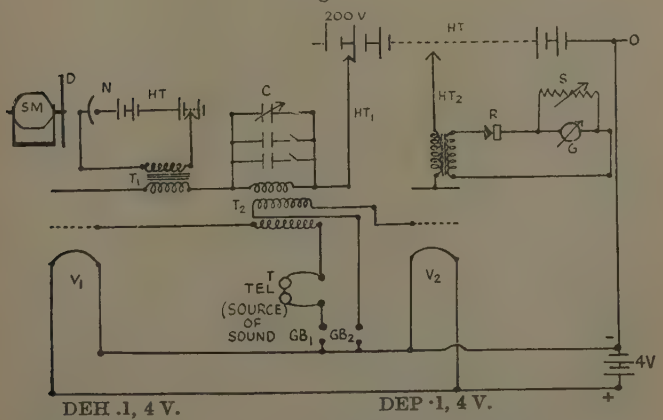

N = Neon lamp.
S = Galvo shunt.
C = Variable condenser.
T_1 = Marconiphone transformer.
T_2 = Air core transformer.
SM = Synchronous motor.
D = Stroboscopic disk.
R = Weston photronic cell rectifier.
T = Source of sound.
G = Reflecting galvo.

of frequencies is possible (200–4000/sec.), with fine adjustment for any required frequency by means of a variable oil condenser (·002 μF). When working normally at frequencies between 900–1000 in the region of the natural frequency of vibration of diaphragm (N = 950), owing to increased sensitivity due to resonance, the one valve arrangement shown in fig. 2 suffices. Outside this range an additional stage of valve amplification is necessary (fig. 3).

The oscillating neon arrangement (fig. 4) is not so sensitive and powerful in output as the valve arrangements, but, owing to the presence of harmonics and the saw tooth characteristics of the wave form of the energizing current which is desirable under certain conditions, the method

Fig. 4.

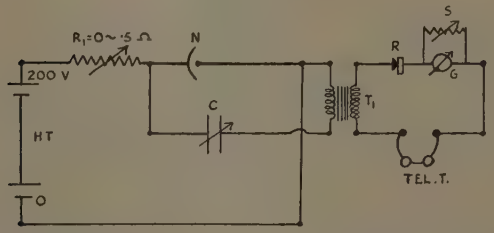

N = Oscillating neon.
C = Variable capacity.
R = Weston photronic cell or Westinghouse instrument metal rectifier.
T = Telephone source.
R_1 = Variable resistance.
T_1 = Intervalve transformer.
G_1 = Reflecting galvo.

possesses certain advantages worthy of recommending (see later).

(c) *Determination and Control of Frequency of Source.*

For precision measurement the A.C. mains supply at 50 cycles/sec. was employed as a standard source of frequency for comparison purposes, but for ordinary measurements the pitch of the source is tuned to a similar note produced on a monochord, the latter being finally calibrated with a reliable tuning-fork (512 vibrations/sec.). In determining the frequency of the source accurately, stroboscopic control is resorted to (fig. 2). The inclusion of an intervalve transformer T_1 (Marconiphone, ratio 1 : 2·50) in the plate circuit of the oscillator, and coupling

its secondary winding to a "Osglim" lamp N in series with a dry H.T. battery, provided a flashing source of same frequency as the oscillator, only when the battery voltage is adjusted initially so as to be just too small for the striking of the lamp without the oscillator working. The "Osglim" was made to illuminate a stroboscopic disk D mounted on the spindle of a synchronous motor S.M., driven from the A.C. mains at 50 cycles/sec., the speed of the disk being 50 revolutions/sec. By suitable selection of different rings containing various numbers of triangles on the disk the oscillator could be adjusted to any required frequency. The variable condenser C connected across the plate coil of the air core transformer T_2 served as a fine control for keeping the frequency constant during an experiment.

In the case of the oscillating neon method (fig. 4) the light emitted by the "Osglim" is very much weaker, but sufficient to illuminate the stroboscopic disk and so enable stroboscopic control of frequency again being utilized. Fine adjustment of control is now effected by means of the variable condenser C. It is also satisfactory to adopt the alternate monochord tuning-fork method for standardization of frequency.

(d) *Measurement of the Reactive Effects at the Source and Computation of Wave-length* (λ).

In the one-valve arrangement (fig. 2) the telephone receiver was coupled *via* a pick-up coil to the grid and plate coils of the oscillator, and also arranged in series with a rectifier R and shunted reflecting galvanometer G. By this means the induced oscillating currents in the pick-up circuit become rectified and produce a steady deflexion of the galvanometer together with an energizing pulse control of the telephone. Any change in the electrical impedance of the pick-up circuit due to variations in acoustical reaction on the telephone diaphragm causes corresponding changes in the rectification, and hence resulting variations in the deflexion of the galvanometer. It is this deflexion which is observed under the varying experimental conditions.

Referring to the two-valve arrangement (fig. 3), the pick-up coil is connected to the grid of the second valve, the plate circuit being transformer coupled to the rectifying circuit comprising the rectifier and shunted reflecting

galvanometer. The telephone receiver in the grid circuit of the first valve thus provides a very sensitive arrangement, and any change in the acoustical reaction upon the diaphragm affects automatically the grid potential of the first valve with corresponding changes in the plate current. The increased amplification then produces simultaneous variations in rectification and deflexion of galvanometer.

When using the oscillating neon device (fig. 4) the telephone earpiece, rectifier, and galvanometer are all in series in a circuit transformer coupled to the oscillating neon lamp.

Three types of rectifiers were tried, namely: (*a*) double wireless crystal, (*b*) Weston photronic cell, (*c*) Westinghouse instrument metal rectifier (1. M.A.). The double crystal, although more sensitive than the photronic cell, is susceptible to changes in sensitivity due to variations in pressure and heating effects at the contact, and with the two-valve arrangement changes in zero of the galvanometer became troublesome. For reliability the photronic cell serves admirably in conjunction with the one-valve amplifier. For a frequency range 900–1000 there is no need to shunt the galvanometer. Of the three rectifiers the Westinghouse proved most sensitive, and in certain experiments (Part II.) it was used without valve amplification. Thus in view of its cheapness (17*s*. 6*d*.)* and sensitivity its use in such acoustical measurements is to be recommended.

In each of the pipe systems the sound waves originating at the telephone diaphragm are propagated along the pipe and undergo reflexion at the other end, R, and finally arrive back at the source, where they react with the diaphragm. The phase difference between the outgoing and reflected waves at the diaphragm depends upon the pipe length. The resultant amplitude of the diaphragm at any instant depends upon the electrical driving force and the phase relationship between the two sets of waves at that instant. Upon varying the length of the air column (figs. 1 (*a*), (*b*), & (*c*)) the phase difference between the transmitted and reflected waves arriving back at the source is altered with consequent change in acoustical damping of the diaphragm.

When conditions are favourable for resonance within

* Supplied by the Westinghouse Co., Ltd.

the pipe the diaphragm vibrates with maximum amplitude, and hence production of maximum rectification and galvanometer deflexion. On gradually increasing the pipe length by any number of half wave-lengths the path difference between the transmitted and reflected waves arriving back at the source is increased by a number of wave-lengths, and resonance occurs at each setting with resulting maximum deflexion of the galvanometer.

Thus upon plotting the galvanometer deflexion or response against either the reading of the oil level (resonance tube, fig. 1 (*a*)), or reading of the index carried by the adjustable rod or sliding tube (figs. 1 (*b*) & (*c*)), curves with maxima and minima are obtained, the distance between successive maxima or minima being equivalent to half the wave-length of the sound vibrations within the pipe at the particular frequency employed.

(e) *Specimen Results for Velocity of Sound in Air contained in Pipes.*

In figs. 5 and 6 are exhibited results using the resonance tube with telephone source controlled by the valve oscillator and oscillating neon. Fig 7 (*a*) contains typical response curves for the Kundt's tube arrangement, and figs. 7 (*b*) & (*c*) results with the open and closed sliding pipes, the source being operated in each case by the valve oscillator.

With the valve oscillator controlled source, when working near the resonant frequency of the diaphragm, although larger galvanometer deflexions are obtained the peaks of the response curves are not so sharp as those corresponding to frequencies remote from that natural to the diaphragm. Reduction in sensitivity is regained by an additional stage of amplification (two-valve). The curves now show much sharper peaks (figs. 5 (*b*) & (*c*)). Two methods were adopted in computing the wave-length from the graphs : (1) with non-sharp maxima or minima, interpolation of the successive mid-points between maxima and minima, *i. e.*, along XY (figs. 5 (*a*) & (*b*)) ; (2) interpolation of the peak positions when the response curves are sharp enough.

In most cases the second method is adopted, and when sufficient peaks are available the Gaussian method is employed in deducing the wave-length. Typical results

Fig. 5.

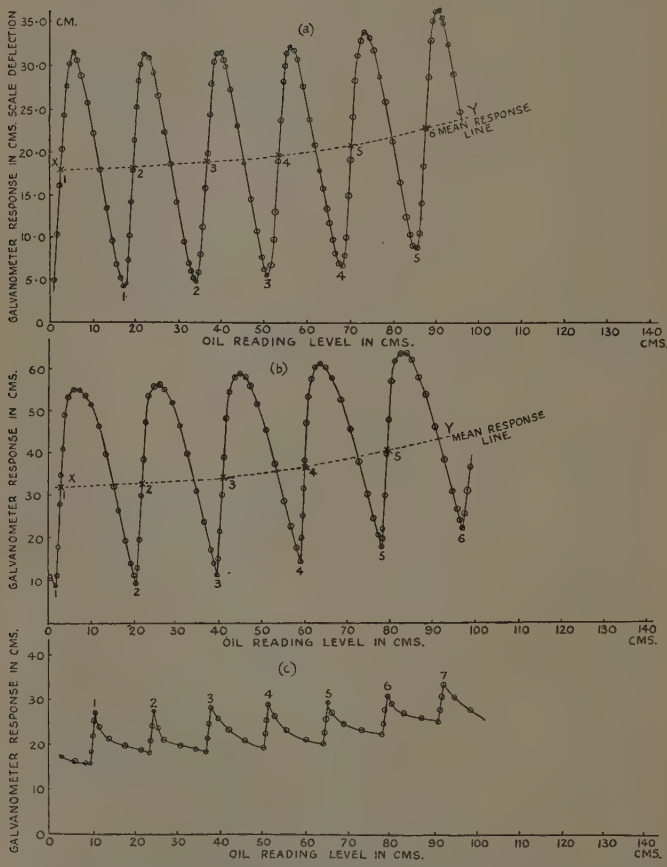

(*a*) Resonance tube results in air. Valve oscillator controlled source (fig. 2). Diameter of tube = 2·50 cm. (Glass.) N = 1000 vib./sec. Temp. = 17·5. (See Table I.)

(*b*) Resonance tube results in air. Valve oscillator controlled source (fig. 3). Tube diameter = 2·50 cm. (Glass.) N = 890 vib./sec. Temp. = 18·5° C. (See Table I.)

(*c*) Resonance tube results in air. Valve oscillator controlled source (fig. 3). Tube diameter = 2·50 cm. (Glass.) N = 1250 vib./sec. Temp. = 19·0° C. (See Table I.)

for both methods of analysis are shown in Tables I., II., and III. As an alternate method we could first observe the galvanometer deflexions at successive turning points corresponding to maxima and minima and then critically adjust the length of air column until the spot of light on the scale is coincident with the scale reading relevant to the mid-point between the successive turning points.

Fig. 6.

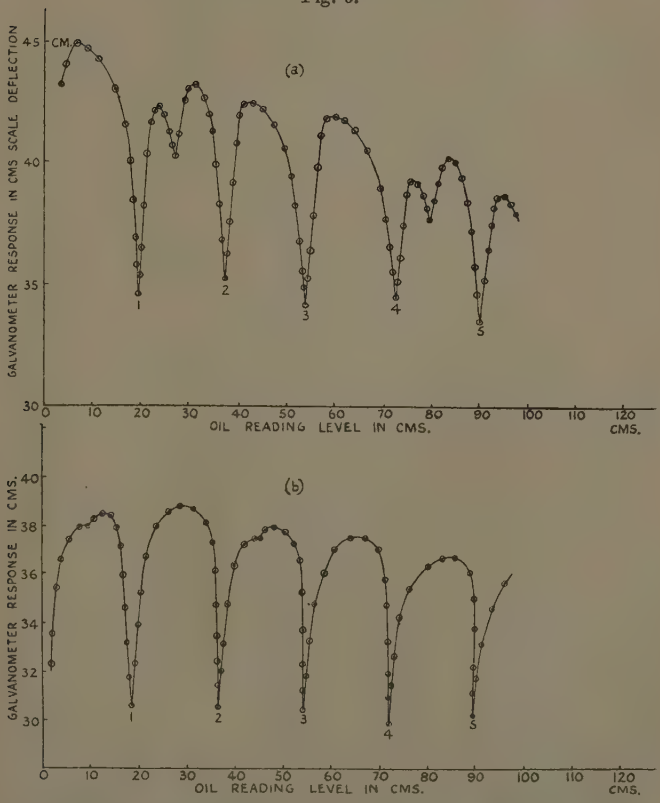

(*a*) Resonance tube results in air. Tube diam. = 2·50 cm. Oscillating neon controlled source (fig. 4). N = 322 vib./sec. Temp. = 18·5° C. (See Table II.)

(*b*) Resonance tube results in air. Tube diam. = 2·50 cm. Oscillating neon controlled source (fig. 4). N = 479 vib./sec. Temp. = 15·5° C. (See Table II.)

Fig. 7.

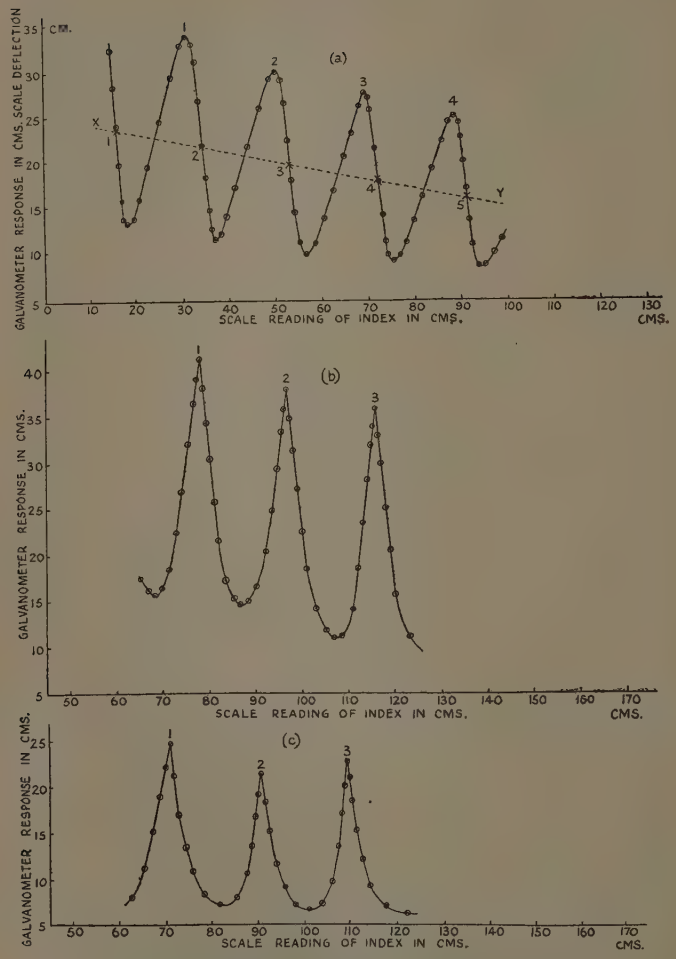

(*a*) Kundt's tube results in air. Valve oscillator controlled source (fig. 2). N=916 vib./sec. Temp.=22·5° C. (See Table III.) XY=mean response line.

(*b*) Sliding pipe results in air. Open pipe. Valve oscillator controlled source (fig. 2). N=916 vib./sec. Temp.=21·0° C. (See Table III.)

(*c*) Sliding pipe results in air. Closed pipe. Valve oscillator controlled source (fig. 2). N=916 vib./.sec. Temp.=21·0° C. (See Table III.)

The corresponding oil reading level or index reading is then observed on the attached scale, and from the series of observations made at the different resonant lengths the wave-length is obtained. In the case of the resonance tube such mid-points between successive turning points represent the conditions at which there is greatest change in resonance response for a small change in the air column.

Table IV. contains a specimen set of results obtained by this method. With reference to the results using the oscillating neon controlled source (figs. 6 (*a*) & (*b*)), although the acoustical output from the telephone is much smaller than in the case when controlled by the valve oscillator, much sharper response curves are obtained, and despite the smaller galvanometer deflexions the curves are so steep as to permit excellent interpolation of the peaks, and hence reliable values of the wave-length. Such steep response curves is an attribute of the saw-tooth characteristics of the energizing current in the telephone, derived from the oscillating neon. Reversal of the peak directions is due to a reversal in the telephone leads relative to the remainder of the circuit.

In view of the reduction in output of the oscillating neon with increase in frequency it was found advantageous to operate the telephone at a sub-multiple of its natural frequency of vibration (N_0), *i. e.*, at $N_0/2$ or $N_0/3$ etc. More acoustical energy is now available for sounding the pipe, thus giving larger galvanometer deflexions. Pre-selection of these sub-multiple frequencies enables excellent response curves to be obtained with separation distances between the peaks corresponding to a frequency N_0.

It is therefore clear that the pipe responds to the overtones of the frequency at which the telephone is driven, and if these overtones coincide with the natural frequency of the diaphragm the latter responds to the aerial vibration, thus producing marked response curves with sharp resonance peaks. Even when the telephone was driven at its natural frequency by the oscillating neon the peaks of the curves were very much smaller than those obtained with the sub-multiple frequencies. Furthermore, it was also noticeable that immediately the resonant length of pipe was reached the frequency of the source suddenly changed to a lower value, evidently due to an unstable condition existing and brought about by the sudden operation of the reaction effects due to the

Table I.

Resonance Tube Results in Air.

Valve oscillator controlled source. (Figs. 2 and 3.)
V_t = velocity of sound in air at $t°$ C. V_0 = velocity of sound in air at 0° C.

Reference curve.	Peak number or mid transit point.	Readings (cm.).	Wave-length λ (cm.).	Mean λ (cm.).	Temp. ($t°$ C.).	Frequency, N.	V_t (metres per sec.).	V_0 (metres per sec.).
Fig. 5 (*a*)...	1 (min.)	17·20	(3)–(1)	34·06	17·5	1000 (strob)	340·6	330·3
	2	34·10	=34·10					
	3	51·30	(4)–(2)					
	4	68·10	=34·00					
	5	85·40	(5)–(3)					
			=34·10					
Fig. 5 (*a*)...	1 (mid pt.)	2·25	(3)–(1)	34·17	17·5	1000 (strob)	341·7	331·2
	2	19·25	=34·10					
	3	36·35	(4)–(2)					
	4	53·50	=34·25					
	5	70·50	(5)–(3)					
	6	87·70	=34·15					
			(6) (4)					
			=34·20					

TABLE I. (*contd.*).

Reference curve.	Peak number or mid transit point.	Readings (cm.).	Wave-length. λ (cm.).	Mean λ (cm.).	Temp. (t° C.).	Frequency, N.	V_t (metres per sec.).	V_0 (metres per sec.).
Fig. 5 (*b*) ...	1 (min.)	1·50	(3)–(1)	38·25	18·5	890 (mon)	340·5	329·6
	2	20·70	= 38·20					
	3	39·70	(4)–(2)					
	4	59·00	= 38·30					
	5	78·00	(5)–(3)					
	6	97·20	= 38·30					
			(6)–(4)					
			= 38·20					
Fib. 5 (*b*) ...	1 (mid pt.)	2·80	(3)–(1)	38·21	18·5	890 (mon)	340·1	329·2
	2	22·00	= 38·20					
	3	41·00	(4)–(2)					
	4	60·15	= 38·15					
	5	79·30	(5)–(3)					
			= 38·30					
			(2λ)					
Fig. 5 (*c*) ...	1 (max.)	10·60		27·33	19·0	1250 (strob)	341·7	330·6
	2	24·40	(5)–(1)					
	3	38·00	54·70					
	4	51·75	(6)–(2)					
	5	65·30	54·70					
	6	79·10	(7)–(3)					
	7	92·60	54·60					
			Mean = 54·66					

Table II.

Resonance Tube Results in Air.

Oscillating neon controlled source. (Fig. 4.)
V_t = Vel. of sound at $t°$ C. V_0 = Vel. of sound at 0° C.

Response. curve.	Number of peak.	Readings (cm.).	Wave-length λ (cm.).	Mean λ (cm.).	Temp. ($t°$ C.).	Frequency, N.	V_t (metres per sec.).	V_0 (metres per sec.).
Fig. 6 (*a*)	1 (min.)	19·50	(3)–(1)	35·20	18·5	(N)	341·1	330·1
	2	37·50	=34·40			322		
	3	53·90	(4)–(2)			(3 N)		
	4	72·60	=35·10			966		
	5	90·00	(5)–(3)			(mon)		
			=36·10					
Fig. 6 (*b*)	1 (min.)	19·00	(3)–(1)	35·26	15·5	(N)	337·7	328·5
	2	36·50	=35·10			479		
	3	54·10	(4)–(2)			(2 N)		
	4	72·00	=35·50			958		
	5	89·20	(5)–(3)			(mon)		
			=35·20					

Table III.

Kundt's Tube and Sliding Pipe Results in Air.

Valve oscillator controlled source. (Fig. 2.)

Response curve.	Number of peak or mid-transit point.	Readings (cm.).	Wave-length λ (cm.).	Mean λ (cm.).	Temp. ($t°$ C.).	Frequency, N.	V_t (metres per sec.).	V_0 (metres per sec.).
Fig. 7 (*a*). Kundt's tube.	1 (max.)	31·00	(3)–(1)	38·00	22·5	916 (mon)	348·1	334·7
	2	50·00	=38·00					
	3	69·00	(4)–(2)					
	4	88·00	=38·00					
	1 (mid pts.)	15·40	(3)–(1)	37·80	22·5	916	346·2	332·9
	2	24·20	=37·70					
	3	53·10	(4)–(2)					
	4	72·00	=37·80					
	5	91·00	(5)–(3)					
			=37·90					
			(λ/2).					
Fig. 7 (*b*). Sliding pipe. Open end.	1 (peak)	78·40	(2)–(1)	37·60	21·0	916 (mon)	344·4	332·0
	2	97·15	=18·75					
	3	116·00	(3)–(2)					
			=18·85					
			(λ/2).					
Fig. 7 (*c*). Sliding pipe. Closed end.	1 (peak)	71·60	(2)–(1)	37·80	21·0	916 (mon)	346·2	333·7
	2	90·50	=18·90					
	3	109·40	(3)–(2)					
			=18·90					

Table IV.

Resonance Tube Results in Air by observing Oil Reading Levels corresponding to Mid Transit Points of Spot of Light moving across Scale.

Valve oscillator controlled source. (Fig. 2.)
Temp. 19·5 C. N 1000 vib./sec. (Strob).

Number of transit of spot of light.	Direction of movement, left-right or right-left.	Readings of oil level in tube. (cm.).	λ R. L. (cm.).	$3/2 \cdot \lambda$ L. R. (cm.).	Mean λ (cm.).	V_t (metres per sec.).	V_0 (metres per sec.).
1	L. R.	96·45					
2	R. L.	87·75	(2)–(6)	(1)–(7)			
3	L. R.	79·05	= 34·35	= 50·85			
4	R. L.	70·55					
5	L. R.	62·10	(4)–(8)	(3)–(9)			
6	R. L.	53·30	34·25	51·10	34·14	341·4	329·9
7	L. R.	45·60					
8	R. L.	36·30	(6)–(10)	(5)–(11)			
9	L. R.	27·95	34·30	51·00			
10	R. L.	19·65					
11	L. R.	11·10	(8)–(12) = 34·45	(7)–(13) = 50·90			
				λ 33·98 (0)			

saw-tooth characteristics of the energizing current in the telephone. The change in pitch of the note emitted by the source is so sudden as to provide a sensitive aural method of detecting accurately the resonant pipe-length. Fine control for adjusting critically the length of the air column is now essential.

Measurement of the Velocity of Sound in Free Air by Stationary Wave Method, using a Single Telephone Receiver.

The principle of this method is similar to the interferometer method adopted by Pierce * for measuring the wave-length of supersonic vibrations generated by a quartz oscillating crystal. Instead of using the quartz oscillator use is made of the maintained telephone. This is mounted vertically in the centre of a wooden baffle facing a plane reflector of glass (fig. 8), also arranged symmetrically and parallel to the telephone diaphragm. The source is kept fixed and the distance between it and the reflector varied by traversing the latter along the baseboard of an optical bench provided with a reference scale. The resulting reactions at the source are observed for each setting of the reflector in the same manner as before with the pipes. If the distance between the source and the reflector is an exact number of half wave-lengths of the vibrations in the intervening medium, stationary waves will be formed with a corresponding alteration in the reaction on the diaphragm. The magnitude of this reaction will vary accordingly as the distance between the source and the reflector is altered. In consequence, the rectified currents due to the superposed fluctuations in anode current of the oscillator pass through a series of maxima and minima as the distance between the source and reflector is increased. The observed galvanometer deflexions exhibit similar behaviour, and the distance between successive maxima or minima is a measure of the half wave-length.

Owing to the small percentage amount of the transmitted energy arriving back at the source after reflexion, increased amplification is necessary. This sometimes causes changes in zero of the galvanometer due to internal heating within the amplifier. A change in the procedure

* Amer. Acad. Arts and Sci. Proc. lx. p. 271 (1925).

of recording observations is therefore necessary; either balance out any changes in current by means of an auxiliary circuit (not shown in figs. 2 & 3), or reduce all observations relatively to those for one definite distance between the source and the reflector. Galvanometer readings for the latter condition must now be made immediately before each observation at the varying distances. Sometimes disturbances may arise owing to movement of the observer. If possible the experiment should be performed in the middle of a large empty room

Fig. 8.

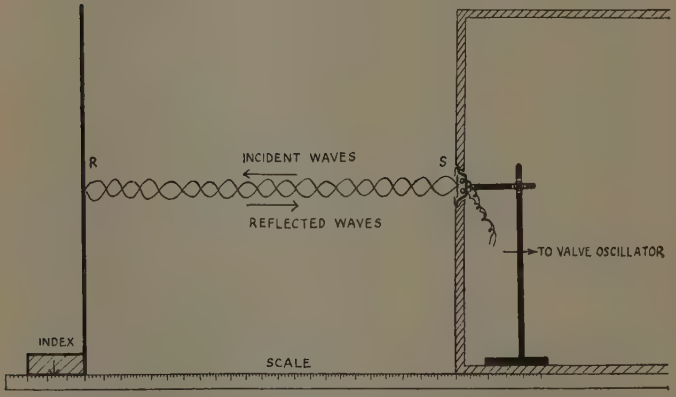

Stationary wave arrangement for measuring the velocity of sound in free air. S=maintained telephone source (fig. 3.). R=reflector.

and the observer occupy the same position while recording observations.

Specimen Results for the Velocity of Sound in Free Air using Stationary Wave Method.

Two typical response curves and results are shown in Table V. and fig. 9, using the two-valve arrangement. It will be observed there is a marked falling off in the reaction on the source as the distance between it and the reflector is increased, which, of course, is to be expected. The variations in the galvanometer deflexions between successive maxima and minima are sufficiently big enough,

TABLE V.

Results using Plane Reflector and Single Telephone (Stationary Wave Method) in Air.

Valve oscillator controlled source. (Fig. 3.)

Response curve.	Number of peak or mid transit point.	Readings (cm.).	Wave-length λ (cm.).	Mean λ (cm.).	Temp. (t° C.).	Frequency, N.	V_t (metres per sec.).	V_0 (metres per sec.).
Fig. 9 (*a*) ...	1 (peak)	39·00	(3)–(1)	40·00	22	860 (mon)	344·0	331·0
	2	58·00	40·00					
	3	79·00	(4)–(2)					
	4	98·00	=40·00					
	1 (mid pts.)	34·00	(3)–(1)	40·00	22	860	344·0	331·0
	2	54·00	=40·00					
	3	74·00	(4)–(2)					
	4	94·00	=40·00					
Fig. 9 (*b*) ..	1 (peak)	26·50	(3)–(1)	42·50	18	800 (mon)	340·0	329·4
	2	49·50	=43·00					
	3	69·50	(4)–(2)					
	4	91·50	=42·00					

however, for plotting purposes. The peaks of the curves are not so sharp as with some of the pipe results, but owing to their symmetry, interpolation of the intersecting points along the mean response line (fig. 9) is resorted to in the deduction of the half-wave-length. It is sufficient

Fig. 9.

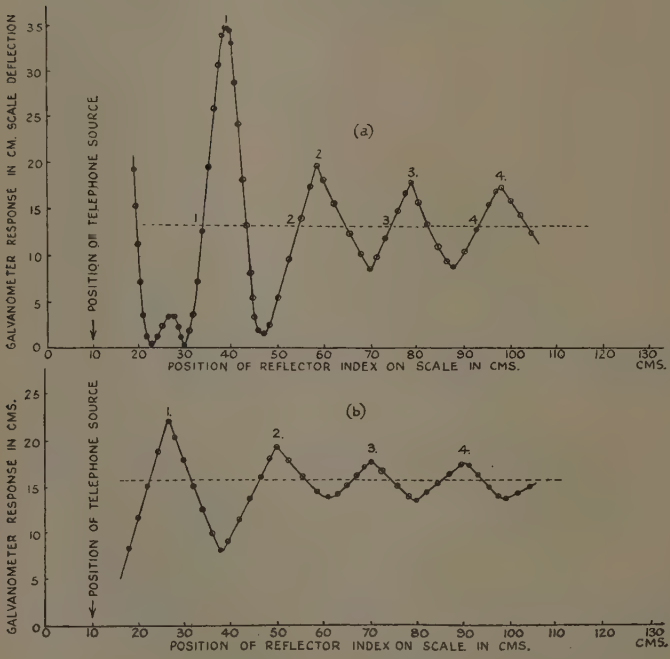

(*a*) Results by Plane Reflector—Stationary wave method. N=860 vib./sec. Temp. 22° C. (See Table V.)

(*b*) Results by Plane Reflector—Stationary wave method. N=800 vib./sec. Temp.=18° C. (See Table V.)

to note the results obtained compare well with the pipe results. A modification of this method employing a second telephone receiver is described in Part II.

(For Discussion of Results, see Part II.)

LXII. *Free Two-Dimensional Crystals of Silicon Pentoxide.* *By* N. A. Shishacow, *Colloido-Electrochemical Institute of Academy of Sciences, Moscow* *.

[Plate V.]

THE opinion is widely held that vitreous silica and pumice stone are amorphous substances. I have succeeded in obtaining, however, surprisingly good electron diffraction patterns of these substances exhibiting several prominent rings. It has been concluded on the basis of the intensity distribution that the crystals have in both cases nearly the same structure as that of high cristobalite †. There are, however, two facts which have given rise to objections against this conclusion—namely, the different character of both these substances and the many unsuccessful attempts which have been made to obtain distinct X-ray diagrams from them. The objection has been raised (Prof. A. A. Lebedeff) that the patterns might be due to the presence of some organic impurities to which the electron rays are very susceptible. It was also objected (Acad. I. W. Grebenstschikoff) that the patterns are due rather to the presence of a thin crystalline film of hydrous silica on the surface of the otherwise amorphous grains. The following experiments were carried out in order to refute these objections.

If silica, in general, is able to retain oriented organic molecules on the grain surface, then one might detect them also in the case of its crystalline modifications as well as in the case of silica gels. Experiments have shown, however, that every modification of silica yields its characteristic electron diffraction pattern. Ordinary sand, for example, yields thoroughly distinct rings of low quartz ‡.

The characteristic lines of low cristobalite (Table I.) were obtained very distinctly in the same manner from dinas brick.

These X-ray data are in good agreement with those of other investigators §.

* Communicated by the Author.

† N. A. Shishacow, 'Nature,' cxxxvi. p. 514 (1935); J. tech. Phys. (Russ.) v. p. 1834 (1935).

‡ N. A. Shishacow, *C. r. U.R.S.S.* i. (x), p. 19 (1935); see also Pl. V. fig. 1.

§ See, for instance, I. Levin and E. Ott, *Z. Krist.* lxxxv. p. 305 (1933).

Low tridymite and several silica gels are among the other modifications of silica that may be mentioned here. The first gives only a few very faint rings, most of which presumably belong to the low quartz (the specimen contained a very large amount of the latter). None of the silica gels, however, have given distinct patterns with the exception of three diffuse rings unfortunately coinciding with those of the celluloid film. It must be noted,

TABLE I.

Bragg Spacings according X-ray and Electron Reflexions from Dinas Brick.

X-ray diagram.		Average from electron diagrams.	
Very strong	4·089	Very strong	4·005
Strong	3·157	Strong	3·143
,,	2·849	,,	2·829
Very strong	2·495	Very strong	2·460
Fair	2·129	Weak	2·129
Weak	2·022	Very weak	2·032
Strong	1·930	,, ,,	1·928
,,	1·871	Strong	1·862
,,	1·684	Weak	1·656
,,	1·604	Fair	1·599
,,	1·530	Weak	1·542
,,	1·486	,,	1·478
Fair	1·427	,,	1·418
,,	1·360	Weak, broad	1·344
,,	1·329		
Strong	1·295	Weak	1·278
,,	1·276		
Fair	1·180		
,,	1·172	Strong, broad	1·171
,,	1·160		
Very strong	1·094	Weak, broad	1·084

however, that neither of these modifications of silica gives any evidence of the rings characteristic of pumice stone and vitreous silica. It follows from the above argument that these peculiar rings can hardly be due to the presence of organic impurities.

The assumption of superficial crystalline films is apparently rejected by the above check experiments and also by electron diffraction experiment with powders of pumice and tripolite that were deposited on the celluloid film in dry air*. The electron diffraction

* The mode of operations is described by myself in *C. r. U.R.S.S.* i. p. 461 (1935).

patterns obtained in this way were obviously the same as those earlier observed with pumice and vitreous silica by the method of water suspension (Table II.).

Now several other puzzolanes were systematically investigated. The samples were always prepared by drying a drop of a water suspension on a celluloid film. The results may be briefly summarized as follows. Nearly all the puzzolanes give identical electron diffraction patterns which are almost the same as those of the above mentioned vitreous silica. They differ from the latter only by the absence of some " extra " rings.

TABLE II.

Electron Diffraction from Tripolite dried at 110° C. and precipitated in dry air.

Intensities.	Bragg spacings.	Indices (compare Table III.).
Very diffuse strong ring	4·4–4·2	(100)
Strong, thin	2·529	(110)
Weak, broad	1·972 †	—
Very weak	1·646	(120)
„ „	1·454	(300)
Very weak, broad	1·203	(220) and (310)

A most astonishing fact was, finally, that exactly the same electron diffraction patterns were obtained for several clay minerals as for the puzzolanes. The only difference was that in the former case they appeared especially sharp and almost free from background (Pl. V. fig. 2).

Some good specimens of puzzolanes and of clays were mixed with pure sodium chloride, and exposures were taken again in order to obtain the most exact values of the Bragg spacings. The necessity of measuring the accelerating voltage and computing the electron wave-lengths was thus done away with. The value $a = 5{\cdot}626$ Å. was taken as the constant for the sodium chloride lattice. The results of these calculations are given in Table III.

† As the tripolite has, perhaps, sea origin, this reflexion belongs presumably to (022)—plane of NaCl.

It is seen from this table that the assumption of a hexagonal lattice leads to a satisfactory value for the constant $a=5{\cdot}161\pm$maximum 0·5 per cent., and that the indices are apparently quite regular. The most striking fact is that the third index is everywhere equal to zero. It may be noted, in addition, that such a successful identification would hardly be possible under any other

TABLE III.

Mean Bragg Spacings according Electron Reflexions from Kaolines and Puzzolanes.

Intensities.	Bragg spacings.	Constants of hexagonal lattice.	Indices of hexagonal lattice.
Very strong	4·450	5·138	(100)
„ „	2·561	5·122	(110)
Weak	2·235	5·162	(200)
Fair.....	1·688	5·157	(210)
Strong	1·491	5·165	(300)
Fair.....	1·291	5·164	(220)
„	1·240	5·162	(310)
Weak	1·120	5·173	(400)
„	1·028	5·174	(320)
„	0·974	5·154	(410)
„	0·895	5·167	(500)
Very weak	0·858	5·148	(330)
„ „	0·842	5·145	(420)
Traces.....	0·808	5·195	(510)
Not seen.....	—	—	(600)
„ „	—	—	(430)
Traces.....	0·720	5·192	(520)

assumption as to the system of the crystals in question. The low symmetrical lattices, in fact, should give rise to a much larger number of reflexions than has been observed, while the postulation of comparatively simple ones appeared impossible after checking the various assumptions with the aid of the Hull and Davey nomograms.

The above-mentioned fact that $l=0$ can only mean that crystals in question are oriented in such a manner that their basic planes lay parallel to the celluloid film,

assumed to be perpendicular to the electron beam, or that they are two-dimensional. Let us consider both of these possibilities.

Hendricks * has recently obtained beautiful electron diagrams from powdered kaolinite and anauxite. This pattern is obviously quite the same as that in Pl. V. fig. 2. Transforming the indices of the orthohexagonal cell (h_1k_1) given by Hendricks into the indices of the ordinary hexagonal cell (hk) by means of the equations

$$h=h_1,$$
$$k=\frac{k_1-h_1}{2},$$

one obtains quite the same indices as given here in Table III. Therefore the structure is the same in both cases.

In Hendrick's opinion " the clay minerals tend to break up into very thin crystalline plates that settle from the solution with their extended surfaces parallel to the surface upon which they deposit. Now if these settled aggregates are used for electron diffraction by transmission, only those planes whose normals are approximately in the surface would be expected to reflect." It is hardly possible, however, to agree with this conclusion.

The ($h\ k\ 0$) reflexions in fact should only be obtained when the cathode beam is normally incident to the celluloid film. Crystals oriented in this way should also give the ($h\ k\ l$) reflexions at other angles of incidence. This has not been observed, however. The failure to obtain distinct X-ray diagrams from the puzzolanes, while the clay minerals give in this case many good reflexions corresponding to their monoclinic structure, and the fact that the electron diagrams are identical for both, also contradicts this point of view. In fact, the chemical composition of both is very different. This may mean that the puzzolanes do not belong to the class of clay minerals and that the latter undergo a change under the influence of the electron rays leading to a structure identical with that of the puzzolanes. It seems, therefore, most probable that the electron diffraction in both cases is due to randomly distributed two-dimen-

* S. B. Hendricks, *Z. Krist.* xcv. p. 247 (1936).

sional crystals. The following considerations serve as confirmation of this assumption.

According to a recent theory of Laue * a specimen consisting of two-dimensional crystals oriented at random should give almost the same rings on transmission of monochromatic rays as those obtained in the Debye-Scherrer powder method of three-dimensional crystals. These rings must be disposed in just the same places as the corresponding (h k 0) reflexions of three-dimensional crystals.

A peculiar feature of such a two-dimensional diffraction is the asymmetrical intensity distribution across the breadth of every ring ; the intensity abruptly decreases from a maximum to small angles of reflexion, and in general more slowly to large angles.

The work of Wilm and Hofmann † experimentally confirms Laue's theory. They observed such an asymmetrical intensity distribution in the X-ray reflexions from almost wholly randomly oriented two-dimensional crystals of graphite. Very similar phenomena were also observed by Burgers ‡ with electron rays in the case of very thinly etched iron-nickel films. The electron diffraction from powders of mica apparently also belongs to the same class of phenomena §. The patterns obtained in this case have quite the same character as those of clays and puzzolanes.

The close resemblance of the electron diagrams of clays and puzzolanes may be explained in the following manner. The monclinic lattices of the clay minerals are so unstable that they disintegrate at temperatures of 400–500° C. It may therefore be imagined that they behave analogously under the influence of cathode rays, part of which are absorbed by the powder, causing the formation of amorphous alumina and free two-dimensional crystals with the composition Si_2O_5, which are, as is well known, the basic units in the structure of micas and clay minerals. These two-dimensional crystals, which are *in statu nascendi* free from any adsorbed or chemically bound substances, and which are distributed at random on the

* M. v. Laue, *Z. Krist.* lxxxii. p. 127 (1932).
† D. Wilm and H. Hofmann, *Koll. Z.* lxx. p. 21 (1935).
‡ W. G. Burgers, *Z. Krist.* xciv. p. 301 (1936).
§ A. Steinheil, *Z. Phys.* lxxxix. p. 50 (1934) ; G. I. Finch, A. G. Quarrel, and H. Wilman, Trans. Farad. Soc. xxxi. p. 1160 (1935).

celluloid film, are the cause of the surprisingly sharp and clear electron diagrams of clays. The free amorphous alumina which is admixed with such a powder of Si_2O_5 crystals has a very small effect upon the character of the electron diffraction pattern. This may be thought of as due to its small amount (about 30 per cent.), in virtue of which its influence is about the same as that of the amorphous celluloid film, so that expositions of one or two seconds are insufficient to form haloes or additional background. The puzzolanes are to be thought of as consisting of two-dimensional crystals even in their natural state. The difficulty of detecting these crystals by means of X-rays is probably due to their greater wave-length as compared with that of the electron rays, or that these crystals retain so much of adsorbed foreign substances on their surfaces that the X-ray diffraction pattern disappears from these crystals in the intense general background due to the adsorbed layers, which may be thicker than the crystals themselves. The success of electron ray investigation may be thought of as due, on the one hand, to the sufficiently small electron wave-lengths, and, on the other hand, to the influence of the vacuum, which conceivably causes the volatilization of some adsorbed layers. It may be imagined also that this cleaning of the two-dimensional crystals in vacuum is not complete, thus causing much more background on the electron diffraction patterns from puzzolanes than from clay minerals.

Now there is also the numerical evidence for the above point of view. The above-mentioned constant $a=5{\cdot}161$ Å. was found by the assumption of hexagonal system. On the other hand, it was established that all electron reflexions, which are characteristic of the puzzolanes, are observed also in the case of vitreous silica, so that their crystals are composed only of silicon and oxygen, not of any complex silicates. Therefore the infinite two-dimensional sheets, consisting of SiO_4-tetrahedra, must have here the same structure as those which are the basis of all micas and clay minerals. If, in fact, we will take instead of one parameter $a=5{\cdot}161$ Å. of the ordinary hexagonal cell the corresponding two parameters of orthohexagonal cell, *i. e.*,

$$a^1=5{\cdot}161 \text{ Å.} \quad \text{and} \quad b^1=a\sqrt{3}=8{\cdot}939 \text{ Å.},$$

we may check the latter with known parameters of micas and clay minerals. We have, thus, for

Margarite	$a^1=5{\cdot}12$	$b^1=8{\cdot}90$
Muskovite	5·17	8·94
Lepidolite	5·20	8·95
Zinnwaldite	5·26	9·07

and for

Kaolinite	$a^1=5{\cdot}14$	$b^1=8{\cdot}90$
Metahalloysite.....	5·15	8·90
Halloysite	5·20	8·92

The agreement is quite satisfactory.

Now it has to be shown that the above constant $a=5{\cdot}161$ Å. is, apparently, more exact than might seem as a result of such a comparison. These two parameters for different minerals in fact cannot be quite identical, because the Si_2O_5-sheets in three-dimensional structures are under the influence of adjacent sheets, say, of $Al(OH)_3$. The free two-dimensional crystals must have the same constant a no matter what their origin, since there is no such influence on them. The constant $a=5{\cdot}161$ Å. $\pm 0{\cdot}3$ per cent. in fact was obtained from my best measurements both for clays and puzzolanes. Why, then, did Hendricks obtain the constant $a=5{\cdot}125$ Å. as against my 5·161 Å. ?

It may be mentioned here that in my experiments the measurements of wave-lengths were made by means of sodium chloride, which have already proved successful in the study of the oxide layer of iron * and in the determination of the lattice constant of magnesia †.

In both cases the results obtained were very close to the best X-ray data. Now in Hendricks's work very thin films of metallic gold for the same purpose were used, which are hardly reliable for exact measurements. In fact, according to the recent work of Riedmiller ‡, the crystals of gold in very thin films have the lattice constant not 4·08 Å., as have the crystals of normal sizes, but about 0·8 per cent. more. If, therefore, Hendricks had taken for his computation the usual value 4·08 Å. instead of more correct 4·11 Å., this oversight might lead not

* N. A. Shishacow, *C. r. U.R.S.S.* i. p. 458 (1935).
† *Ibid.* ii. p. 164 (1934).
‡ A. Riedmiller, *Z. Phys.* cii. p. 408 (1936).

to correct constant $a = 5{\cdot}161$ Å., but just to $5{\cdot}125$ Å. It follows from this that there is hardly any difference between the two-dimensional crystals which were obtained by Hendricks from kaolinite and anauxite and which were obtained by myself from different clays and observed in the free state in several puzzolanes, *i.e.*, for all two-dimensional crystals of Si_2O_5 the constant a must be the same.

It remains now to answer the question of relationship between these two-dimensional crystals Si_2O_5 and the crystals of vitreous silica. It is quite certain that several diffraction rings of vitreous silica are the same as of two-dimensional crystals Si_2O_5; the latter are also present in vitreous silica without doubt. It is now not yet clear what is the origin of the "extra rings," which were, besides, observed in electron diffraction patterns from vitreous silica. The first assumption would be that they belong to some second crystalline phase. I am inclined to think, however, that there is no such second phase, and that these "extra rings" are due rather to the presence of third-dimension in the crystals of vitreous silica which are built up of the two-dimensional layers in such a way that the whole structure is near to the structure of high cristobalite. The fact that some crystalline modifications of silica are really built of two-dimensional identical crystals was revealed recently by Niuwenkamp * by means of X-rays. It follows from this that there is no contradiction between these and previous conclusions from my experiments.

April 27, 1937.

LXIII. *Note on certain combined Alternating Stress Systems and a Stress Criterion of the "Fatigue Limit."* By W. Mason, *D.Sc.*†

1. *Introductory. Symbols used.*

DR. H. J. GOUGH and Mr. H. V. Pollard published in 1935 [1] some results of experiments in which alternating bending and torque were applied simultaneously and in various proportions to round bars

* W. Niuwenkamp, *Z. Krist.* xc. p. 377 (1935).
† Communicated by the Author.

of steel. The bending and torque were applied in simple harmonic cycles in phase with each other; it was found that the fatigue limit was reached when the alternating direct stress was $\pm$OM (fig. 1) and the simultaneous shear stress $\pm$MN, OM and MN being the coordinates of a point N on an ellipse. The semi-axes of this ellipse, herein referred to as "Gough's ellipse," were f_1 and q_1, where $\pm f_1$ is the range of applied alternating direct stress that just induced the fatigue limit condition without any torsion, and $\pm q_1$ the range of applied alternating shear stress without any bending. These stresses were calculated on the assumption of perfect elasticity; and initially in the testing are sensibly the same as the real stresses.

Fig. 1.

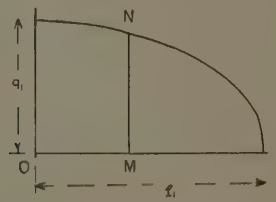

The two steels which Gough and Pollard used in this research were a 0·1 per cent. carbon steel (normalized), for which $\frac{f_1}{q_1}$ was 1·76, and a 3½ per cent. nickel chrome steel (hardened and tempered), for which $\frac{f_1}{q_1}$ was 1·55. It is convenient to express the ratio $\frac{f_1}{q_1}$ as "m," and also to write OM (fig. 1) as $af_1 = amq_1$, and MN as $q_1\sqrt{(1-a^2)}$, where a varies from 0 to 1. OM and MN then satisfy the equation to Gough's ellipse

$$\frac{\mathrm{OM}^2}{m^2{q_1}^2}+\frac{\mathrm{MN}^2}{{q_1}^2}=1.$$

In some theories concerning the criterion of change under static stresses from the elastic to the plastic state,

e. g., those of Haigh and of von Mieses, an element of volume of the material is considered; in others, *e. g.*, those of Guest and of Möhr, the criterion is sought in the limit of resistance of the material on planes within it. With alternating stressing the problem is, of course, entirely different; but there is a choice in dealing with fatigue limit conditions whether the basis shall be the consideration of a stressed element of volume or a stressed plane. In this note the latter basis is chosen.

In the experiments which established this ellipse one of the three principal stresses was always zero, and the resultant stress on any plane was therefore parallel to the plane containing the directions of the other two, viz., p_1, the larger numerically, and p_2, the smaller. The range of stress systems was from $p_2=0$ (alternating bending only) to $p_1=-p_2$ (alternating torsion only). For $p_2=0$ there is circular symmetry of stress about p_1; as p_2 increases numerically it may be shown that both normal and tangential components on a plane decrease as its normal moves, with some constant angle α to p_1, from parallelism to the plane of p_1 and p_2; but when α is greater than an angle α_1 depending on the numerical ratio $\frac{p_1}{p_2}$ the tangential stress on the plane increases slightly at first during the movement of the normal from parallelism to the plane of p_1 and p_2. The smallest value of α_1 for the stress systems of those experiments was 60°, when $p_1=-p_2$. It will appear that 45° is the largest angle that occurs in the argument of this note, and the stress systems may therefore be treated as two-dimensional. Only the stresses on planes whose normals are parallel to the plane of p_1 and p_2 (*i.e.*, planes perpendicular to a radius of the cylindrical specimen in the plane of the applied bending moment) need be considered.

2. *Representation of the Relevant Stress Systems by "Stress Circles."*

With simultaneous alternating stress applied by bending and torsion of period of cycle T, in phase, the principal stresses p_1 and p_2 at any instant t which form the same stress system as OM and MN (fig. 1) are

$$\tfrac{1}{2}[amq_1 \pm \sqrt{(a^2m^2q_1^2+4q_1^2(1-a^2))}]\cos 2\pi\frac{t}{\mathrm{T}}.$$

On a plane whose normal is inclined θ to the direction of the greater of these principal stresses, viz., p_1, the normal stress is

$$\frac{p_1+p_2}{2}+\frac{p_1-p_2}{2}\cdot\cos 2\theta$$

$$=\tfrac{1}{2}q_1[am+\sqrt{(a^2m^2+4(1-a^2))}\cos 2\theta], \quad . \qquad (1)$$

and the tangential stress is

$$\tfrac{1}{2}(p_1-p_2)\sin 2\theta=\tfrac{1}{2}q_1\sqrt{(a^2m^2+4(1-a^2))}\,.\sin 2\theta. \quad . \quad (2)$$

These expressions (1) and (2) have each of them a factor $\cos 2\pi\frac{t}{T}$ omitted, and have their maximum cyclic value

Fig. 2.

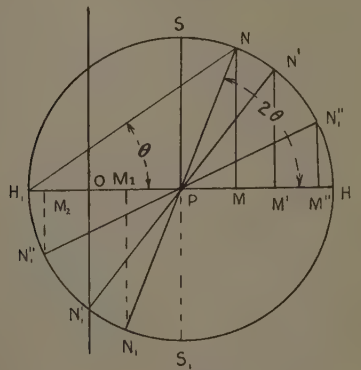

OM = Normal Stress } on
MN = Tangential Stress } plane θ

when $t=T$. If we plot these normal and tangential stresses as abscissa and ordinate we obtain the circle (Möhr's [2] "stress-circle for plane tress")

$$x^2-amq_1\,.\,x+y^2-q^2(1-a^2)=0. \quad . \quad . \quad . \quad (3)$$

The radius of this circle is

$$\tfrac{1}{2}q_1\sqrt{(a^2m^2+4(1-a^2))}, \quad . \quad . \quad . \quad . \quad . \quad (4)$$

and its centre is on the x-axis at distance $\frac{1}{2}amq_1$ from the origin.

In fig. 2 OM is the normal and MN the tangential stress on the plane whose normal is inclined θ to the

direction of p_1. The principal stresses are OH and OH_1. On planes at $\frac{\pi}{2} - \theta$ the normal and tangential stresses are respectively OM_1 and M_1N_1, where NPN_1 is a straight line through the centre of the circle. When $\theta = \frac{\pi}{4}$ the stresses are OP and PS. The stresses due to bending and torsion, *i. e.*, the stresses actually applied, are OM^1 and M^1N^1, N^1 being one extremity of a diameter $N^1PN_1{}^1$ which cuts the y-axis at $N_1{}^1$, the direct stress on the plane $\frac{\pi}{2} - \theta$ being then zero. On the plane of a shear stress $M^{11}N^{11}$ smaller than M^1N^1 the normal stress is OM^{11}, and on the plane of the complementary shear $M_2N_1{}^{11}$ the normal stress is OM_2, which is of opposite sign to OM^{11}. There is, of course, a stress circle for each value of "a."

3. *Superposition of Normal Stress on the Planes of Maximum Shear Stress.*

Assume that there is a material for which $m = 2$ and that Gough's ellipse for this hypothetical material expresses the fatigue limit stress condition for all combinations of the applied direct and shear stress for values of "a" from 0 to 1. Whatever the value of "a" in this range the radius of the corresponding stress circle is always $\frac{1}{2}q_1 \sqrt{4} = q_1$: the shear stress on some plane for each value of "a" is always equal to the maximum shear q_1. When $a = 0$ there is no normal stress on the plane of q_1: when "a" $= 1$ there is a normal stress q_1 on the planes of the maximum shear q_1. Intermediate values of "a" correspond also to a maximum shear q_1 with a normal stress given by the expression (1). These normal stresses are in each case of the same sign. For this material the fatigue limit condition is obviously induced by the shear q_1, and the addition of normal stress on the planes of maximum shear has no effect at all.

Next conside a material, conforming to Gough's ellipse, with a value "m" between 2 and $\sqrt{2}$, the latter value being, as will appear, a critical one. (See Conclusion.)

(α) For $a=0$ (applied torque only) there is a maximum shear stress q_1 with no normal stress on its planes.

(β) For $1>a>0$ there is a maximum shear $\frac{1}{2}q_1\sqrt{(a^2m^2+4(1-a^2))}$, and on the planes of this shear a normal stress $\frac{1}{2}amq_1$ of the same sign on either plane.

(γ) For $a=1$ (applied bending only) there is a maximum shear stress $\frac{1}{2}mq_1$, and on the planes of this shear normal stresses $\frac{1}{2}mq_1$ of the same sign.

Now the stress systems that are the equivalents of (α), (β), (γ) just induce the fatigue limit condition in the material of specific value of "m," and it is clear that normal stress on the planes of maximum shear has some effect. In the hypothetical material $m=2$ the superposition of a "fluid" stress (in two dimensions) has no effect at all; when $2>m>\sqrt{2}$ such superposition accompanies a reduction of the maximum shear that is associated with the fatigue limit condition. It does not follow, however, that a normal stress (see γ above) of $\frac{1}{2}mq_1$ has reduced the resistance to maximum shear by an amount (see (α) and (γ)) $q_1-\frac{1}{2}mq_1$, because the effect of normal stress in reducing resistance to shear on planes other than those of *maximum* shear has not yet been considered.

4. "*Enveloping Curve*" *of the Stress Circles.*

Suppose that an envelope (Mohr's "enveloping curve for plane stress"), F_1BB^1E (fig. 3), be drawn touching the family of stress circles drawn for values $a=0$ to $a=1$ for a particular value of m. This envelope, for the stresses at the commencement of testing, is the ellipse

$$x^2\Big/\frac{4.{q_1}^2}{4-m^2}+\frac{y^2}{{q_1}^2}=1,$$

and its tangent point with the circle

$$x^2-amq_1x+y^2-{q_1}^2(1-a^2)=0$$

is the point

$$x=\frac{2aq_1}{m},\ y=q_1\sqrt{\left(1+a^2-\frac{4a^2}{m^2}\right)}.$$

The circle of smallest radius $R^{11}E$ of the family is that for which $a=1$, and its tangent point E, viz.,

$$\frac{2q_1}{m};\ q_1\sqrt{2-\frac{4}{m^2}},$$

is the end of the chain of tangent points with the family of circles. The envelope extends from this point E to the point F, which is the tangent point of the circle of radius q_1. For a material of a particular value m between 2 and $\sqrt{2}$ the stress circles have positions as shown in fig. 3, and as "a" increases the tangent point of the stress circles with the envelope moves continuously to the right up to the point E.

It is clear that if any point, *e. g.*, K, on one of the stress circles ABC lies within another stress circle then the

Fig. 3.

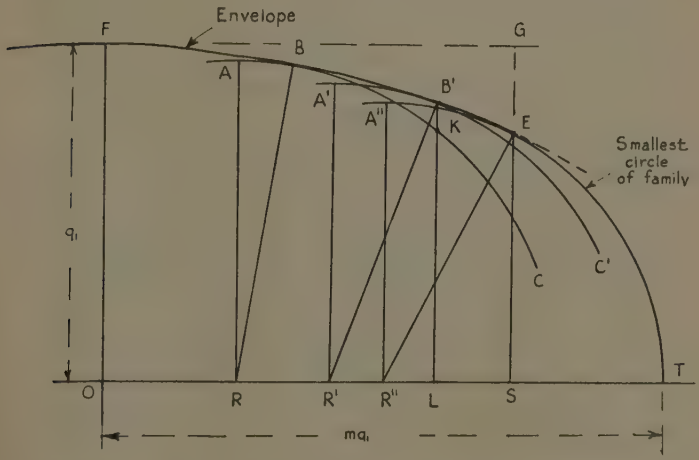

stresses OL, LK cannot induce the fatigue limit condition. For let LK be prolonged to cut the envelope at B^1; B^1 is the tangent point of some stress circle $A^1B^1C^1$ with the envelope. And while OL, LB^1 may induce the fatigue limit condition, OL and LK cannot. The point where ABC touches the envelope is the only point of this circle whose stress coordinates may induce the fatigue limit. The same argument applies to the tangent points with the envelope of the whole family of stress circles from the tangent point E of the smallest circle to F, the tangent point of the circle of radius q_1 *.

* The envelope FE may be regarded as one-quarter of the complete curve, the latter being symmetrical about OS and OF produced.

As he abscissa increases from that of the point E—corresponding to $a=1$—this argument ceases to apply, because the arc ET is not interior to any other stress circle. If the material reaches the fatigue limit condition under the stress coordinates of the arc ET there would be a change at E from an ellipse to a circle in the graph which exhibits the stresses that induce the fatigue limit condition. Moreover, from E to T along this circle the shear component decreases at a more rapid rate than along the envelope from F to E, and this with progressively smaller increments of normal stress. We conclude, therefore, that OS, SE are the only stress components of this smallest stress circle, of radius $\frac{1}{2}mq_1$, that induce the fatigue limit.

Conclusion.

If it is assumed that alternating stress on some plane or planes induces the fatigue limit condition in metals of heterogeneity of grain orientation for which Gough's ellipse can be experimentally established, and for which $2>m>\sqrt{2}$, the following conclusion is arrived at.

For any one combination C of alternating bending and twisting of the same phase there is only one plane A on which the component alternating normal and tangential stresses can induce the fatigue limit condition in a material of specific value "m." The normal to A is parallel to the plane containing the directions of the two principal stresses, and makes an angle α with the greater principal stress given by

$$\tan 2\alpha = \frac{LB^1}{R^1L} = \frac{LB^1}{OL - OR^1} \text{(fig. 3)},$$

where

OL is the normal alternating stress
LB^1 the alternating shear stress } on A

R^{1}B^1 is the radius of the "Mohr stress circle" that represents the particular combination C, and B^1 is the tangent point of this stress circle with the envelope of the family of the stress circles that represent the various combinations of the stresses. For the stresses at the commencement of testing,—

$$OL = \frac{2a}{m} q_1 \; ; \; OR^1 = \tfrac{1}{2} amq_1,$$

$$LB^1 = q_1\sqrt{\left(1-\frac{a^2}{m^2}(4-m^2)\right)},$$

$$\tan 2\alpha = \frac{2\sqrt{(m^2-a^2(4-m^2))}}{a(4-m^2)}.$$

With alternating bending only, the two steels of Gough and Pollard's experiments ($m=1{\cdot}76$ and $1{\cdot}55$) have the angles $\alpha = 36\frac{1}{2}°$ and $24°$ respectively, the larger angle relating to the ductile steel.

This result has some general interest, since it entails quantitative evaluation of the effect, in inducing fatigue, of a normal alternating stress upon planes of alternating shear stress for steels to which Gough's ellipse applies—a range of material that may, very probably, include most of the steels used by engineers.

The envelope of the stress circles (fig. 3) may be regarded as a graph exhibiting the reduction for the fatigue limit condition of alternating shear stress consequent upon the addition of normal stress upon the plane of that shear. The percentage reduction can be shown on fig. 3 by taking FO to represent 100 per cent. and OT to represent m. An abscissa then represents normal stress/q_1, and the percentage reduction is then the intercept between the envelope FBE and a line through F parallel to OT. For Gough and Pollard's two steels,

$$EG = \frac{1}{q_1}\left(q_1 - q_1\sqrt{2-\frac{4}{m^2}}\right)\times 100,$$

is 15 and 42 per cent. respectively for alternating bending only.

If a steel exists for which $m=\sqrt{2}$, Gough's ellipse for it would coincide with the envelope of the stress circles, and the maximum reduction of the shear component would be 100 per cent.—*e. g.*, a normal stress $\sqrt{2}q_1$ with no shear on its plane, and a shear q_1 with no normal stress on its plane, would be equally effective in inducing the fatigue limit condition. The planes on which the stresses are *applied* are, in this case, the critical planes, and the tangent points of the stress circles with the envelope are points such as N^1 on fig. 2.

References.

(1) " The Strength of Metals under Combined Alternating Stresses," H. J. Gough, M.B.E., D.Sc., F.R.S., and H. V. Pollard, A.M.I.Mech.E. Proc. Inst. Mech. Eng. vol. cxxxii. (1935).

(2) ' Plasticity,' A. Nadai. McGraw-Hill, 1931, pp. 45 & 61.

LXIV. *The Flow past a Flat Plate, to Oseen's Approximation. By* V. D. H. Rutland, *B.Sc., D.I.C., and* W. G. Bickley, *D.Sc., Imperial College of Science and Technology.**

1. In a recent paper by one of us [1] exact solutions were obtained of an equation which is formally identical with the well-known equations proposed by Oseen for the approximate solution of problems of viscous fluid motion. It was realized when these solutions were obtained that the solution of the Oseen equations for the flow of a viscous fluid past a flat plate was inherent in them. The details have now been worked out, and the results are here put on record, and compared with the solution of the Prandtl " boundary layer " equations for the same problem.

The Oseen equations have been subjected to considerable criticism, since the approximation inherent in them ceases to be adequate in the neighbourhood of the obstacle except at quite small Reynolds numbers. Garstang [2] has shown some alarming discrepancies which occur when the Oseen equations are applied to certain cases of the flow past spinning obstacles, and has tracked down the source of the errors. At the same time it is to be remembered that the Oseen approximation was the first which indicated mathematically the existence of a " wake," while it is generally admitted that the equations are valid at a distance from the obstacle—apart, that is, from the phenomena of turbulence, which supervene at high Reynolds numbers.

Although in the problem to be studied in this paper, where the " obstacle " itself extends to infinity, it is not to be expected that the Oseen equations will yield results of high accuracy, so that the agreement with the results of the " boundary layer " theory is unlikely to be close, it is of some interest to see how the Oseen equations acquit themselves in this case, while the solution presents some points of mathematical interest, and gives what the " boundary layer " theory does not, some information as to the motion of the fluid upstream of the obstacle.

* Communicated by the Authors.

2. We consider the steady motion of an incompressible viscous fluid past a plate whose trace is the positive half of the x-axis and whose edge is the z-axis, the undisturbed velocity of the stream being U in the positive x-direction. If u and v are the x- and y-components respectively of the fluid velocity, and p is the pressure, the equations of motion in the approximate form due to Oseen are

$$\mathrm{U}\frac{\partial u}{\partial x}=-\frac{1}{\rho}\frac{\partial p}{\partial x}+\nu\nabla^2 u, \quad . \quad . \quad . \quad (2.1)$$

$$\mathrm{U}\frac{\partial v}{\partial x}=-\frac{1}{\rho}\frac{\partial p}{\partial y}+\nu\nabla^2 v, \quad . \quad . \quad . \quad (2.2)$$

in which ρ and ν are the density and kinematic viscosity of the fluid respectively. In addition to these we have the equation of continuity,

$$\frac{\partial u}{\partial x}+\frac{\partial v}{\partial y}=0. \quad . \quad . \quad . \quad . \quad . \quad (2.3)$$

The solution must be such as to satisfy the conditions of no slip at the surface of the plate, *i. e.*,

$$u=0 \quad \text{and} \quad v=0 \quad \text{for} \quad y=0,\ x>0,$$

and also the condition that

$$u\to\mathrm{U} \ \text{as} \ y\to\infty .$$

Lamb has shown that the solution of Oseen's equations consists of an irrotational part together with a motion possessing vorticity. The former is connected with the pressure, and if ϕ is the velocity potential

$$p=\rho\mathrm{U}\,\partial\phi/\partial x+\text{const.}$$

In our case ϕ is evidently the velocity potential of a uniform stream, so that p will be constant. The equation for u thus reduces to

$$\mathrm{U}\,\partial u/\partial x=\nu\nabla^2 u. \quad . \quad . \quad . \quad . \quad . \quad . \quad . \quad (2{\cdot}4)$$

3. A solution of an equation formally identical with (2·4) satisfying similar boundary conditions was given in the paper cited [1], but we give, for completeness, an outline of the analysis.

It is convenient first to introduce non-dimensional variables given by

$$\mathrm{X}=nx, \ \mathrm{Y}=ny, \ \text{with} \ n=\mathrm{U}/2\nu,$$

when the equation becomes

$$2\frac{\partial u}{\partial \mathrm{X}} = \frac{\partial^2 u}{\partial \mathrm{X}^2} + \frac{\partial^2 u}{\partial \mathrm{Y}^2}. \quad . \quad . \quad . \quad . \quad (3.1)$$

We then introduce parabolic coordinates (λ, μ) defined by

$$\mathrm{X} = \lambda^2 - \mu^2, \ \mathrm{Y} = 2\lambda\mu,$$

for which $\mu = 0$ on the positive half of the x-axis, $\lambda = 0$ on the negative half, λ is everywhere positive, and μ has the sign of y. The transformation formulæ are

$$\frac{\partial}{\partial \mathrm{X}} = \frac{1}{2(\lambda^2+\mu^2)}\left\{\lambda\frac{\partial}{\partial\lambda} - \mu\frac{\partial}{\partial\mu}\right\} \quad . \quad . \quad (3.21)$$

$$\frac{\partial}{\partial \mathrm{Y}} = \frac{1}{2(\lambda^2+\mu^2)}\left\{\mu\frac{\partial}{\partial\lambda} + \lambda\frac{\partial}{\partial\mu}\right\} \quad . \quad . \quad (3.22)$$

$$\frac{\partial^2}{\partial \mathrm{X}^2} + \frac{\partial^2}{\partial \mathrm{Y}^2} = \frac{1}{4(\lambda^2+\mu^2)}\left\{\frac{\partial^2}{\partial\lambda^2} + \frac{\partial^2}{\partial\mu^2}\right\} \quad . \quad (3.23)$$

The equation to be satisfied by u is now

$$\frac{\partial^2 u}{\partial\lambda^2} + \frac{\partial^2 u}{\partial\mu^2} = 4\left(\lambda\frac{\partial u}{\partial\lambda} - \mu\frac{\partial u}{\partial\mu}\right). \quad . \quad . \quad . \quad (3.3)$$

We may also note for future reference that

$$\lambda = [\{(\mathrm{X}^2+\mathrm{Y}^2)^{\frac{1}{2}} + \mathrm{X}\}/2]^{\frac{1}{2}}$$
$$= [\mathrm{U}\{(x^2+y^2)^{\frac{1}{2}} + x\}/\nu]^{\frac{1}{2}}/2, \quad . \quad . \quad . \quad (3.41)$$

$$\mu = [\{(\mathrm{X}^2+\mathrm{Y}^2)^{\frac{1}{2}} - \mathrm{X}\}/2]^{\frac{1}{2}}$$
$$= [\mathrm{U}\{(x^2+y^2)^{\frac{1}{2}} - x\}/\nu]^{\frac{1}{2}}/2, \quad . \quad . \quad . \quad (3.42)$$

appropriate signs being given to μ; if x is large compared with y,

$$\mu \sim \mathrm{Y}/2\mathrm{X}^{\frac{1}{2}} = \frac{1}{2\sqrt{2}}\frac{y}{\sqrt{(\nu x/\mathrm{U})}}. \quad . \quad . \quad (3.43)$$

Thus it is seen that $2\mu\sqrt{2}$ is asymptotically equal to the variable used by Blasius in his transformation of the boundary layer equations.

4. In view of the boundary conditions it is reasonable to seek a solution of (3·3) which is a function of μ only. For such a solution

$$\frac{d^2 u}{d\mu^2} = -4\mu\frac{du}{d\mu}, \quad . \quad . \quad . \quad . \quad . \quad (4.1)$$

whence

$$\log(du/d\mu) = -2\mu^2 + \text{const.},$$

$$u = A\int_{\mu_0}^{\mu} e^{-2t^2}dt.$$

When $\mu=0$, $u=0$, so that the limit $\mu_0=0$. When $\mu\to\infty$, $u\to U$, so that

$$U = A\int_0^{\infty} e^{-2t^2}dt = A\sqrt{\pi}/2\sqrt{2}.$$

Thus
$$u = 2U\sqrt{(2/\pi)}\int_0^{\mu} e^{-2t^2}dt. \quad . \quad . \quad . \quad . \quad (4.2)$$

From this value of u we can derive the stream-function ψ by the relation

$$-\partial\psi/\partial y = u,$$

or

$$\lambda.\,\partial\psi/\partial\mu + \mu.\,\partial\psi/\partial\lambda = -4U\sqrt{(2/\pi)}(\lambda^2+\mu^2)\int_0^{\mu} e^{-2t^2}dt.$$

Suppressing temporarily the constant multiplier $4U\sqrt{(2/\pi)}$, the subsidiary equations are

$$\frac{d\mu}{\lambda} = \frac{d\lambda}{\mu} = -\frac{d\psi}{(\lambda^2+\mu^2)\int_0^{\mu} e^{-2t^2}dt} \quad . \quad . \quad . \quad . \quad (4.3)$$

One integral of this system is

$$\lambda^2-\mu^2 = \text{const.} = X, \quad . \quad . \quad . \quad (4{\cdot}41)$$

and by use of this the equation for ψ may (for positive X) be written

$$d\psi = -\left[\left\{\frac{\mu^2}{\sqrt{(X+\mu^2)}} + \sqrt{(X+\mu^2)}\right\}\int_0^{\mu} e^{-2t^2}\,dt\right]d\mu.$$

Since $\psi=0$ when $\mu=0$, we have

$$\psi = -\int_0^{\mu}\left\{\frac{\beta^2}{\sqrt{(\beta^2+X)}} + \sqrt{(\beta^2+X)}\right\}d\beta\int_0^{\beta} e^{-2t^2}dt.$$

Regarding this as a double integral, and changing the order of integration, we have

$$\psi = -\int_0^{\mu} e^{-2t^2}dt\int_t^{\mu}\left\{\frac{\beta^2}{\sqrt{(\beta^2+X)}} + \sqrt{(\beta^2+X)}\right\}d\beta$$

$$= -\int_0^{\mu}\left\{\mu\sqrt{(\mu^2+X)} - t\sqrt{(t^2+X)}\right\}e^{-2t^2}dt.$$

After some reduction, we obtain finally

$$\psi = -\mu\lambda\int_0^{\mu} e^{-2t^2}\,dt - \tfrac{1}{4}\lambda e^{-2\mu^2} + \tfrac{1}{4}e^{2X}\int_0^{\lambda} e^{-2t^2}dt + \tfrac{1}{4}\left\{\sqrt{X} - e^{2X}\int_0^{\sqrt{X}} e^{-2t^2}\,dt\right\} \quad . \quad . \quad (4{\cdot}42)$$

This formula is valid for positive X, but the terms in the last bracket become imaginary when X is negative. It is easy to verify that the expression in the bracket, along with its X- and Y-derivatives, vanishes for $X=0$, so that we are led to suppose that the remainder of (4.42) may continue to represent the stream-function for negative X. That this is true may be conclusively shown by obtaining another integral of (4.3) for negative X, satisfying the condition that $\psi=0$ when $\lambda=0$, in the form

$$\psi = -\int_0^{\lambda}\left\{\frac{\beta^2}{\sqrt{(\beta^2-X)}} + \sqrt{(\beta^2-X)}\right\}d\beta\int_x^{\sqrt{(\beta^2-X)}} e^{-2t^2}\,dt.$$

By methods similar to those used above this reduces to

$$\psi = -\mu\lambda\int_0^{\mu} e^{-2t^2}\,dt - \tfrac{1}{4}\lambda e^{-2\mu^2} + \tfrac{1}{4}e^{2X}\int_0^{\lambda} e^{-2t^2}dt. \quad (4.43)$$

From these values of ψ we obtain, replacing the factor $4U\sqrt{(2/\pi)}$,

$$\left.\begin{aligned} v &= 2U\sqrt{(2/\pi)}\,.\,e^{2X}\int_{\sqrt{X}}^{\lambda} e^{-2t^2}\,dt \quad (X>0),\\ v &= 2U\sqrt{(2/\pi)}\,.\,e^{2X}\int_0^{\lambda} e^{-2t^2}\,dt \quad (X<0),\end{aligned}\right\} \quad . \quad . \quad (4{\cdot}6)$$

and these values are evidently continuous when $X=0$.

Graphs of u as a function of Y for selected values of X, and as a function of X for selected values of Y, calculated from the above formulæ, are given in figs. 1 and 2, while a drawing of the stream-lines in the upper half of the X-Y plane is given in fig. 3. The values of u shown for negative values of X exhibit the effect of the plate in modifying the velocity distribution upstream of the leading edge. This effect, although quite noticeable, is confined to a small region ; when $X=-0{\cdot}5$ the maximum reduction in the velocity is less than 20 per cent. For water, taking $\nu=0{\cdot}018$ C.G.S., $X=0{\cdot}5$ corresponds to a distance $x=2\nu X/U=0{\cdot}018/U$ cm.

Fig. 1.

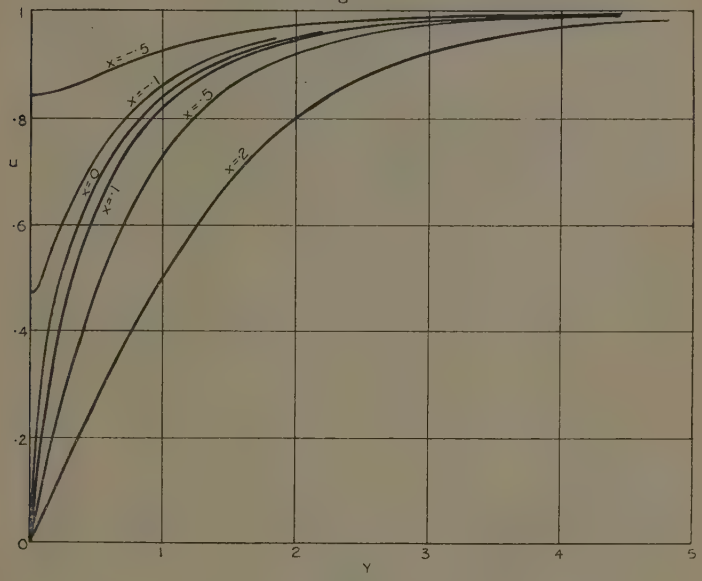

Fig. 2.

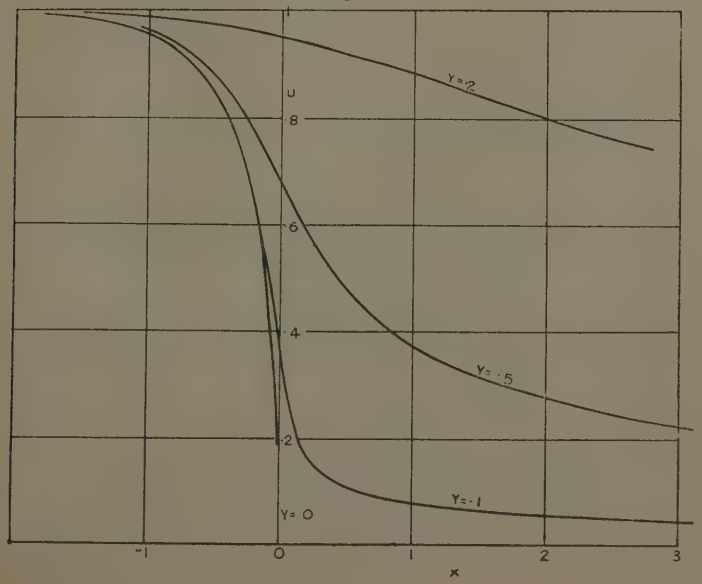

5. The adequacy of the approximation has been investigated by calculating the ratio of $(u\,\partial u/\partial x+v\,\partial U/\partial y)$, as given by the above formulæ, and $U\,\partial u/dx$, at selected points. It appears that the ratio differs from unity to an appreciable extent only near the positive X-axis and near the Y-axis, and that it is the failure to include the $v\,\partial u/\partial y$ term (representing convection across the stream) which is responsible for most of the error.

Fig. 3.

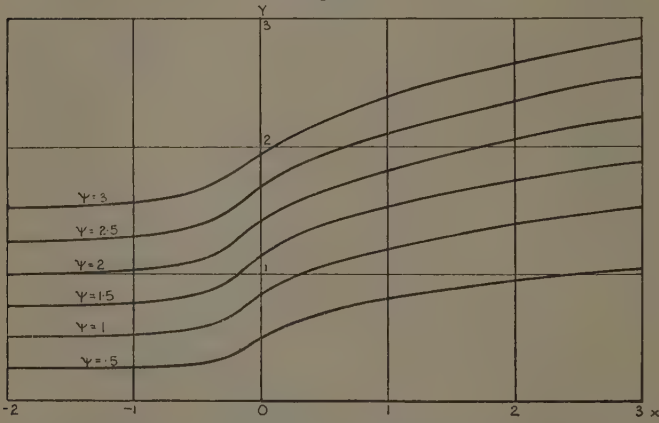

6. The formulæ obtained allow an estimate of the resistance of the plate to be determined. The viscous stress at any point is

$$p_{xy}=\rho\nu(\partial u/\partial y)_{y=0} \quad . \quad . \quad . \quad . \quad . \quad (6.11)$$

$$=\rho\sqrt{(U^3\nu/\pi x)}. \quad . \quad . \quad . \quad . \quad . \quad (6{\cdot}12)$$

For the total resistance F per unit width of plate, over a length l from the leading edge, we have

$$F=2\int_0^l p_{xy}dx$$

$$=4\rho\sqrt{(U^3\nu l/\pi)}. \quad . \quad . \quad . \quad . \quad . \quad (6.2)$$

The resistance coefficient

$$k_D=F/\rho l U^2$$

$$=\frac{4}{\sqrt{\pi}}\sqrt{\frac{\nu}{Ul}}$$

$$=2{\cdot}257R^{-\frac{1}{2}}, \quad . \quad . \quad . \quad . \quad . \quad . \quad . \quad (6.3)$$

R being the appropriate Reynolds number. Blasius's solution of the boundary-layer equations for this case leads to a resistance coefficient

$$k_D = 1{\cdot}328 R^{-\frac{1}{2}}, \quad . \quad . \quad . \quad . \quad . \quad . \quad (6.4)$$

and our result exceeds this by 70 per cent. It is interesting, however, to note that the numerical factor $4 \surd \pi$ was also obtained as a first approximation by Piercy and Preston [3].

To estimate the thickness of the boundary layer we take the distance δ from the plate at which the velocity differs from U by 0·5 per cent. From tables of the probability integral we find that this gives $\mu = \surd 2$ very nearly, so that

$$\delta = 4 \left(\frac{\nu x}{U} \right)^{\frac{1}{2}} \left(1 + \frac{4\nu}{Ux} \right)^{\frac{1}{2}}, \quad . \quad . \quad . \quad (6.51)$$

i. e., unless x is very small,

$$\delta = 4(\nu x / U)^{\frac{1}{2}}. \quad . \quad . \quad . \quad . \quad . \quad . \quad . \quad (6.52)$$

Blasius gives 5·2 as the numerical coefficient, so that our estimate is too low. Both of these discrepancies are in the direction which is to be expected, since the use of U instead of u as the "convection velocity" will increase the velocity gradient near the plate.

7. Some progress has been made in the attempt to obtain a second approximation. If the above value of u is used in the term $u \partial u / \partial x$ and the term $v \partial u / \partial y$ is neglected μ is still the only coordinate appearing in the equation, which can be formally solved, although the final result can apparently only be obtained by quadrature. From rough numerical results it would seem that a process of successive approximation on these lines will lead to a numerical coefficient in the formula (6.3) in the neighbourhood of 1·8. If it were feasible also to include the term $v \partial u / \partial y$ in obtaining the second approximation it seems probable that this approximation would then give a result even closer to Blasius's.

References.

(1) Bickley, Phil. Mag. xx. pp. 322–343 (1935); see especially p. 339.
(2) Garstang, Proc. Roy. Soc. A, cxlii. pp. 491–508 (1933).
(3) Piercy and Preston, Phil. Mag. xxii. pp. 995–1005 (1936).

LXV. *Notices respecting New Books.*

Manual of Experiments in Physics. By J. E. Shrader, Ph.D. [Pp. 262.] (McGraw-Hill Publishing Company, Ltd. Price 12*s.* 6*d.*)

THIS book is intended to be used as a laboratory manual in conjunction with a standard textbook, and for this reason theory is not given in detail except where not found in the textbook, but the relevant theory is recalled by means of questions. Concise but detailed instructions for performing each experiment are given, and a set form for recording the results is provided in each case. Opinions differ as to the advisability of this, but in his preface the author gives adequate reasons for favouring this procedure. It may be added that the remarks in the preface may be read with profit by any student using the book.

Of the sixty-one experiments, selected from all branches of the subject, which are described somewhat less than half are suitable for students who have passed the stage of an "intermediate" course in a university. The author appears to have collected, primarily for the use of his own students, a representative but limited selection of experiments which form part of a particular course of instruction, and no doubt it serves this purpose admirably.

The choice of light experiments is hardly well balanced. One example each of diffraction and interference is given (the grating and the Michelson interferometer), and these follow a determination of refractive index by the measurement of real and apparent depth. The best portion is the collection of electrical experiments, which includes some very useful methods and exercises.

OBITUARY.

We regret to announce the death of Dr. J. R. Airey, M.A., for several years one of the Editors of *The Philosophical Magazine*, at Llwynon, Newtown, Montgomeryshire, on September 16th. An obituary notice will be published in our next issue.

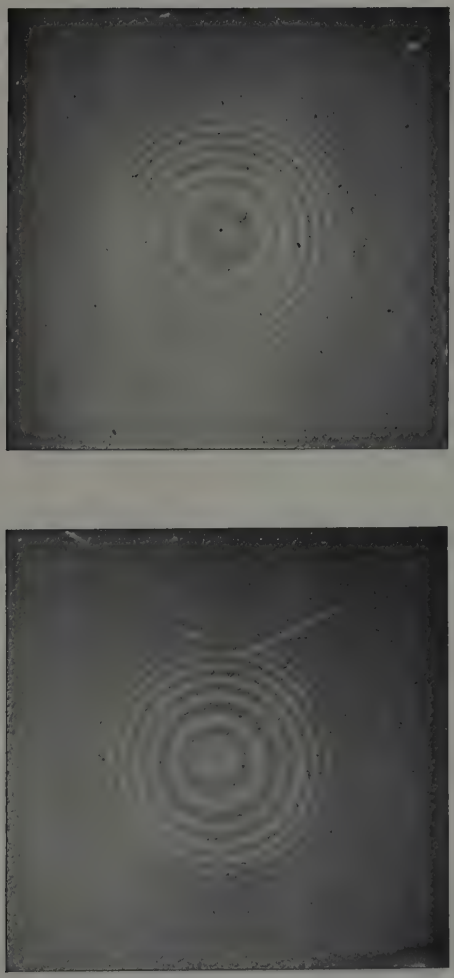

Interferometer pictures of the red line 6300 of distant auroræ with ray structure, taken at Oslo, Oct. 16–17, 1936, towards the northern sky. (*a*) exposure 1^{05}–2^{10}, (*b*) exposure 2^{25}–4^{15}. Enlarged positive copies.

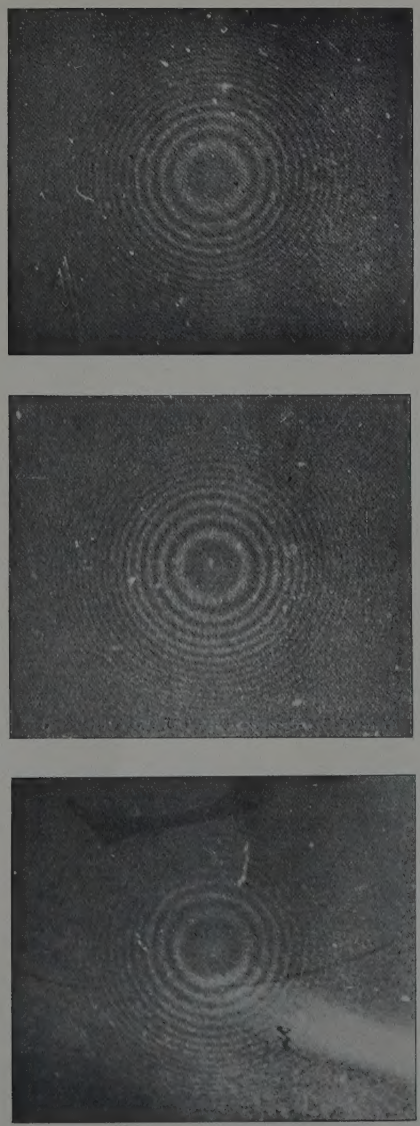

Interferometer pictures of the green auroral line (5577), taken at Oslo, May 4–5, 1937. (*a*) from lower limit, (*b*) medium altitude, (*c*) from upper limit.

FIG. 1.

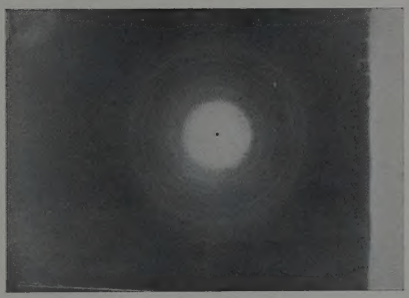

Electron diffraction from quartz sand.

FIG. 2.

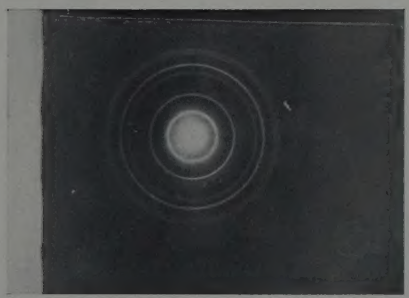

Typical electron diffraction pattern from clays and puzzolanes.